

# The Role of LIN9 in Mouse Development

Dissertation zur Erlangung  
des naturwissenschaftlichen Doktorgrades  
der Bayerischen Julius-Maximilians-Universität Würzburg



vorgelegt von  
**Nina Reichert**  
**aus Marburg an der Lahn**

**Würzburg, 2008**

Eingereicht am:

.....

Mitglieder der Promotionskommission:

Vorsitzender:

1. Gutachter: Prof. Dr. Stefan Gaubatz

2. Gutachter: Prof. Dr. Thomas Brand

Tag des Promotionskolloquiums:

.....

Doktorurkunde ausgehändigt am:

.....

**Für meine Familie & Oliver**

---

|          |  |           |
|----------|--|-----------|
| <b>1</b> | <b>INTRODUCTION.....</b>                                   | <b>1</b>  |
| 1.1      | Cell Cycle & its Regulators.....                           | 1         |
| 1.1.1    | Mammalian Cell Cycle.....                                  | 1         |
| 1.1.2    | Cyclins & CDKs.....  | 2         |
| 1.1.3    | pRB/E2F Pathway.....                                       | 4         |
| 1.2      | pRB/E2F Complexes in Model Organisms .....                 | 5         |
| 1.2.1    | DRM Complex in <i>C. elegans</i> .....                     | 5         |
| 1.2.2    | Myb-MuvB(MMB) & dREAM Complexes in <i>Drosophila</i> ..... | 6         |
| 1.2.3    | Human LIN Complex & its Core Component LIN-9 .....         | 7         |
| 1.3      | Mouse Models for known Cell Cycle Regulators.....          | 10        |
| 1.3.1    | Embryonic Development.....                                 | 10        |
| 1.3.2    | Essential LINC Members .....                               | 12        |
| 1.3.2.1. | pRB/p107/130 .....   | 12        |
| 1.3.2.2. | E2F4 .....   | 15        |
| 1.3.2.3. | B-MYB .....  | 16        |
| 1.4      | Aim of this Project.....                                   | 17        |
| <b>2</b> | <b>MATERIALS &amp; METHODS.....</b>                        | <b>18</b> |
| 2.1      | Materials.....   | 18        |
| 2.1.1    | Chemical Stocks & Reagents.....                            | 18        |
| 2.1.2    | PCR & DNA/RNA Modifying Enzymes.....                       | 19        |
| 2.1.3    | Molecular Kits & Protein/DNA/RNA Markers.....              | 20        |
| 2.1.4    | Buffers.....   | 20        |
| 2.1.4.1. | General Buffers .....                                      | 20        |
| 2.1.4.2. | Buffers for Southern Blot .....                            | 22        |
| 2.1.4.3. | Buffers for Immunohistochemistry.....                      | 23        |
| 2.1.4.4. | Buffers for Western Blot.....                              | 24        |
| 2.1.5    | Oligolist.....   | 25        |
| 2.1.6    | Plasmidlist .....  | 27        |
| 2.1.7    | Antibodies.....  | 28        |
| 2.1.8    | Cell Lines & Cell Culture Media.....                       | 28        |
| 2.1.9    | Bacterial Strains.....                                     | 29        |
| 2.1.10   | Mouse Strains & ES Cell Lines .....                        | 29        |
| 2.1.11   | Microscopic equipment.....                                 | 29        |
| 2.2      | Methods .....  | 30        |
| 2.2.1    | Cell Culture.....  | 30        |
| 2.2.1.1. | Generation of MEFs.....                                    | 30        |
| 2.2.1.2. | Passageing of Cells .....                                  | 30        |
| 2.2.1.3. | Freezing & Thawing of Cells.....                           | 30        |
| 2.2.1.4. | Transient Transfection of Plat-E Cells.....                | 31        |
| 2.2.1.5. | Infection of MEFs .....                                    | 31        |
| 2.2.1.6. | Tamoxifen Induction of Cre.....                            | 31        |
| 2.2.1.7. | Growth Curve .....   | 32        |
| 2.2.1.8. | Determination of Cell Cycle Phases.....                    | 32        |
| 2.2.1.9. | Culturing of Blastocysts .....                             | 32        |
| 2.2.2    | Molecular Methods.....                                     | 32        |

---

|           |   |           |
|-----------|---|-----------|
| 2.2.2.1.  | Isolation of RNA from Cultured Cells.....                           | 32        |
| 2.2.2.2.  | Isolation of RNA from Mouse Organs .....                            | 33        |
| 2.2.2.3.  | Isolation of Plasmid DNA from Bacteria.....                         | 33        |
| 2.2.2.4.  | Isolation of DNA Fragments from Agarose Gels.....                   | 33        |
| 2.2.2.5.  | Extraction of gDNA from Cells.....                                  | 34        |
| 2.2.2.6.  | Extraction of gDNA in Small Scale .....                             | 34        |
| 2.2.2.7.  | Extraction of gDNA from Tails for Southern Blot .....               | 34        |
| 2.2.2.8.  | Standard Cloning Method.....  | 35        |
| 2.2.2.9.  | Tail PCRs (basic protocol).....                                     | 36        |
| 2.2.2.10. | Reverse Transcription.....  | 36        |
| 2.2.2.11. | Quantitative PCR .....  | 37        |
| 2.2.2.12. | TaqMan .....  | 37        |
| 2.2.2.13. | Southern Blot with Radioactively Labeled Probes .....               | 38        |
| 2.2.3     | Immunohistochemical Methods.....                                    | 40        |
| 2.2.3.1.  | Preparation of Paraffin Sections.....                               | 40        |
| 2.2.3.2.  | HE Staining .....   | 41        |
| 2.2.3.3.  | TUNEL Staining .....  | 41        |
| 2.2.3.4.  | <i>In situ</i> Hybridization of Sections .....                      | 41        |
| 2.2.3.5.  | Whole Mount <i>in situ</i> Hybridization of Embryos (WISH) .....    | 43        |
| 2.2.3.6.  | WISH of Blastocysts .....   | 45        |
| 2.2.4     | Mouse .....   | 46        |
| 2.2.4.1.  | Mouse Husbandry.....  | 46        |
| 2.2.5     | Biochemical methods .....   | 47        |
| 2.2.5.1.  | Whole Cell Lysates .....  | 47        |
| 2.2.5.2.  | Tissue Extract.....   | 47        |
| 2.2.5.3.  | Determination of Protein Concentration (Bradford) .....             | 48        |
| 2.2.5.4.  | IP-Western Blot .....   | 48        |
| <b>3</b>  | <b>RESULTS .....</b>  | <b>50</b> |
| 3.1       | Expression of <i>Lin</i> in Mouse .....                             | 50        |
| 3.1.1     | Molecular Analysis of <i>Lin</i> mRNA Expression .....              | 50        |
| 3.1.2     | Histological Analysis of <i>Lin</i> mRNA Expression.....            | 52        |
| 3.2       | Lin9 Gene Trap Mouse Model (GT).....                                | 56        |
| 3.2.1     | Location of the Gene Trap in the Lin9 Allele .....                  | 56        |
| 3.2.2     | Analysis of Lin9 in Early Mouse Development .....                   | 58        |
| 3.2.3     | Early Embryonic Lethality of Lin9 <sup>GT/GT</sup> Embryos .....    | 59        |
| 3.2.4     | Analysis of Apoptosis in Lin9 <sup>GT/GT</sup> Embryos .....        | 62        |
| 3.2.5     | Analysis of Lin9 <sup>GT/GT</sup> Peri-implantation Phenotype ..... | 62        |
| 3.2.6     | Analysis of <i>Lin9</i> mRNA Expression in Blastocysts .....        | 66        |
| 3.2.7     | Analysis of GT Lin9 Heterozygous MEFs .....                         | 67        |
| 3.3       | Generation of a Conditional Lin9 Knockout Mouse Model.....          | 69        |
| 3.3.1     | Construction of the Conditional Lin9 Knockout.....                  | 69        |
| 3.3.2     | Generation of Conditional Knockout Mice.....                        | 70        |
| 3.3.3     | Analysis of Lin9 <sup>fl/fl</sup> MEFs with Cre-Infection.....      | 72        |
| 3.3.4     | Analysis of Lin9 <sup>fl/fl</sup> CreER <sup>T2</sup> MEFs.....     | 75        |
| <b>4</b>  | <b>DISCUSSION .....</b>   | <b>78</b> |
| 4.1       | Expression of <i>Lin</i> mRNA in the Mouse .....                    | 78        |

---

|          |   |           |
|----------|---|-----------|
| 4.2      | Lin9 Gene Trap Mouse Model.....   | 80        |
| 4.2.1    | Establishment of the Lin9 GT Knockout Model .....                                       | 80        |
| 4.2.2    | Early Embryonic Lethality of Lin9 <sup>GT/GT</sup> Embryos .....                        | 80        |
| 4.2.3    | Peri-implantation Lethality of Lin9 <sup>GT/GT</sup> Embryos .....                      | 81        |
| 4.2.4    | Possible Role in Early Embryonic Cell Cycle Regulation &/or Lineage Specification ..... | 83        |
| 4.2.5    | <i>In vitro</i> Analysis of LIN9's Role in Cell Cycle in MEFs.....                      | 86        |
| 4.3      | Conditional Lin9 Knockout .....   | 87        |
| 4.3.1    | Generation of the Conditional Lin9 Knockout Model.....                                  | 87        |
| 4.3.2    | Cre-mediated Excision <i>in vivo</i> .....  | 87        |
| 4.3.3    | Cre-mediated Excision <i>in vitro</i> .....   | 88        |
| 4.3.4    | Inducible Cre-mediated Excision <i>in vivo</i> .....                                    | 88        |
| 4.3.5    | LIN9 Function in Tumorigenesis & Differentiation <i>in vivo</i> .....                   | 89        |
| 4.3.6    | Hypothesis.....   | 90        |
| <b>5</b> | <b>SUMMARY.....</b>   | <b>92</b> |
| <b>6</b> | <b>ZUSAMMENFASSUNG.....</b>   | <b>93</b> |
| <b>7</b> | <b>APPENDIX.....</b>  | <b>94</b> |
| 7.1      | Supplementary Figures.....  | 94        |
| 7.2      | Mouse Genome Informatics (MGI) .....  | 96        |
| 7.3      | Database .....  | 97        |
| 7.4      | Software .....  | 97        |
| 7.5      | Abbreviations & Symbols .....   | 97        |
| 7.6      | List of Figures & Tables .....  | 98        |
| 7.7      | Citations .....   | 100       |
| 7.8      | Acknowledgement .....   | 107       |
| 7.9      | Own publications .....  | 108       |
| 7.10     | Curriculum Vitae .....  | 109       |
| 7.11     | Eidesstattliche Erklärung.....  | 110       |

# 1 INTRODUCTION

## 1.1 Cell Cycle & its Regulators

### 1.1.1 Mammalian Cell Cycle

To ensure proper growth and maintenance of an organism, mammalian cells exhibit a tightly controlled cycle of growth and cell division. Cell division leads, via mitosis and cytokinesis, to two equal daughter cells. Proliferation describes cell growth, accumulation of cell properties and subsequent cell division. There are four main parts of the cell cycle, the M phase (mitosis), and the three interphases, G1 (first gap), S (synthesis) and G2 (second gap) (Fig. 1.1 A).

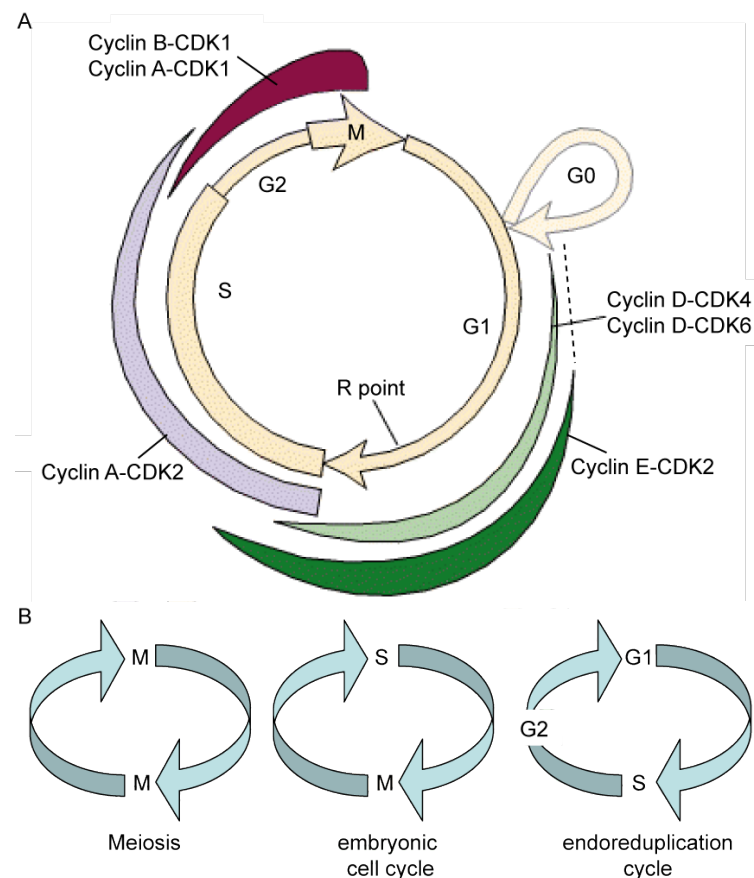


**Fig. 1.1: Simplified representation of the mammalian cell cycle.** (A) Activity of cyclin/CDK complexes through the course of the cell cycle. The width of the colored bands is proportional to the kinase activity. Cyclin D refers to all three D-type cyclins. (adapted & modified from (Coller, 2007). (B) Different cell cycles in which specific phases are absent (adapted from (van den Heuvel, 2005). (R point = restriction point & CDK = cyclin dependent protein kinase)

Immediately after cell division RNA and proteins start to accumulate. This period of the cell cycle between the end of mitosis and the subsequent onset of DNA synthesis is termed G1. Usually this gap takes 12 to 15 hours. Variances in cycle duration are mostly due to

differences in entering and exiting G1 phase, and to an optional break in quiescence state (G0); or even entering the differentiation modus. This is influenced by growth factors in the cell's surroundings. In sufficient concentrations these extracellular signals will encourage a cell to continue cell cycle, or their absence will trigger the cell to proceed into G0. This critical decision point in the cell cycle, several hours before the end of G1, is termed restriction point (R point). This also resembles the point of no return, once the cell has passed this critical point, it will proceed with the G1/S phase transition. The following S phase, during which DNA synthesis occurs, typically requires 6 to 8 hours to reach completion. The second gap (G2) takes 3 to 5 hours. Finally, M phase extends approximately one hour, and includes four distinct subphases: prophase, metaphase, anaphase, and telophase. Mitosis finishes with cytokinesis, the division of the cytoplasm (Coller, 2007; Pardee, 1974; Planas-Silva and Weinberg, 1997). There are several DNA damage control points in G1 and G2 phases, and the spindle-assembly checkpoint in M phase.

The time a cell needs to progress through the cell cycle is greatly depending on cell type and on circumjacent conditions. The indicated lengths of each phase are commonly observed in cultured cells. Hence actively proliferating lymphocytes may double in only 5 hours, and some cells in the early embryo may do so even more rapidly. For example, the pluripotent cells in the epiblast have a cell cycle lacking the gap phases, and more than 50% of the cycle time is devoted to S phase (Mac Auley et al., 1993) (Fig. 1.1 B & Section 1.3.1). This is similar for pluripotent ES cells (embryonic stem cells) (Savatier et al., 1994) and murine embryonal carcinoma cells (Thomson et al., 1998). Cells that only display S and G phases and no mitosis are endoreduplicating such as trophoblast giant cells (Varmuza et al., 1988).

### 1.1.2 Cyclins & CDKs

Controlled cell cycle progression is driven mainly by protein complexes composed of two subunits: a cyclin and a corresponding cyclin dependent protein kinase (CDK). CDKs are small serine/threonine kinases that require association with a cyclin subunit for their activation. Cyclin/CDKs catalyze the phosphorylation of specific target substrates. These phosphorylation events are transient and reversible. When the cyclin/CDK complex disappears, the phosphorylated substrates are rapidly dephosphorylated by protein phosphatases (reviewed in (Morgan, 1997; Murray, 2004)).

Active cyclin/CDK complexes lead to the activation of transcription factors which induce the transcription of the next set of cyclins and CDKs. Consequently there is a rapid turnover and tight regulation, which involves controlled transcription and degradation of cyclins.



Regulation also involves activating and inhibiting phosphorylation, dephosphorylation of the CDKs, and control of inhibitory proteins that associate with cyclin/CDK complexes (Hadwiger et al., 1989; Nash et al., 1988; Sanchez and Dynlacht, 2005)).

During G1 phase, the D-type cyclins (D1, D2, and D3) bind and activate CDK4 and CDK6 (Bates et al., 1994; Matsushime et al., 1992; Meyerson and Harlow, 1994). Both CDKs have similar enzymatic activities. In late G1, after the R point CDK2 primarily interacts with E-type cyclins (E1 and E2) to phosphorylate specific substrates required for the initiation of DNA replication and centrosome duplication in S phase (Dulic et al., 1992; Gudas et al., 1999; Koff et al., 1992; Lauper et al., 1998; Leone et al., 1999; Zariwala et al., 1998). When the cells enter S phase, the A-type cyclins (A1 and A2) substitute the E-type cyclins (E1 and E2) as partners of CDK2 to promote progression through S phase. Cyclin A phosphorylates proteins involved in DNA replication, such as CDC6 (Coverley et al., 2000; Petersen et al., 1999; Yan et al., 1997). Hence at the end of the S phase, the A-type cyclins switch partners to associate with CDK1 (CDC2) (Girard et al., 1991; Pagano et al., 1992; Yan et al., 1997). Moving further into G2 phase, CDK1 largely associates to the mitotic B-type cyclins (B1 and B2). During G2/M transition cyclin A activity is needed for the initiation of prophase (Furuno et al., 1999). At the mitotic exit, the cyclin/CDK complexes are required for chromosomal alignment and progression to anaphase (den Elzen and Pines, 2001; Minshull et al., 1990) (Draetta et al., 1989). At the onset of M phase, the B-type cyclin/CDK1 complex triggers many of the essential procedures that constitute mitosis and end in cytokinesis (Obaya and Sedivy, 2002; Wheatley et al., 1997) (Fig. 1.1 A).

The levels of CDKs slightly vary during cell cycle, only the cyclins fluctuate in a cell cycle dependent manner. For example, cyclin B strongly increases at the onset of mitosis to associate with CDK1. At the end of the M phase cyclin B levels drop due to rapid degradation. It is undetectable at the beginning of the next cell cycle. The only exceptions in fluctuating levels are the D-type cyclins, which are constantly expressed (Sherr and Roberts, 2004; Silver and Montell, 2003).

Mammalian cells are thought to require the sequential activation of the CDKs and cyclins to precede though interphase and mitosis. Most prominent downstream targets of cyclin/CDK complexes include pRB and E2F.

### 1.1.3 pRB/E2F Pathway

The retinoblastoma family of proteins consists of the retinoblastoma protein (pRB) and two related proteins p107 and p130. pRB was the first tumoursuppressor identified and is mutated in approximately one third of all human tumors (Lee et al., 1987; Sherr, 1996). These proteins are called pocket proteins because they share a pocket domain, which consists of two highly conserved regions A and B, separated by a linker (Lipinski and Jacks, 1999). The pocket domain mediates interactions with transcription factors of the E2F family and histone deacetylases (HDACs) (Felsani et al., 2006; Giacinti and Giordano, 2006). The best characterized targets of the pocket proteins are members of the E2F family of transcription factors. To date, eight different E2F family members have been identified in mammals. E2Fs can be divided into two major groups, the transcriptional activators E2F1, E2F2 and E2F3 and the transcriptional repressors E2F4, E2F5, E2F6, E2F7 and E2F8. The E2Fs bind to DNA as heterodimers together with either DP1 or DP2, except for the two most recently identified, E2F7 and E2F8, which bind to DNA DP-independently. E2F6-8 are pocket protein independent transcriptional repressors.

The transcriptional activators E2F1-3 promote the cell cycle and exclusively bind to pRB, and not to p130 or p107. In G0 and early to mid G1, hypophosphorylated pRB binds to E2F activator proteins, preventing them from transactivating E2F target genes (Rayman et al., 2002). The following G1/S transition is promoted by the cyclin D/CDK4/6 complex phosphorylating pRB (Kato et al., 1993). The hyperphosphorylation of pRB leads to released and thereby activated E2Fs/DP heterodimers, For example, free E2F1 activates genes required for DNA synthesis, such as cyclin E, cdc6 and cyclin A (Arroyo and Raychaudhuri, 1992; Leone et al., 1999; Mudrak et al., 1994). pRB remains hyperphosphorylated throughout the rest of the cell cycle, due to cyclin E/CDK2 activity.

In contrast, the repressor E2Fs, E2F4 and E2F5, are localized in the nucleus, associated to the pRB-related proteins p130 and p107, thereby silencing E2F-regulated promoters in quiescent cells (G0) and in early G1. Indirectly this prevents binding of activators and moreover these complexes silence genes directly by recruitment of further repressive complexes. For example, E2F4 recruits HDAC complexes, which causes deacetylation of histone tails and repression of many E2F target genes, like B-Myb, CDK1, E2F1, and cyclin A (Frolov and Dyson, 2004; Humbert et al., 2000; Leone et al., 1999; Trimarchi and Lees, 2002; Wu et al., 2001). If the cell reenters cell cycle, many E2F target genes become activated. E2F4 is released, due to CDK-dependent phosphorylation of p130. The HDAC repressor complex dissociates from the promoter because E2F4 relocates to the cytoplasm (Gaubatz et al.,

2001; Verona et al., 1997). In parallel, the phosphorylation of pRB by cyclin D/CDK4/6 promotes the release of the E2F activators, which leads to HAT recruitment, consequent histone H3/H4 acetylation and transcriptional activation of E2F target genes (Morris et al., 2000; Rayman et al., 2002).

## 1.2 pRB/E2F Complexes in Model Organisms

Pocket proteins are able to counteract E2F-mediated transactivation in two different ways, first by simply binding and masking the E2F activation domain and second by actively repressing their transcription with corepressors complexes (Frolov and Dyson, 2004). Due to the complexity of the pRB/E2F pathways in mammalian cells, a lot of the functional studies were performed in model organism where the pRB/E2F network appears to be less complex.

### 1.2.1 DRM Complex in *C. elegans*

Genetic studies of the nematode *Caenorhabditis elegans* (*C. elegans*) identified pRb/E2F as essential in chromatin remodeling processes during development. Of high interest are the studies concerning vulva development. Here, the synthetic multivulva (synMuv) genes antagonize, in a redundant fashion, the Ras-MAPK (mitogen-activated protein kinase) signaling pathway (Fay and Han, 2000; Ferguson and Horvitz, 1985; Horvitz and Sulston, 1980; Kornfeld, 1997; Lipsick, 2004). These synMuv genes are grouped into three classes, namely A, B, and C, on the basis of their genetic interactions (Ceol and Horvitz, 2004; Ferguson and Horvitz, 1989). The class B synMuv genes encode among other proteins homologues of pRB (*lin-35*), DP (*dpl-1*) and E2F (*efl-1*) (Ceol and Horvitz, 2001; Lu and Horvitz, 1998). However, their biochemical properties and pathways regulated by these proteins were largely unknown.

Recently biochemical approaches implied that synMuv proteins form distinct transcriptional regulatory complexes. The group of Horvitz was able to identify the components of an evolutionarily conserved pRB/E2F complex in *C. elegans*, namely the DP, pRB, and class B synMuv (DRM) complex (Ceol and Horvitz, 2001; Harrison et al., 2006). The DRM complex consists of the following members: LIN-9, LIN-35, LIN-37, LIN-52, LIN-53, LIN-54, DPL-1, and EFL-1. The main members, the heterodimeric EFL-1/DPL-1 and the WD40-repeat histone-binding protein LIN-53 (RbAp48) interact and bind directly to LIN-35 (pRB) (Ceol and Horvitz, 2001; Lu and Horvitz, 1998).

## 1.2.2 Myb-MuvB(MMB) & dREAM Complexes in *Drosophila*

The Myb-MuvB and dREAM complexes in *Drosophila melanogaster* (*Drosophila*) are nearly identical to the DRM complex and were purified biochemically from *Drosophila* embryos by the groups of Brehm and Botchan (Korenjak et al., 2004; Lewis et al., 2004). The *Drosophila* genome encodes two pocket protein homologues termed RBF1 and RBF2, a single dDP protein and only two E2F homologues, the activating dE2F1 and the repressive dE2F2 (Du et al., 1996; Stevaux and Dyson, 2002). The native multi-subunit complex identified by Brehm's group is termed dREAM (*Drosophila* RBF, dE2F, and dMyb-interacting proteins) and contains dE2F2, dDP, RBF1 or RBF2, CAF1p55 (RbAp48), and dMyb (B-Myb) as well as the dMyb-interacting proteins Mip40 (LIN-37), Mip120 (LIN-54), and Mip130/TWIT (LIN-9) ((Korenjak et al., 2004); Tab. 1.2). Interestingly, all of these proteins except Myb are homologues of the class B synMuv genes of *C. elegans* and members of the DRM complex described above. Thus it is possible that the DRM complex does not need a Myb protein, or that the functional ortholog of the *Drosophila* dMyb protein might not be identified in *C. elegans*, yet (Harrison et al., 2006).

The second complex, termed Myb-MuvB or MMB by the Botchan group is similar to dREAM but contains three additional subunits, namely the histone deacetylase Rpd3 (HDAC), dLin52 (LIN-52), and the tumor suppressor L(3)MBT (lethal malignant brain tumor/*C. elegans* LIN-61) (Lewis et al., 2004). The different complex composition may be due to the less stringent purification procedures applied.

Both complexes were shown to repress gene transcription and localize to promoters of dE2F2-regulated genes (Dimova et al., 2003). Both groups performed RNAi knockdown studies and demonstrated that the dE2F2 repressor and other components are necessary to effectively silence developmentally regulated genes, except dMyb, which does not seem to be essential for repression (Korenjak et al., 2004; Lewis et al., 2004). These and other studies, only described a function for replication (Beall et al., 2004; Beall et al., 2002) and transcriptional repression with a passive role of dMyb (Dimova et al., 2003; Korenjak et al., 2004; Lewis et al., 2004), but not for transcriptional activation. Moreover the exact mechanisms of the transcriptional repression are still unclear. Combining these studies a model was proposed, where dMyb activates the complex, cell context-dependent (Beall et al., 2004; Beall et al., 2002).

Recently this model was supported by analysis of the DNA-binding properties of each dREAM/MMB component in a genome-wide screen using RNAi (Georlette et al., 2007). Georlette and colleagues could confirm that dREAM/MMB represses many developmental

genes and additionally functions as an activator of G2/M genes. They further showed that the complex members preferentially co-localize near transcriptional start sites (Georgette et al., 2007). The dREAM/MMB complexes are widely expressed in various tissues in *Drosophila*. Recently one tissue-specific complex, termed tMAC (testis Meiotic Arrest Complex) was purified from *Drosophila* testes extract suggesting that in *Drosophila* context-dependent complexes may also exist (Beall et al., 2007).

### 1.2.3 Human LIN Complex & its Core Component LIN-9

Recently, our lab was able to identify predicted homologues of all subunits of the dREAM/Myb-MuvB complex in the human and mouse genome. It was also known from previous work that an important component, LIN-9 associates with pRB and B-MYB (Gagrica et al., 2004; Osterloh et al., 2007; Pilkinton et al., 2007). Our group in cooperation with the group of Alexander Brehm has also biochemically purified and characterized a human dREAM/Myb-MuvB like complex which was called LINC (LIN complex) (Schmit et al., 2007). LINC differs from the invertebrate complexes in that it consists of a stable core complex which interacts cell cycle-dependent and context-dependent with pocket proteins, E2F4 and B-MYB. The core module consists of the LIN proteins LIN-9, LIN-54, LIN-52, LIN-37 and RbAp48 (Tab. 1.1). The cell cycle-regulated pocket protein p107 is only loosely associated to LINC. The composition of LINC was further analyzed with binding assays in synchronized cells. These assays revealed that LINC associates in G0 to E2F4 and p130. This binding is lost in S-phase where LINC switches to B-MYB and p107 (Schmit et al., 2007).

The cell cycle regulated LINC assembly was further analyzed with chromatin immunoprecipitation (ChIP) experiments, demonstrating that LINC directly binds to E2F-regulated promoters in quiescent cells (G0). Moreover, LINC leaves the promoters of genes activated at G1/S upon cell cycle entry (G1), but remains bound to G2/M promoters (Schmit et al., 2007). The role of LINC in cell cycle progression and proliferation was analyzed by RNAi in immortalized BJ fibroblasts (BJ-ET cells). Depletion of either LIN-9 or B-MYB inhibited proliferation and delayed entry into mitosis because it regulates genes essential for entry into mitosis such as cyclin A2, cyclin B1 and *cdc2* (CDK1), as well as genes regulating the mitotic spindle checkpoint such as PLK1, Aurora-A, and Bub1, Birc5 (survivin). Additionally genes important for chromosome segregation like CENP-E as well as genes essential to exit mitosis like Ubch10 and many others are also regulated by LINC (Osterloh et al., 2007; Schmit et al., 2007) (Tab. 1.2). These LINC G2/M target genes are responsible for entry into, progression

through and exit from mitosis. Although LINC associates with E2F-regulated promoters in G<sub>0</sub>, it is not necessary for their repression.

| <b>Drosophila melanogaster</b> |                      | <b>C. elegans</b>    | <b>Homo sapiens</b>   |          |
|--------------------------------|----------------------|----------------------|---|----------|
| Lewis et al. 2004              | Korenjak et al. 2004 | Harrison et al. 2006 | Schmit et al. 2007 (LINC)<br>Litovchick et al. 2007 (DREAM) |          |
| <b>Myb-MuvB</b>                | <b>dREAM</b>         | <b>DRM</b>           | <b>G<sub>0</sub></b>  | <b>S</b> |
| Mip130                         | Mip130/TWIT          | LIN-9                | LIN-9   | LIN-9    |
| Mip40                          | Mip40                | LIN-37               | LIN-37  | LIN-37   |
| dLin52                         |                      | LIN-52               | LIN-52  | LIN-52   |
| Mip120                         | Mip120               | LIN-54               | LIN-54  | LIN-54   |
| CAF1p55                        | CAF1p55              | LIN-53               | RbAp48  | RbAp48   |
| dDP                            | dDP                  | DPL1                 | DP  | DP       |
| dE2F2                          | dE2F2                | EFL1                 | E2F4  |          |
| RBF1/2                         | RBF1/2               | LIN-35               | p130  | (p107)   |
| dMyb                           | dMyb                 |                      |   | B-MYB    |
| RPD-3                          |                      |                      |   |          |
| L(3)MBT                        |                      |                      |   |          |

**Tab. 1.1: Summary of pRB/E2F complexes in different species.** p107 is present in LINC but not in DREAM (adapted and modified from (Schmit et al., 2007)).

Independently, the group of DeCaprio identified a similar complex, using an unbiased proteomics approach with human cell extracts. This so called DREAM (p130-associated DP, RB-like, E2F and MuvB) complex contains in quiescence cells p130, E2F4 or E2F5, Dp1 or DP2, LIN-9, LIN-54, LIN-52, LIN-37, and RbAP48. With this composition DREAM is able to bind to E2F-regulated promoters, as shown with ChIP analysis. The DREAM complex dissociates in S phase and only the LINs (LIN-9, LIN-54, LIN-52, LIN-37, and RbAP48) together with B-MYB form a sub-complex which is no longer associated with E2F-regulated promoters (Litovchick et al., 2007). These findings are consistent apart from our observation of LINC binding to G<sub>2</sub>/M promoters. Furthermore, although our work suggests a role for LINC in gene activation, DREAM was reported to function in G<sub>0</sub> to repress cell-cycle dependent genes, shown by single RNAi depletion experiments. Further experiments are necessary to resolve these issues.

LIN-9, a component of the core complex, is not only part of the LINC complex, but also binds to pRB (Gagrica et al., 2004; Korenjak et al., 2004). This binding is restricted to the N-terminal part of LIN-9, interacting with the pocket domain of pRB. LIN-9 cooperates with pRB during flat cell formation in human Saos-2 cells (Gagrica et al., 2004). The flat cell formation is similar to a senescent-like phenotype and is a marker for differentiation (Sellers

et al., 1998), suggesting that human LIN-9 promotes pRB-mediated differentiation. Notably LIN-9 is not involved in pRB-regulated G1 arrest and in the repression or activation of E2F-dependent cell cycle genes, in Saos-2 or Hela cells.

| Gene symbol | Gene name                                      | Expression | Function                     |
|-------------|--|------------|------------------------------|
| BIRC5       | Baculoviral IAP repeat-containing 5 (Survivin) | G2/M       | mitotic checkpoint           |
| CDC2        | Cell division cycle 2                          | G2/M       | cytokinesis                  |
| CCNA2       | Cyclin A2                                      | S/G2/M     | entry in S & transition in M |
| CCNB1       | Cyclin B1                                      | G2/M       | entry & transition in M      |
| CENPE       | Centromere Protein E                           | G2/M       | mitotic checkpoint           |
| BUB1        | Budding uninhibited by benzimidazoles 1        | G2/M       | mitotic checkpoint           |
| AURKA       | Serine/threonine kinase 6; Aurora A            | G2/M       | mitotic spindle assembly     |
| PLK1        | Polo-like kinase 1                             | G2/M       | entry & exit from M          |

**Tab. 1.2: List of important LINC target genes.** Summary of downregulated G2/M genes in LIN-9 depleted BJ-cells (adapted from (Osterloh et al., 2007)). (M = mitosis)

Moreover the depletion of LIN-9, like the pRB depletion, lead to transformation in primary human fibroblasts (BJ-ET cells). LIN-9 overexpression rescued morphological changes induced by oncogenic RasV12 in immortalized murine fibroblasts (NIH-3T3) and inhibited growth of colonies in soft agar assays pRB-dependently in murine embryonic fibroblasts (MEFs). This suggests a role for LIN-9 in tumorigenesis (Gagrica et al., 2004).

Sandoval and colleagues generated a Lin9 mutant allele (termed BARA/LIN-9 $\Delta$ 84) that expresses a truncated protein in mouse. Homozygous mutant mice were viable. This truncated LIN9 protein rescued defects associated with a CDK4 knockout mouse including growth retardation, infertility and a decreased proliferation rate of MEFs (Sandoval et al., 2006). However, questions concerning the role of LIN9 in tumorigenesis, and differentiation as well as its cell cycle regulation potential remained unclear. This is probably due to the fact that the knockout approach resulted in only a partial knockout that deleted solely the first 84 amino acids of LIN9. However nothing is known about the other LINC *in vivo* so far.

Since we were able to identify homologues of all subunits of the dREAM/synMuvB complex in the human and mouse genome, and studied LIN-9 in detail, it is of immense interest to investigate LIN-9 and subsequently the function of LINC in mouse models. This could also shed light on LIN-9 physiological function in differentiation and tumorigenesis.

## 1.3 Mouse Models for known Cell Cycle Regulators

LINC regulates the expression of genes whose products are important for mitosis entry, progression and exit, such as Bub1, Birc5, cyclin A2, cyclin B1 and cdc2 (CDK1). As the aim of this study was to analyze the role of LIN9 in mouse development, the roles of LINC target genes in development, as it is known from knockout studies in mice, are described in the following section and summarized in table 1.3.

Additionally, an analysis about major LINC components in development, such as B-Myb, E2F4 and the pocket proteins is included. For further understanding of embryogenesis pre-/peri- and post-implantation development will be briefly explained.

### 1.3.1 Embryonic Development

At the beginning of embryonic development, the fertilized oocyte divides and starts to differentiate on its way to the uterus. The mature oocyte contains abundant amounts of RNA, proteins and ribosomes, some of which last until the early blastocyst stage (Gardner, 1996; Schultz, 1993). Maternal factors are probably responsible for the earliest events of embryogenesis, such as the first embryonic transcription, zygotic gene activation (ZGA), (Nothias et al., 1995; Schultz, 1993). ZGA occurs during the second cell cycle and is followed by major gene activation (MGA) during the third division (Aoki et al., 1997; Ram and Schultz, 1993; Wang and Dey, 2006).

Early development is characterized by a series of cleavages, which are fairly different to somatic cell cycles. After fertilization, the cell passes in 18 to 20 hours through S and M phase with a very short G1, and a nearly undetectable G2 phase (Howlett, 1986; Howlett and Bolton, 1985; Luthardt and Donahue, 1975) (Fig. 1.1 B). The second round of cell division at 1.5 dpc (days post coitus), resulting in four cells, is similar. The next four cell cycles each takes ~12 hours, from 8 blastomeres which asynchronously divide to the early blastocyst (~64 cell), at 3.5 dpc. The totipotent blastomeres of the compact morula loosen to form the blastocoel, a fluid filled cavity. The blastocyst consists of an outer layer, the multipotent trophoectoderm (TE) and the pluripotent inner cell mass (ICM). These are restricted tissue lineages, since the TE contributes only to the trophoblasts and extraembryonic ectoderm and the ICM disperses to the pluripotent epiblast, the multipotent primitive endoderm (PE) and extraembryonic mesoderm (Gardner, 1983) (Fig. 1.2).

The final pre-implantation cell division to the late blastocyst (~120 cells) takes ~24 hours (Bolton et al., 1984; Goldbard and Warner, 1982; Hogan, 1994). Peri-implantation defines the



stage in which the blastocyst hatches from the zona pellucida to implant into the uterine wall at day 4.5. This happens in three steps: apposition, attachment and penetration. The stroma differentiates into decidual cells which results in the decidual swelling (Hogan, 1994; Parr and Parr, 1989; Psychoyos et al., 1986). The TE layer gives rise mainly to trophoblast giant cells (TG), these mediate implantation and vascularization.

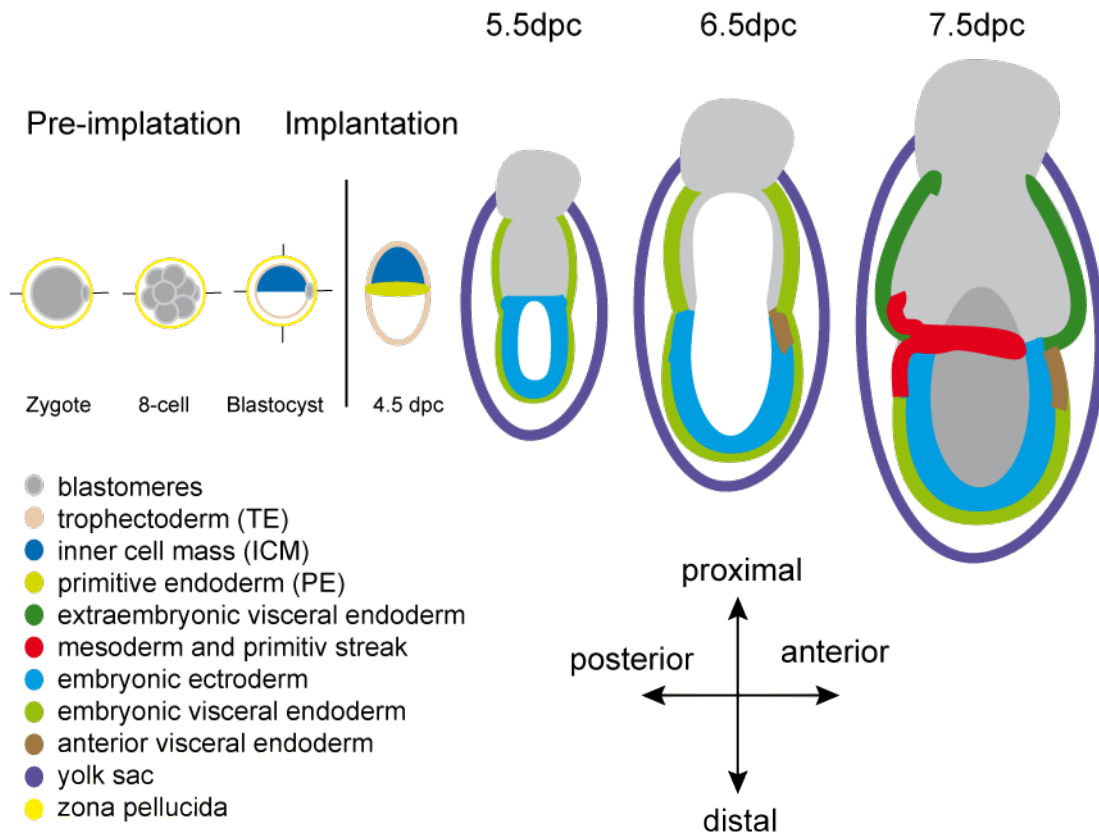


**Fig. 1.2: Mouse development from zygote to onset of primitive streak formation.** Schematic illustrations of embryonic development, the tissues are color labeled. The double-crossed arrows show the orientation of the proximal-distal and anterior-posterior embryonic axes (illustration based on (Pfister et al., 2007; Rivera-Perez, 2007)).

Next, in embryos 5.0 to 6.0 dpc, the polar TE develops into thick layers of extraembryonic ectoderm (ExE), which expands and bears distal the epiblast. Both ExE and the epiblast are enclosed by the visceral endoderm (VE) and the distal visceral endoderm (DVE), which are derived from the PE (Martin and Finn, 1968; Welsh and Enders, 1991). The epiblast as well as the PE will contribute to the extraembryonic mesoderm, which later forms the yolk sac, the allantois and the amnion. This formation becomes visible with the proamniotic cavity. The embryonic germ layers result in the assembly of the primitive streak and gastrulation at 6.5 dpc (Hogan, 1994).

The cell cycle speed starts to vary and largely increases during the subsequent gastrulation. This is especially obvious within the embryonic ectoderm, where the epiblast undergoes massive rearrangements such as primitive streak formation. Therefore cells move out of the

ectodermal layer, which has to proliferate rapidly to form the future embryonic mesoderm and endoderm. The cells in the proliferative zone display several distinct features. First their cycle tempo increases to only ~2 hours (Snow, 1977) with non-existent or very short G1 and G2 phases (Section 1.1.1). Second the cells populating primitive streak are smaller compared to their precursors, due to the short G1 phases, during which cellular growth usually occurs (Mac Auley et al., 1993). Third these pre-gastrulation cycles lack checkpoints that inhibit mitosis in the presence of DNA damage, these cells will rather die than arrest and repair (Heyer et al., 2000). However, the ExE tissue of the developing extraplacental cone does not undergo particularly rapid cycles (Hogan, 1994). Next, the germ layers form as gastrulation proceeds and organogenesis starts, at stage 7.5 to 9.5 dpc. The germ layers will contribute to all subsequent tissues.

## 1.3.2 Essential LINC Members

### 1.3.2.1. pRB/p107/130

The pocket protein family consists of three members, pRB, p107 and p130. They all represent major targets of cyclin D/CDK4/6 complexes (Sherr and Roberts, 1999; Sherr and Roberts, 2004). LINC binds to p130 in quiescent cells and then switches to p107 progressing to mitosis (Schmit et al., 2007).

The pocket proteins are differently expressed during mouse development. At pre-implantation stages pRb is absent, but expressed at blastocyst stage (Iwamori et al., 2002). Expression patterns of p107 and p130 at pre-implantation stages have not yet been studied. Later in embryogenesis, expression levels are restricted to selected tissues, e.g. in E13.5 only pRB is expressed in muscle, lens and retina, while the heart, lung, kidney and intestines express only p107. However, CNS and liver express all three pocket proteins (Jiang et al., 1997).

pRB belongs to the best studied tumor suppressor *in vivo*. There are several classical and conditional knockout approaches and chimeras generated with tetraploid complementation techniques. Some of these models are described below.

First the classical knockout model showed that mice lacking pRB die in utero at midgestation, due to severe anemia. pRB-deficient embryos have also obvious defects in lens development and massive cell death within the nervous system (Clarke et al., 1992; Jacks et al., 1992; Lee et al., 1992). These results strongly suggested a critical role for pRB in embryonic development.

Recently the phenotypes observed could be unraveled using the tetraploid complementation technique. This allowed Leone and his group to dissect the placental malformation from the abnormal embryonic development of pRB knockouts (Wu et al., 2003). These tetraploid pRB-deficient embryos developed to term. However they die soon after birth due to respiratory problems. However, none of the before examined defects in the CNS, nor other causes mentioned for embryonic lethality, were observed. Only defects in erythropoiesis persisted, though less severe, implying a delay in erythroid differentiation. New defects in skeletal muscle development were observed with these pRB newborns (Wu et al., 2003). Taken together, the vast majority of pRB knockout phenotypes are probably due to placental abnormalities.

Interestingly, mice mutants for either p107 or p130 revealed no obvious abnormalities, which is due to their redundant functions in most tissues (Cobrinik et al., 1996; Lee et al., 1996). However, this was only observed in knockout mice generated in the 129/Sv x C57BL/6 genetic background. p107 and p130 knockouts in the BALB/cJ background lead to severe phenotypes. p107-deficient weanlings display apparent growth retardation and myeloid hyperplasia, and MEFs display increased proliferation rates (LeCouter et al., 1998a). Furthermore, p130 mutant embryos died in utero between stage 11 to 13 dpc, in the BALB/cJ background, because of defects in neurogenesis and myogenesis (LeCouter et al., 1998b). These pronounced phenotypes are probably due to reduced p16INK4a activity in BALB/cJ mice (Zhang et al., 2001).

p107 and p130 double knockout animals, in the mixed genetic background, died immediately after birth (Cobrinik et al., 1996). Similar is the phenotype of mutants for pRB/p107 or pRB/p130, which died in utero between stage 11 to 13 dpc and showed obvious apoptosis in the liver and CNS (Lee et al., 1996). These observations indicated that the pocket proteins have redundant functions in development and substitute for each other. However, this may also be caused by pronounced placental defects observed for pRB knockout embryos.

| Gene name        | Gene symbol | k.o. | Survival                                  | Phenotype   | Function  | Expression   | Interesting facts   | References   |
|------------------|-------------|------|---|---|---|--|---|--|
| <b>Survivin</b>  | Birc5       | yes  | embryonic lethal E4.5                     | fail to hatch, blastomeres deteriorate, mitotic defects                       | apoptotic inhibitor & mitotic checkpoint                                    | ubiquit. until E11.5; later restricted to high proliferative tissue e.g. lung, CNS; largely absent in adults             | expressed in many common human tumors; brain dev. model   | Conway et al. (2002); Kawamura et al. (2002); Okada et al. (2004); Uren et al. (2000); Xing (2004)   |
| <b>Cdk1</b>      | Cdc2a       | yes  | embryonic lethal prior to E1.5            | essential for earliest cell cycle division in the absence of interphase       | interacts with Cyclin A & B from S to M phase                               | -  | only essential cell cycle CDK, drives solitary embryogenesis until midgestation, in k.o. for all other interphase CDKs (Cdk2, 3, 4 & 6)   | Santamaria et al. (2007)   |
| <b>Cyclin A2</b> | Ccna2       | yes  | embryonic lethal E5.5 to E6.5             | abnormal reminiscent implants E6.5  | entry in S & transition in M phase  | ubiquit.; in cell cycle dependent manner; from oocyte on   | unclear whether the unexpected long survival is due to maternal transcripts or redundancy   | Murphy et al. (1997)   |
| <b>Cyclin B1</b> | Ccnb1       | yes  | embryonic lethal before E10.5             | fail to develop, reason not exactly determined                                | entry & transition in M phase   | ubiquitously expressed from oocyte on  | represents an important regulator in M phases, overexpressed in most human cancer cells   | Brandiset al. (1995)   |
| <b>CENP-E</b>    | Cenpe       | yes  | embryonic lethal E4.5                     | if the blastocysts attach & develop smaller ICM                               | mitotic checkpoint  | cell cycle dependent   | Haploinsufficiency promotes or prevents tumorigenesis this is context dependent   | Putkey et al. (2002); Weaver et al. (2007)   |
| <b>Bub1</b>      | Bub1a       | yes  | embryonic lethal prior to E4.5            | cultured blastocysts developed no ICM but trophoblasts                        | mitotic checkpoint  | -  | defects in spindle assembly & chromosomal aberrations; co MEFs show decreased proliferation   | Jeganathan et al. (2007); Perera et al. (2007)   |
| <b>Aurora-A</b>  | Aurka       | no   | ?   | ?   | mitotic spindle assembly  | in oocytes & during meiotic maturation, fertilization & early cleavages  | overexpressed in a variety of cancers; overexpression in mice lead to mitotic defects & mammary hyperplasia, hence not to malignant transformation  | Yao et al. (2004)  |
| <b>Plk</b>       | Plk1        | no   | ?   | ?   | entry, spindle assembly & exit of mitosis                                   | in oocytes & during embryogenesis; in adult restricted to ovary & testis... associated with proliferative tissues        | overexpressed in a range of human tumors & coincides with bad prognosis; prognostic marker, RNAi experiments displayed cleavage failures  | Zahng et al. (2007)  |
| <b>B-myb</b>     | Mybl2       | yes  | embryonic lethal E3.5 to E6.5             | cultured blastocysts developed little or no ICM, but trophoblasts             | various functions in cell cycle progression, differentiation & apoptosis    | ubiquit. during development, highest in proliferative tissue   | co MEFs show decreased proliferation; k.o. in ES cells leads to G2/M arrest; new spindle complex Myb-Clafl  | Garcia et al. (2005); Iwai et al. (2001); Tanaka et al. (1999); Yamauchi et al. (2008)   |
| <b>pRB</b>       | Rb1         | yes  | embryonic lethal E12.5 to E15.5           | defects in erythroid, neuronal & lens dev.; severe abnormalities in placental | various functions in cell cycle progression & essential for differentiation | no expression in perimplantation stages, but in E3.5, later restricted to several tissues E13.5 lens, retina & muscle... | Tetraploid complementation resulted in completion of embryogenesis; best studied tumor suppressor   | Clarke et al. (1992); Jacks et al. (1992); Lee et al. (1992); Wu et al. (2003)   |
| <b>p107</b>      | Rb1         | yes  | viable (129/BL6); weanlings die (BALB/cJ) | retardation, myeloid hyperplasia  | cell cycle progression & differentiation                                    | restricted to E13.5 heart, kidney, lung & intestine  | p107 & p130 are redundant, MEFs show proliferation defects; double k.o. p107/130 neonatally lethal; double k.o. combinations with pRB die E11 to E13 due to placental defects; earlier death in BALB/cJ background probably due to the lack of p16INK4a | Cobrinik et al. (1996); LeCouter et al. (1998a); Lee et al. (1996); Robanus-Maandag et al. (1998); Cobrinik et al. (1996); LeCouter et al. (1998b) |
| <b>E2F4</b>      | E2f4        | yes  | die postnatally                           | arrested embryonic growth & defects in neurogenesis & myogenesis              | cell cycle progression & differentiation                                    | unknown in earlier stages, later in dev. & adult ubiquit. expressed  | susceptibility to bacterial infection; MEFs showed a decrease expression of E2Fs but cell cycle progression not altered   | Humbert et al. (2000); Rempel et al. (2000)  |

Tab. 1.3: LINC members, target genes and their functions in mouse.

Triple knockouts had not been generated, thus ES cells that lack all three pocket proteins were created and showed normal proliferation rates (Dannenberg et al., 2000; Sage et al., 2000). However, they had very limited, to no differentiation potential (Dannenberg et al., 2000). This indicated that ES cells do not necessitate pocket proteins for proliferation, but for differentiation (Dannenberg et al., 2000; Iwamori et al., 2002). Recent experiments showed that ES cells lacking Dicer1 are also unable to differentiate (Benetti et al., 2008; Sinkkonen et al., 2008). Factors like Oct4 are normally silenced for differentiation by DNA methylation of the promoter, accompanied by accumulation of repressive histone marks. These differentiation marks are only poorly initiated in dicer-deficient ES cells, probably due to p130 and other transcriptional repressors which are not properly downregulated, and therefore inhibit the expression of *de novo* DNA methyltransferases (Dnmts). This defect was reversible by reintroducing the miR-290 miRNAs (Sinkkonen et al., 2008).

#### 1.3.2.2. E2F4

One of the best understood functions of the pocket proteins is their binding to and thereby inhibiting the activity of E2F transcription factors during the cell cycle progression. E2F4 is one of the repressive E2Fs and also an important component of the LINC complex (Blais and Dynlacht, 2004; Schmit et al., 2007). E2F4 is constitutively synthesized (Sardet et al., 1995) and is widely expressed during mouse development (Dagnino et al., 1997a; Dagnino et al., 1997b).

The E2F4 knockout mice are neonatally lethal. They display noticeable growth retardations, hematopoietic, craniofacial and intestinal defects (Humbert et al., 2000; Rempel et al., 2000). This analysis of the mutant mice revealed that E2F4 plays an important role during the differentiation of certain cell lineages, such as the hematopoietic lineages. Analysis of the thymus in E2F4-deficient embryos showed an increase of immature cells, such as reticulocytes, nucleated erythrocytes, granulocyte precursors, and immature T-cells (Humbert et al., 2000; Rempel et al., 2000).

The analysis of E2F4 knockout MEFs revealed a dramatic decrease in the amount of total cellular E2Fs. Hence the expression of E2F target genes and cell cycle progression in general remained unaffected (Humbert et al., 2000).

E2F5, which is also a repressive E2Fs, leads as knockout to an early postnatal death caused by a hydrocephalus (Lindeman et al., 1998). Interestingly double knockouts E2F4 and E2F5 result in a late embryonic lethality post 13.5 dpc. At least one functional allele is required for postnatal viability, suggesting that the two E2Fs may play an overlapping function in

development (Gaubatz et al., 2000). Moreover, double mutant MEFs are resistant to cell cycle arrest in response to overexpression of the CDK inhibitor p16<sup>INK4a</sup>, which indicates a direct role for the repressive E2Fs in mediating cell cycle exit (Gaubatz et al., 2000).

### 1.3.2.3. B-MYB

The Myb family consists of three members, A-MYB, B-MYB (MYBL2) and C-MYB (Nomura 1988). All three members are transcription factors involved in the control of cell cycle progression, differentiation and apoptosis (Oh and Reddy, 1999; Sala, 2005). They have conserved regulation and transactivation domains that exhibit sequence-specific DNA-binding activity to the consensus sequence C/TAACNG (Ness, 2003; Ogata et al., 1994). Although they recognize the same binding sequence their expression patterns as well as knockout phenotypes are quite diverse.

C-Myb is mainly expressed in bone marrow and is essential to develop the hematopoietic cell lineage (Gonda and Metcalf, 1984). C-myb-deficient embryos are late embryonic lethal due to the failure of fetal liver haematopoiesis (Bender et al., 2004; Mucenski et al., 1991). A-Myb is required for spermatogenesis and in mammary gland proliferation. Hence, A-Myb knockout results in growth defects and male infertility (Toscani et al., 1997; Trauth et al., 1994).

In contrast, B-Myb is ubiquitously expressed during mouse development (Sitzmann et al., 1996), and elevated expression levels are detectable in brain, kidney, heart, skeletal muscle, testis and ovary. The observed expression is proportional to the degree of cell proliferation (Latham et al., 1996). B-Myb expression is induced by E2Fs and is highest at the G1/S transition. Moreover its activity is regulated by cyclin A/CDK2-mediated phosphorylation (Bessa et al., 2001; Garcia et al., 2005; Joaquin and Watson, 2003; Sala, 2005). B-Myb persists throughout the cell cycle and is essential for G2/M progression (Osterloh et al., 2007; Schmit et al., 2007; Zhu et al., 2004).

Knockout of B-Myb results in embryonic lethality at 4.5 to 5.5 dpc, shortly after implantation, due to failure in inner cell mass (ICM) formation (Tanaka et al., 1999). This phenotype suggests that B-Myb is crucial for growth of the ICM during the post-implantation phase. Based on studies in ES cells using an inducible dominant-negative form of Myb called MERT (C-Myb engrailed-estrogen receptor-tag), the faulty development is attributed to a defect in cell cycle progression through G1 (Iwai et al., 2001). Since B-Myb is known to be present in murine ES cells (Sitzmann et al., 1996), Tarsov and colleagues recently established a B-Myb shRNA approach in ES cells. They were able to show that B-Myb depletion leads to G2/M arrest and results in severe mitotic spindle and centrosome defects (Tarasov et al., 2008a;

Tarasov et al., 2008b). This seems to promote either differentiation coupled to apoptosis or generation of aneuploid ES cells. Furthermore, two other groups generated conditional B-Myb knockout mice and were also able to detect decreased proliferation abilities and genomic instabilities in knockout MEFs (Garcia et al., 2005; Yamauchi et al., 2008). Interestingly a new B-Myb complex was characterized termed Myb-Clafi. This complex contains clathrin and filamin, and is required for normal localization of clathrin to the mitotic spindle (Yamauchi et al., 2008).

## 1.4 Aim of this Project

From previous experiments we know that LINC regulates the transcription of many genes essential during the G2/M transition (Osterloh et al., 2007; Schmit et al., 2007). Homologue complexes in model organisms such as *Drosophila* and *C. elegans* regulate the transcription of developmental genes (Harrison et al., 2006; Korenjak et al., 2004). One evolutionary highly conserved and essential component of the LINC-core module is LIN-9. To deeper investigate the role of Lin9 in cell cycle and differentiation, *in vivo* and *in vitro*, the mouse was used as a model organism. The following analyses were performed:

First *Lin* expression was analyzed in adult mouse and during mouse development, in tissue samples and on sections, to examine whether the LINC components are expressed in mouse. For this, the necessary tools like *in situ* hybridization probes and protocols had to be established.

Second a Lin9 gene trap mouse model was obtained and analyzed to further understand the physiological role of Lin9. For the phenotypical examination histological and biochemical analyses were performed.

An additional important goal was to design and generate a conditional Lin9 knockout mouse model. To be able to knockout Lin9 in a more controlled manner and establish further inducible mouse models.

## 2 MATERIALS & METHODS

### 2.1 Materials

#### 2.1.1 Chemical Stocks & Reagents

| Chemicals   | Stock concentration              |
|---|----------------------------------|
| Ammonium Persulfate (APS)                         | 10% in H <sub>2</sub> O          |
| Ampicillin (Roth)                                 | 100 mg/ml in H <sub>2</sub> O    |
| Blasticidin (Invivogen)                           | 10 mg/ml in 10 mM Hepes, pH 7.4  |
| BM Purple AP Substrate (Roche)                    | ready to use                     |
| BrdU (Sigma)                                      | 32.5 mM in PBS                   |
| Bovine Serum Albumin (BSA)                        | 20 mg/ml                         |
| DAB with Metal Enhancer (Sigma)                   | ready to use                     |
| [ $\alpha^{32}$ -P]-dCTP (Hartmann Analytic)      | 50 $\mu$ Ci/ $\mu$ l             |
| DEPC (Roth)                                       | ready to use                     |
| DMSO p.a.   | Roth                             |
| DNA, MB grade (SS DNA)                            | Roche                            |
| dNTPs (Promega)                                   | 2 mM dATP, dCTP, dGTP, dTTP each |
| DTT (Invitrogen)                                  | 1 M in H <sub>2</sub> O          |
| Ethidium Bromide (Sigma)                          | 10 mg/ml in H <sub>2</sub> O     |
| ExpressHyb Hybridization Solution (Clontech)      | ready to use                     |
| Glutaraldehyd solution, Grade I, 25%              | ready to use                     |
| Glycogen (Invitrogen)                             | ready to use                     |
| 4-Hydroxytamoxifen (Sigma)                        | 10 mg/ml in PBS                  |
| Immobilized Protein G (Pierce)                    | ready to use                     |
| ImmunoPure Immobilized Protein A (Pierce)         | ready to use                     |
| IPTG Isopropylthio- $\beta$ -D-galactoside (Roth) | 1.0 M in H <sub>2</sub> O        |
| Kaisers Glygeringelantine (Merck)                 | ready to use                     |
| Levamisol (Sigma)                                 | 200 mM in H <sub>2</sub> O       |
| Luminol (Roth)                                    | 250 mM in DMSO                   |
| p-Coumaric acid (Sigma)                           | 90 mM in DMSO                    |
| PMSF (Phenylmethylsulphonyl-fluoride) (Roche)     | 10 mg/ml in isopropanol          |



| <b>Chemicals</b>   | <b>Stock concentration</b>   |
|--|--|
| Polybrene (Hexadimethrine bromide)                                     | 4 mg/ml in H <sub>2</sub> O  |
| Ponceau S solution   | 0.1% Ponceau S in 5% glacial acetic acid   |
| Propidium iodide (PI)  | 1 mg/ml in H <sub>2</sub> O  |
| Protease Inhibitors (PI) Mix   | 0.1 mg/ml Aprotinin<br>10 mg/ml AEBSF<br>0.5 mg/ml Bestatin<br>0.5 mg/ml E64<br>1 mg/ml Leupeptin<br>0.1 mg/ml Pepstatin |
| Proteinase K (Promega)   | 10 mg/ml in 50 mM Tris-HCl pH 8.0, 1 mM CaCl <sub>2</sub>  |
| ProtoGel, 30% (Biozym)   | ready to use   |
| Random Primer (Roche)  | 0.5 mg/ml in H <sub>2</sub> O  |
| RNase A  | 10 mg/ml in 10 mM Tris-HCl pH 7.4,<br>150 mM NaCl  |
| Roti®-Histokitt (Roth)   | ready to use   |
| Temed 99% p.a. (Roth)  | ready to use   |
| Trizol/Trifast/Total RNA Isolation Reagent (Invitrogen/Peqlab /Thermo) | ready to use   |
| tRNA (brewer's yeast) (Roche)  | 100 mg/ml in H <sub>2</sub> O (DEPC)   |
| X-gal (5-bromo-4-chloro-3-indolyl-β-D-galactopyranoside) (AppliChem)   | 20 mg/ml in DMF (N,N-dimethylformamide)  |
| XyloI (Roth)   | ready to use   |

Unless otherwise indicated, commonly used chemicals were purchased from AppliChem, Roth, Merck or Sigma with analysis quality.

## 2.1.2 PCR & DNA/RNA Modifying Enzymes

| <b>Enzymes</b>                    | <b>Company</b>          |
|-----------------------------------|-------------------------|
| Absolute QPCR SYBR Green Mix      | ThermoFisher            |
| Advantage cDNA PCR Kit            | BD Biosciences          |
| Advantage Genomic PCR Kit         | BD Biosciences          |
| Dnase I, RNase-free               | Roche                   |
| GoTaq® DNA Polymerase             | Promega                 |
| Long PCR Enzyme Mix               | Fermentas               |
| M-MLV-RT Transcriptase (100 U/μl) | Promega & Thermo Fisher |

| <b>Enzymes</b>                       | <b>Company</b>                                       |
|--------------------------------------|--|
| Phosphatase, alkaline (10 U/μl)      | Roche  |
| Phusion™ (2 U/μl)                    | Finnzymes  |
| qPCR Core kit for SYBR® Green I      | Eurogentec   |
| Random Primers DNA Labeling System   | Invitrogen   |
| Restriction endonucleases            | New England BioLabs (NEB),<br>Invitrogen & Fermentas |
| RiboLock (RNase-Inhibitor) (40 U/μl) | Fermentas  |
| SAWADY Taq-DNA-Polymerase            | peqLab   |
| T4-DNA-ligase (400 U/μl)             | NEB  |
| T7 & Sp6 & T3 RNA Polymerase         | Roche  |

### 2.1.3 Molecular Kits & Protein/DNA/RNA Markers

| <b>Kits</b>                           | <b>Company</b>      |
|---------------------------------------|---------------------|
| DIG RNA Labeling Mix                  | Roche               |
| In Situ Cell Death POD                | GENOMED             |
| JETSTAR Plasmid Midi-/Maxi-prep Kit   | GENOMED             |
| MassRuler™ DNA Ladder, Mix            | Fermentas           |
| NucleoSpin® Tissue XS Kit             | Macherey-Nagel (MN) |
| QIAquick® PCR Purification Kit        | Qiagen              |
| Page Ruler™ Prestained Protein Ladder | Fermentas           |
| ProbeQuant™ G-50 Micro Columns        | GE Healthcare       |
| RNA Ladder, Low Range                 | Fermentas           |
| TOPO-TA Cloning® Kit                  | Invitrogen          |
| Wizard Mini-/Midi-/Maxi-preps Kit     | Promega             |

### 2.1.4 Buffers

#### 2.1.4.1. General Buffers

10x PBS

130 mM NaCl  
 3 mM KCl  
 64 mM Na<sub>2</sub>HPO<sub>4</sub>  
 15 mM KH<sub>2</sub>PO<sub>4</sub>  
 adjust pH to 7.4 with HCl

## 50x TAE buffer

200 mM Tris base  
250 mM glacial acetic acid  
500 mM EDTA, pH 8.0

## 10x TBS

500 mM Tris-HCl, pH 7.4  
1500 mM NaCl

## 10x TE

100 mM Tris-HCl, pH 7.5  
10 mM EDTA

## 20x SSC

3 M NaCl  
0.3 M Na-Citrat  
adjust pH to 7.0 with NaOH

## 0.5 M EDTA pH 8.0

0.5 M EDTA  
adjust pH to 8.0 with NaOH pellets

## 3.0 M Sodium Acetate pH 5.8

3 M Na Acetate  
adjust pH to 5.2 with glacial acetic acid

## Miniprep-Solution S1

50 mM Tris-HCl, pH 8.0  
10 mM EDTA  
100 µg/ml RNase A

## Miniprep-Solution S2

200 mM NaOH  
1% SDS

## Miniprep-Solution S3

3.1 mM Potassium Acetate  
adjust pH to 8.0 with glacial acetic acid

## 5x DNA Loading buffer

15% Ficoll  
0.05% Bromphenol Blue  
0.05% Xylene Cyanol  
0.05 M EDTA

## 2x HBS

280 mM NaCl  
1.5 mM Na<sub>2</sub>HPO<sub>4</sub>  
50 mM HEPES-KOH, pH 7.05

**Lysis buffer (cultured cells)**

150 mM NaCl  
20 mM Tris pH7.5  
5 mM EDTA  
0.5% SDS  
250 mg/ml Proteinase K (added fresh)

**Tail buffer (mouse tails)**

100 mM TrisCl, pH 8.5  
5 mM EDTA  
0.2% SDS  
200 mM NaCl  
250 mg/ml Proteinase K (added fresh)

**Citrate buffer (TUNEL-staining)**

9 ml Solution A (0.1 M Citricacid  $C_6H_8O_7 \times H_2O$ )  
41 ml Solution B (0.1 M Natiumcitrat  $Na_3C_6H_5O_7 \times 2H_2O$ )  
ad 500 ml

**MOPS (RNA Gel)**

0.8 g Agarose  
54.8 ml  $H_2O$   
3.4 ml 20xMOPS

**20x MOPS pH7.5**

0.4 M MOPS  
0.1 M Sodium acetate  
100 mM EDTA

**2.1.4.2. Buffers for Southern Blot****Southern buffer I**

0.25 M HCl

**Southern buffer II (Denaturation Solution)**

1.5 M NaCl  
0.5 M NaOH

**Southern buffer III (Neutralization Solution)**

3.0 M NaCl  
0.5 M Tris Cl, pH 7.2

**Southern Wash buffer I**

3x SSC  
0.1% SDS

**Southern Wash buffer II**

1x SSC  
0.1% SDS

## Southern Wash buffer III

0.2x SSC  
0.1% SDS

## 2.1.4.3. Buffers for Immunohistochemistry

Hybridization Buffer Solution (HBS for *in situ* & WISH)

500 ml Formamid deionized  
65 ml 20x SSC  
10 ml EDTA [0.5 M]  
50 ml 10% CHAPS  
1 ml Heparin [100 mg/ml]  
2 ml Tween 20  
ad 1 l H<sub>2</sub>O (DEPC)

## NTMT

20 ml NaCl [5 M]  
50 ml MgCl<sub>2</sub> [1 M]  
100 ml Tris [1 M] pH9.5  
1 ml Tween 20  
ad 1 l H<sub>2</sub>O

## 1xMABT pH7.5

23.2 g Maleic acid  
17.5 g NaCl  
1.6 ml Tween 20  
ad 1.6 l H<sub>2</sub>O

## NTE

100 ml NaCl [5 M]  
10 ml Tris [1 M] pH7.5  
10 ml EDTA [0.5M] pH8.0  
ad 1 l H<sub>2</sub>O

## Proteinase K buffer

20 ml Tris [1 M] pH7.5  
2 ml EDTA [0.5 M]  
ad 1 l H<sub>2</sub>O (DEPC)

## Tris/Glycine buffer

12.1 g Tris  
7.5 g Glycine  
ad 1 l H<sub>2</sub>O (DEPC)

## 4% PFA (DEPC)

4% PFA in PBS  
adjust pH to 7.0 with NaOH

#### 2.1.4.4. Buffers for Western Blot

##### 10x SDS running buffer

0.25 M Tris pH 8.3  
1.92 M Glycin

##### ACK buffer

0.15 M  $\text{NH}_4\text{Cl}$   
1.0 M  $\text{KHCO}_3$   
0.1 mM  $\text{Na}_2\text{EDTA}$   
adjust pH to 7.2-7.4

##### Blotting buffer (1x)

0.6 g Tris base  
2.258 g Glycine  
150 ml Methanol  
ad 1 l  $\text{H}_2\text{O}$

##### Blocking solution

5% (w/v) milk powder in TBST

##### Luminol solution

10 ml Tris pH8.5 [100 mM]  
3  $\mu\text{l}$   $\text{H}_2\text{O}_2$  [30%]  
50  $\mu\text{l}$  Luminol [250 mM]  
22  $\mu\text{l}$  p-coumaric acid [90 mM]

##### Protease Inhibitors

1:200 PMSF [10 mg/ml]  
1:100 PI

##### Ponceau S

0.1% Ponceau S  
5% glacial acetic acid

##### Bradford solution

50 mg Coomassie Brilliant Blue G250  
23.75 ml Ethanol  
50 ml 85% ortho-phosphoric acid  
ad 500 ml  $\text{H}_2\text{O}$  filter twice

##### 3x Electrophoresis Sample Buffer (3x ESB)

300 mM Tris-HCl, pH 6.8  
15 mM EDTA  
150 mM DTT  
12% SDS  
15% Glycerol  
0.03% Bromphenol Blue

## 1% SDS TNN lysis buffer

50 mM Tris-HCl, pH 7.5  
 120 mM NaCl  
 5 mM EDTA  
 0.5% NP-40  
 10 mM Na<sub>2</sub>P<sub>2</sub>O<sub>7</sub>  
 2 mM Na<sub>3</sub>VO<sub>4</sub>  
 100 mM NaF

## 2.1.5 Oligolist

| Internal no.            | Name        | Product size (bp)             | Sequence 5' to 3'                      |
|-------------------------|-------------|-------------------------------|--|
| <b>Mouse genotyping</b> |             |                               |  |
| SG 893                  | Co (fw)     | co 298,<br>wt 192             | CCT GGC TGC CTA GCA TTT AC             |
| SG 894                  | Co (rev)    |                               | CCA GGC CAG GCT AAC ATT AC             |
| SG 657                  | β-gal (fw)  | 475                           | ACT GGC AGA TGC ACG GTT ACG ATG        |
| SG 658                  | β-gal (rev) |                               | CAC ATCTGAACTTCAGCCTCCAG               |
| SG 722                  | FRT (rev)   | co 498,<br>wt 624             | GCA AAA GCT GCA AGT CCT CT             |
| SG 506                  | FRT (fw)    |                               | AGT CTT GCC TGC ACA GGG A              |
| SG 930                  | BxB (fw)    | 400                           | GAG GAG AGG AGA GCA TAG CAC C          |
| SG 931                  | BxB (rev)   |                               | ACA TCT CCG TGC CAT TTA CCC            |
| SG 926                  | pMC-Cre2    | 400                           | GGC ATT TCT GGG GAT TGC                |
| SG 927                  | pMC-Cre3    |                               | CAG ACC AGG CCA GGT ATC TC             |
| SG 722                  | Δfl (rev)   | Δfl 289,<br>wt 541,<br>fl 770 | GCA AAA GCT GCA AGT CCT CT             |
| SG 893                  | Δfl (fw)    |                               | CCT GGC TGC CTA GCA TTT AC             |
| SG 913                  | Flp (rev)   | 725                           | CAC TGA TAT TGT AAG TAG TTT GC         |
| SG 914                  | Flp (fw)    |                               | CTA GTG CGA AGT AGT GAT CAG G          |
| SG 887                  | GT (rev)    | GT 215,<br>wt 302             | TAA AGT GTG GCC CAT CAC AA             |
| SG 885                  | GT (fw)     | GT 215                        | CCC ACT GAC CAG AAG GAA AG             |
| SG 662                  | GT (fw)     | wt 302                        | CCT GCT AGT CTA AAA TTT CTT TTG GT     |
| SG 644                  | GT 2 (rev)  | GT 776,<br>wt 620             | GCC CAA CAG TTA TCT TGT TTG TT         |
| SG 659                  | GT 2 (fw)   | wt 620                        | TGC CTG TGA AAC CAC TAC CA             |
| SG 711                  | GT 2 (fw)   | GT 776                        | CGA TTA AGT TGG GTA ACG CCA GGG<br>TTT |
| IMR0013                 | Neo         | 280                           | CTT GGG TGG AGA GGC TAT TC             |

| Internal no. | Name        | Product size (bp) | Sequence 5' to 3'          |
|--------------|-------------|-------------------|----------------------------|
| IMR0014      | Neo         |                   | AGG TGA GAT GAC AGG AGA TC |
| SG 928       | wt & ko p53 | 600               | ATA GGT CGG CGG TTC AT     |
| SG 929       | wt p53      |                   | CCC GAG TAT CTG GAA GAC AG |
| SG 175       | ko p53      |                   | CCG TCC TGT AAG TCT GCA GA |

#### Taqman primer and probes

|        |                |   |
|--------|----------------|---|
| SG 899 | lacZ/neo       | CGG TCG CTA CCA TTA CCA GT                |
| SG 900 | lacZ/neo       | CGT GCA ATC CAT CTT GTT CA                |
| SG 906 | lacZ/neo probe | FAM-TCA TAT TGG CTG CAG CCC GGG-BHQ-1     |
| SG 895 | ngf            | TGC ATA GCG TAA TGT CCA TGT TG            |
| SG 896 | ngf            | TCT CCT TCT GGG ACA TTG CTA TC            |
| SG 907 | ngf probe      | Hex-ACG GTT CTG CCT GTA CGC CGA TCA-BHQ-1 |

#### RT-qPCR

|        |         |     |                                   |
|--------|---------|-----|-----------------------------------|
| SG 785 | Lin9    | 94  | TTG GGA CTC ACA CCA TTC CT        |
| SG 786 | Lin9    |     | GAA GGC CGC TGT TTT TGT C         |
| SG 802 | Lin37   | 70  | GTA CCC CCG ATG ATG AAC CT        |
| SG 803 | Lin37   |     | CGT TGC ATG TTG CGA TAG AT        |
| SG 800 | Lin52   | 67  | GGT ACG AGG CCT ACA GAA CCT       |
| SG 801 | Lin52   |     | TCC CCT TGT CAT CTC TCT GG        |
| SG 798 | Lin54   | 69  | CCC CAG TGT AAA CAC ACA GC        |
| SG 799 | Lin54   |     | CAT CCG TAC AGG GGT GGT AT        |
| SG 820 | b-myb   | 70  | TTA AAT GGA CCC ACG AGG AG        |
| SG 821 | b-myb   |     | TTC CAG TCT TGC TGT CCA AA        |
| SG 854 | c-myb   | 62  | TGT CAA CAG AGA ACG AGC TGA       |
| SG 855 | c-myb   |     | GCT GCA AGT GTG GTT CTG TG        |
| SG 822 | a-myb   | 111 | GAA CTG ATG ATT GGA CTC TAA TTG C |
| SG 823 | a-myb   |     | TCC AAG GAC CCT TTA TCA ATT C     |
| SG 783 | Hprt    | 90  | TCC TCC TCA GAC CGC TTT T         |
| SG 784 | Hprt    |     | CCT GGT TCA TCA TCG CTA ATC       |
| SG 671 | GT lin9 | 88  | AGG ACG ATC GTT GCG TAT CT        |
| SG 969 | GT lin9 |     | GGG AGA TGA ACA CAG AAG CAG       |
| SG 967 | Fl lin9 | 80  | CAA AGA TCT CCC CGA TGA AA        |
| SG 968 | Fl lin9 |     | CAT CGT GAA TGC CAC GTA C         |



| Internal no.            | Name                 | Product size (bp) | Sequence 5' to 3'                 |
|-------------------------|----------------------|-------------------|-----------------------------------|
| <b>Classical RT-PCR</b> |                      |                   |                                   |
| SG 153                  | Lin9 (fw)            | 249               | ACT CAA GCT TCC CAA AGC AC        |
| SG 154                  | Lin9 (rev)           |                   | CTG ATT TTC TGC CGC TTC TG        |
| SG 670                  | Lin9 (fw)            | wt 178,<br>GT 426 | CGT TAG GAG GCT TTC CAG TG        |
| SG 671                  | Lin9 (rev)           | wt 178            | AGG ACG ATC GAA GCT TGC GTA TT    |
| SG 669                  | Lin9 (rev)           | GT 426            | GAC AGT ATC GGC CTC AGG AAG ATC G |
| SG 106                  | $\beta$ -actin (fw)  | 500               | TGT CAT GGT GGG AAT GGG TCA G     |
| SG 107                  | $\beta$ -actin (rev) |                   | TTT GAT GTC ACG CAC GAT TTC C     |
| <b>SB blot probes</b>   |                      |                   |                                   |
| SG 634                  | Probe C fw           | 332               | TGC TGT GTA GCC TCA GAT GG        |
| SG 635                  | Probe C rev          |                   | CCA GCT TTT CTG CTT CTG TG        |
| SG 739                  | Probe A fw           | 193               | TTG CAC ACC TGT GAA AAT GC        |
| SG 740                  | Probe A rev          | 193               | TTC TCT ACT TGA TTT CTC CCC TAG C |

### 2.1.6 Plasmidlist

| Internal no. | Name                      | Purpose                               |
|--------------|---------------------------|---------------------------------------|
| 822          | pBS lox lin9              | Conditional targeting vector          |
| 67           | pBS246 (loxP)             | LoxP backbone (Sauer, 1993)           |
| 694          | pBS-2FRT-Ires $\beta$ geo | FRT cassette (Mountford et al., 1994) |
| 838          | Topo Lin9 probe C         | Southern blot probe                   |
| 824          | Topo Lin9 probe A         | Southern blot probe                   |
| 729          | pYX-Asc IRAKp961F22132Q   | Lin9 cDNA                             |
| 754          | pCS2+ Lin9 B              | <i>in situ</i> probe                  |
| 839          | pCS2+ B-Myb               | <i>in situ</i> probe                  |
| 846          | pCS2+ Lin52               | <i>in situ</i> probe                  |
| 857          | pCS2+ Lin54               | <i>in situ</i> probe                  |
| 845          | pCS2+ Lin37               | <i>in situ</i> probe                  |
| 921          | pSport $\Delta$ Oct4      | <i>in situ</i> probe                  |
| 936          | pBSK+ H19                 | <i>in situ</i> probe                  |
| 937          | pBluescript Sox2          | <i>in situ</i> probe                  |
| 746          | pBabe-H2B-GFP             | Retroviral transfection/infection     |
| 915          | pMMP Hit & Run CreGFP     | Retroviral transfection/infection     |

## 2.1.7 Antibodies

### Primary antibodies

| Antibody                  | Company          | Origin                                    | Application    | Conc.   | Internal no. |
|---------------------------|------------------|---|----------------|---------|--------------|
| hLIN-9                    | Dauids Biotech   | Rabbit polyclonal (Osterloh et al., 2007) | IP             | 1:50    | # 136        |
|                           |                  |   | WB             | 1:500   | # 137        |
|                           |                  |   | WB             | 1:100   | # 81         |
| $\beta$ -Tubulin          | Chemicon MAB3408 | Mouse monoclonal (1 mg/ml)                | WB             | 1:5000  | # 102        |
| IgG                       | Sigma I5006      | Rabbit polyclonal (1 mg/ml)               | IP             | 1:500   | # 104        |
| $\alpha$ DIG-AP conjugate | Roche            |   | <i>in situ</i> | 1:5 000 | non          |

### Secondary antibodies

| Antibody                  | Company  | Application | Concentration |
|---------------------------|----------|-------------|---------------|
| Anti-mouse HRP-linked     | Amersham | WB          | 1:5000        |
| Anti-protein A HRP-linked | Amersham | WB          | 1:5000        |

## 2.1.8 Cell Lines & Cell Culture Media

| Media components                        | Company   |
|---|---|
| DMEM (4.5 g Glucose/L-Glutamine)        | Cambrex   |
| Penicillin/Streptomycin (10 U/ $\mu$ l) | Cambrex   |
| Trypsin (EDTA) (200 mg/l)               | Cambrex   |
| Trypsin (EDTA) 0.25%                    | Invitrogen  |
| Foetal Bovine Serum (FCS)               | Invitrogen  |
| NEAA (nonessential amino acids)         | Lonza   |
| $\beta$ -Mercaptoethanol                | Roth  |
| LIF (Leukemia Inhibitory Factor)        | AG Gessler  |
| Cell lines                              | Media composition   |
| MEFs                                    | DMEM + 10% FCS + 1% PenStrep  |
| Plat-E                                  | DMEM + 10% FCS + 1% PenStrep  |
| ES media for Blastocysts                | DMEM + 10% FCS + 1% PenStrep + 1% NEAA + 50 $\mu$ M $\beta$ -mercaptoethanol + 1.2% LIF |

## 2.1.9 Bacterial Strains

| <b>E.coli</b> | <b>Description</b> |   | <b>Reference</b> |
|---------------|--------------------|---|------------------|
| DH5 $\alpha$  | chemical competent | SupE44, $\Delta$ lacU169 ( $\phi$ 80lacZ $\Delta$ M15), hsdR17, recA1, endA1  | (Hanahan, 1983)  |
| Top10         | chemical competent | F <sup>+</sup> The Role mcrA $\Delta$ (mrr-hsdRMS-mcrBC) $\phi$ 80lacZ $\Delta$ M15, $\Delta$ lacX_74, recA1, deoR, araD139, $\Delta$ (ara-leu)7697, galU, galK, rpsL, (Str <sup>R</sup> ), endA1, nupG | Invitrogen       |

## 2.1.10 Mouse Strains & ES Cell Lines

| <b>Inbred strains</b>       | <b>Outbred strain</b>                         |
|-----------------------------|---|
| 129/OlaHsd (129P2)          | CD-1  |
| C57BL/6                     | <b>ES cell lines:</b>                         |
| FVB/NHanHsd (UK)            | GT: E14TG2a (RR1306 GT Lin9) (BayGenomics)    |
| B6-SJL-Tg(ACTFLPe)9205Dym/J | Co: 129/SvEvTaq TC-1 (PolyGene Transgenetics) |
| B6-ROSA26-CreERT2           |   |

## 2.1.11 Microscopic equipment

| <b>Binocular/microscope</b> | <b>Company</b> |
|-----------------------------|----------------|
| SMZ1500 (HR Plan APO 1x)    | Nikon          |
| Axiovert 100                | Zeiss          |
| Inverted Microscope         | Leica          |
| Camera                      |                |
| Axio Cam Color HRc          | Zeiss          |
| DFC350 FX                   | Leica          |

## 2.2 Methods

### 2.2.1 Cell Culture

#### 2.2.1.1. Generation of MEFs

Murine embryonic fibroblasts (MEFs) were gained from 13.5 dpc embryos from timed pregnancies. Embryos were prepared in PBS and continuously rinsed in PBS. The yolk sac, placenta, head, and the blood containing organs were removed. For genotyping by PCR the heads were further processed. They were incubated at 55°C in 300 µl tail buffer plus 20 µl Proteinase K (10 mg/ml), shaking o/n. The following day, the samples were heat inactivated for 10 min at 95°C and stored at -20°C until genotyping. The remaining body was cut up into small pieces with razorblades, in a 10 cm dish containing 2 ml 0.25% Trypsin and was incubated for 10 min at 37°C, 5% CO<sub>2</sub>. Next, 2 ml of fresh Trypsin were added, the cells were separated by pipetting them up and down, and incubating for 10 min. Then, 6 ml cell culture medium was added and the cells were transferred into falcon tubes and centrifuged for 10 min at 1200 rpm. Finally, the supernatant was discarded and the cell pellet was resuspended in 10 ml fresh media in 10 cm dishes. The following day, these cells (passage 0) were split 1 to 4 (passage 1). One or two days later, when the cells were grown to 90-100% density, they were trypsinized and frozen (passage 2).

#### 2.2.1.2. Passageing of Cells

MEFs were cultivated in 10 cm cell culture dishes in a tissue culture incubator at 37°C and with 5% CO<sub>2</sub>. For passageing, the cells were washed twice with PBS and shortly incubated with 1 ml in Trypsin/EDTA at 37°C. The detached cells were replated in new media and culture dishes. The standard splitting ratio was 1 to 4.

#### 2.2.1.3. Freezing & Thawing of Cells

##### Freezing

To freeze cells, they were first trypsinized (MM 2.2.1.2). Then 5 ml of medium were added and transferred into 15 ml falcon. Next, they were centrifuged for 5 min at 1000 rpm, the supernatant was discarded and 1 ml ice cold freeze medium (DMEM media containing 10% DMSO) was added. Pellets were resuspended and transferred into cooled cryotubes. Cells were stored at -80°C for short term, or in liquid nitrogen for long term.

## Thawing

Cells were quickly thawed in a 37°C water bath. The cell suspension was mixed with 9 ml fresh medium and centrifuged for 5 min at 1000 rpm. The supernatant was discarded and pellets were resuspended in 10 ml fresh medium and seeded into 10 cm dishes.

### 2.2.1.4. Transient Transfection of Plat-E Cells

For the production of ecotrophic viral supernatant, Plat-E cells carrying the ecotrophic receptor were transiently transfected with the plasmid of interest (Morita et al., 2000). Plat-E cells were plated at a density of  $5 \times 10^6$  per 10 cm dish. The following day, they were transfected using Calcium/Phosphate. Therefore 30  $\mu$ g of plasmid was precipitated with 50  $\mu$ l of 2.5 M  $\text{CaCl}_2$  in a final volume of 500  $\mu$ l with  $\text{H}_2\text{O}$ . 500  $\mu$ l of 2x HBS was continuously bubbled while DNA/ $\text{CaCl}_2$  mixture was added. This solution was carefully added to the cells. After circa 16 h of incubation, cells were washed with PBS and fed with fresh medium. 48 h after transfection, the viral supernatant was harvested twice in 12 h intervals and used immediately, collected at 4°C on ice or frozen in liquid nitrogen and stored at -80°C until infection.

### 2.2.1.5. Infection of MEFs

For retroviral infection, MEFs were plated at a density of  $6.5 \times 10^5$  per 10 cm dish. The next day, the cells were infected with a retrovirus carrying an expression construct for Cre-recombinase. For the infection, the viral supernatant was filtered (0.45  $\mu$ m), mixed with Polybrene at a final concentration of 10  $\mu$ g/ml and added to the cells. The first infection took place for approximately 16 h, then a second round for another 8 h. After infection, the cells were fed with fresh medium.

### 2.2.1.6. Tamoxifen Induction of Cre

Wild type and floxed MEFs additionally harboring an expression construct for Cre-recombinase fused to the mutated ligand-binding domain of the human estrogen receptor (Cre-ER<sup>T2</sup>) were used. These MEFs were plated in passage 3, at a density of  $5.5 \times 10^5$  cells per 10 cm dish. To induce the deletion of the floxed allele, cells were cultured for 48 h in medium containing 1  $\mu$ M 4-hydroxytamoxifen (4-OHT). After ~60 h recovery in fresh media the cells were harvested for further experiments.

### 2.2.1.7. Growth Curve

To determine cell growth and proliferation ability,  $1 \times 10^4$  and  $0.5 \times 10^4$  MEFs were plated in triplicates in several 24-well plates. At interval of approximately every 24 h, one of the plates was fixed. For fixation, cells were rinsed with PBS, incubated with 3.7% formaldehyde for 10 min and air dried. The different time points were collected. Finally, the cells were stained with crystal violet (solved in 20% ethanol), for 30 min at RT and rinsed with tap water. The dye was extracted with 0.5 ml 10% acetic acid per well. 100  $\mu$ l of each extract was transferred into a microtiter plate and absorption at 590 nm was measured with an Elisa reader. Mean values of the absorption were plotted against time.

### 2.2.1.8. Determination of Cell Cycle Phases

For flow cytometry measurement (FACS), the cells were harvested by trypsinization (MM 2.2.1.2), washed with PBS, fixed with 1 ml 80% ethanol and incubated o/n at  $-20^\circ\text{C}$ . The centrifugation was performed for 5 to 10 min at 1200 rpm, at  $4^\circ\text{C}$ . Next the cells were washed with PBS and resuspended in 500  $\mu$ l 38 mM NaCitrate plus 25  $\mu$ l RNase A (10 mg/ml). The cells were incubated for 1-2 h at  $37^\circ\text{C}$ . Finally they were stained with 30  $\mu$ l Propidium Iodide (1 mg/ml) and measured by FACS.

### 2.2.1.9. Culturing of Blastocysts

To isolate blastocysts the uterine horns with the oviducts and the cervix were dissected from pregnant mice at day 3.5. A syringe with a 2 ml volume and a 22 gauge needle was used to flush the uterus horns with PBS or ES media. The liquid filled uterus was hold with forceps and cut open with scissors. The solution was collected in small cell culture dishes and the blastocysts were collected in PBS drops. Therefore the binocular and long thin glass capillaries were used. Each blastocyst was transferred through several PBS drops. The 4-well plates were coated with 0.2% Gelatin/PBS. Each blastocyst was separately grown in 500  $\mu$ l ES media in a tissue culture incubator at  $37^\circ\text{C}$  with 5%  $\text{CO}_2$  and documented every 24 h.

## 2.2.2 Molecular Methods

### 2.2.2.1. Isolation of RNA from Cultured Cells

Total RNA was isolated from cultured cells with TRIzol reagent. After removing the medium, e.g. from 6-well dishes, 0.5 ml TRIzol was added. The cells were scraped, transferred into a reaction tube and mixed with 100  $\mu$ l  $\text{CHCl}_3$ . After vortexing the solution was centrifuged at 11400 g for 10 min at  $4^\circ\text{C}$ . The upper aqueous phase was precipitated with 500  $\mu$ l

isopropanol. After a short incubation on ice, the sample was centrifuged at 11400 g for 15 min at 4°C. The pellet was washed with 75% ethanol and resuspended in 25-50 µl H<sub>2</sub>O (DEPC).

#### 2.2.2.2. Isolation of RNA from Mouse Organs

Circa 80-100 mg tissue was prepared, transferred into 2 ml reaction tubes and frozen in liquid nitrogen (for long term storage: tissue samples were frozen at -80°C). To proceed, 1 ml TRIzol reagent was added. Next homogenization with an Ultra-Turrax was performed, twice for 1 min with a 1 min break on ice. (Optional for protein rich tissues, like muscle and fat, the insoluble material was removed through centrifugation.)

The homogenate was incubated for 5 min and 2 min at RT, in between 200 µl CHCl<sub>3</sub> were added and vortexed for 15 sec. After centrifugation at 11400 g for 15 min at 4°C, the upper colorless aqueous RNA containing phase was transferred into a new tube.

To precipitate the RNA, 500 µl isopropanol were added and the samples were incubated for 10 min at RT. After centrifugation at 11400 g for 15 min at 4°C, the RNA pellet was washed with 1 ml 75-80% ethanol. Finally the pellet was air dried for 10 min and solved in 25-50 µl H<sub>2</sub>O (DEPC). The RNA was incubated for 10 min at 60°C and quantified at 260 nm.

#### 2.2.2.3. Isolation of Plasmid DNA from Bacteria

After transformation, single colonies from an LB agar plate were picked and incubated in 3 ml LB media containing ampicillin in a shaker at 37°C o/n. The following day, 1.5 ml bacterial solution was pelleted and resuspended in 200 µl S1. The bacteria were lysed by adding 250 µl S2 and incubating them for 5 min. This reaction was neutralized with 250 µl S3. The bacterial debris were pelleted by centrifugation for 10 min at full speed. The plasmid DNA in the supernatant was precipitated with 700 µl isopropanol and centrifugation for 30 min at 4°C. The plasmid pellet was washed with 1 ml 75% ethanol and air dried for 10 min. The plasmid DNA was resuspended in 40 µl TE and the correct plasmids were identified by restriction digest.

#### 2.2.2.4. Isolation of DNA Fragments from Agarose Gels

Plasmid DNA was incubated at 37°C with the desired restriction endonuclease for approx. 2 h. The sample was loaded on a 0.8 to 1.2% agarose gel and the fragments were separated by electrophoresis at 100 Volt for about 1 h. The desired bands were excised and the DNA was eluted with JetStar gel extraction kit (Genomed) according to the manufacturer's manual.

### 2.2.2.5. Extraction of gDNA from Cells

The cells, e.g. cultured in 6cm dishes, were washed once with PBS and incubated with 500  $\mu$ l Lysis buffer (plus Proteinase K) for 30 min at 37°C. Next the lysate was transferred into tubes and mixed with 500  $\mu$ l Phenol/ $\text{CHCl}_3$ . After centrifugation for 3 min at full speed, the upper aqueous phase was transferred into a new tube, mixed with 500  $\mu$ l  $\text{CHCl}_3$  and again centrifuged. The DNA containing upper phase was again transferred and precipitated by adding 50  $\mu$ l 3 M NaAc pH5.8 and 500  $\mu$ l isopropanol. After incubation for 20 min at -20°C the sample was centrifuged for 30 min at full speed at 4°C. The supernatant was discarded and the pellet was washed with 1 ml 70-75% ethanol. The final DNA pellet was air dried for 10 min and solved in 50  $\mu$ l TE.

### 2.2.2.6. Extraction of gDNA in Small Scale

NucleoSpin® columns for small tissue samples (Macherey-Nagel) were used to isolate gDNA of either cultured blastocysts or paraffinated fixed 7.5 dpc embryos on sections. Isolation was performed according to the manufacturer's manual. The resulting gDNA was genotyped with TaqMan qPCR.

gDNA from blastocysts directly after isolation was prepared as follows: the blastocysts were transferred through several drops of PBS (MM 2.2.1.9), incubated for 2 h at 65°C in 2  $\mu$ l Tail buffer and inactivated at 95°C for 10 min. Next the solution was diluted 1:5 and TaqMan qPCR was performed with 3  $\mu$ l per reaction.

### 2.2.2.7. Extraction of gDNA from Tails for Southern Blot

The mouse tails were digested in 300  $\mu$ l Tail buffer at 55°C shaking o/n. The following day the samples were heat inactivated for 10 min at 95°C.

#### Phenol/ $\text{CHCl}_3$ Extraction

First 300  $\mu$ l Phenol/ $\text{CHCl}_3$  were added and inverted for 40 times. Next the samples were centrifuged for 3 min at full speed at RT. The supernatant was transferred into a new tube, again 300  $\mu$ l  $\text{CHCl}_3$  were added and centrifuged for 3 min at RT.

#### Ethanol Extraction

The supernatant was transferred into a new tube, and 1/10 volume 3 M NaAc plus 2 1/2 volume 100% ethanol were added. The solution was inverted until the DNA formed a visible clump. Next the solution was centrifuged for 15-30 min at full speed and 4°C. After discharging the supernatant, the pellet was washed with 1 ml 70% ethanol and centrifuged



for further 10 min. The resulting pellet was air dried and eluted in 50-100  $\mu$ l H<sub>2</sub>O. To rehydrate the gDNA the sample was incubated at 4°C o/n or 10-30 min at 55-65°C. 0.5  $\mu$ l gDNA were used for PCR and 10  $\mu$ g for Southern Blot.

### 2.2.2.8. Standard Cloning Method

#### Restriction

Restriction from plasmid DNA and PCR fragments was performed with an adequate restriction endonuclease. As standard preparative set up, 5  $\mu$ g plasmid DNA was mixed with 5 to 10 Units Enzyme and the appropriate buffer in a 50  $\mu$ l volume and incubated for approximately 3 h at 37°C. The resulting DNA fragments were either directly isolated with ethanol precipitation or separated on an agarose gel (MM 2.2.2.4 & 2.2.2.7). Optionally the vector ends were dephosphorylated with calf intestine alkaline phosphatases (CIPed), e.g. for subsequent ligation with only one restriction site.

#### Proofreading PCR

To generate DNA fragments for cloning, the more specific proof reading polymerases were used for PCR amplification. To clone directly or for subsequent preparative restrictions a 50  $\mu$ l PCR mixture was set up, according to the manufacturer's manuals, e.g. Phusion™ (Finnzymes), Advantage Genomic PCR Kit or Advantage cDNA PCR Kit (BD). The PCR products were either directly isolated with ethanol precipitation, QIAquick® PCR Purification Kit (Qiagen) or separated on an agarose gel (MM 2.2.2.4). If needed the PCR product was restricted. As alternative, the PCR was directly processed with the TOPO-TA Cloning® Kit (Invitrogen).

#### Ligation

Classical ligation was performed with T4-DNA-ligase (NEB) in a molar ratio of 1:3 (vector to insert). The mixture was set up in a 10  $\mu$ l volume, with 1 Unit T4-ligase and ~50 ng vector DNA. The samples were incubated at RT o/n.

#### Transformation (heat shock)

DH5 $\alpha$  or Top10 chemical competent bacterial cells were used for transformation. The bacterial cells were thawed on ice for about 10 min. The 10  $\mu$ l ligation reaction was mixed with 50  $\mu$ l bacteria and incubated for 20 min on ice. Next the tube was heat shocked for 2 min at 42°C and cooled on ice. After addition of 500  $\mu$ l cold LB-media (without Amp.), the sample was incubated for 40 min vigorous shaking at 37°C. The bacterial cells were

centrifuged for 1 min at 8000 rpm and the supernatant was discarded. The pellet was plated on LB-agar plates and incubated at 37°C o/n. The colonies were picked for plasmid isolation and restriction analysis (MM 2.2.2.3).

#### 2.2.2.9. Tail PCRs (basic protocol)

Tail PCRs for genotyping were performed with the lysed tails, still in Tail buffer (MM 2.2.2.7), but without Phenol/CHCl<sub>3</sub> extraction. As standard, 0.3 µl of tail gDNA, 2.5 µl dNTPs [2 mM] and 1.0 µl of forward and reverse primer [10 µM] were added to a 25 µl PCR-mixture (according to the manufacturer's manual, e.g. GoTaq® DNA Polymerase (Promega)). For PCR mixtures, the number of samples plus 1 was prepared and tail gDNA was added.

PCR program (30 cycles):

94°C 30 s  
58-60°C 1 min  
72°C 1 min

The annealing temperature for each primer set was calculated with oligo calculator (Appendix 7.2). The samples were mixed with 2 µl gel loading buffer and loaded on a 1% agarose gel for 60 min at 110 Volt.

#### 2.2.2.10. Reverse Transcription

To transcribe RNA into cDNA 2.0 µg RNA was mixed with 0.5 µl random primers (0.5 µg/µl) and brought to a final volume of 10 µl with H<sub>2</sub>O (DEPC). This mixture was incubated for 5 min at 70°C and chilled on ice. The following mixture was added:

5 µl M-MLV 5x reaction buffer  
6.25 µl dNTPs [2 mM]  
0.5 µl Ribolock RNase inhibitor [40 U/µl]  
0.5 µl M-MLV-RT [100 U]  
1.75 µl H<sub>2</sub>O (RNase-free)

The samples were incubated for 60 min at 37°C and inactivated for 15 min at 70°C.

### 2.2.2.11. Quantitative PCR

To determine the amount of a specific mRNA compared to a housekeeping gene, the following reaction was prepared with the Absolute QPCR SYBR Green Mix (ThermoFisher):

12.5  $\mu$ l Absolute QPCR SYBR Green Mix  
 10.5  $\mu$ l H<sub>2</sub>O  
 1  $\mu$ l Primer Mix [10  $\mu$ M]  
 1  $\mu$ l cDNA

PCR program (40 cycles):

95°C 15 min  
 95°C 15 s  
 60°C 1 min

The relative expression of a gene compared to a housekeeping gene was calculated with the following formula:  $2^{-\Delta\Delta Ct}$

with  $\Delta\Delta Ct = \Delta Ct$  (sample) –  $\Delta Ct$  (reference)

and  $\Delta Ct = Ct$ (gene of interest) –  $Ct$  (housekeeping gene)

The standard deviation of  $\Delta\Delta Ct$  was calculated with:  $s = \sqrt{(s_1^2 + s_2^2)}$

with  $s_1$  = standard deviation (gene of interest)

and  $s_2$  = standard deviation (housekeeping gene)

The margin of error for  $2^{-\Delta\Delta Ct}$  was determined by this formula:  $2^{-\Delta\Delta Ct \pm s}$

and the error used for the error bars was calculated with:  $\text{error} = 2^{-\Delta\Delta Ct + s} - 2^{-\Delta\Delta Ct}$

Standard deviation, error margins and error were calculated as shown above.

### 2.2.2.12. TaqMan

TaqMan probes were labeled with a standard reporter fluorophore opposite to a black hole quencher. The polymerase which carries a 5'-exonuclease activity will degenerate the annealed probe while synthesizing the complementary strand. This leads to a separation of the two dyes and the extinction of the reporter fluorophore will be set free and measured. Additionally using two different dyes made it possible to run the TaqMan qPCR in one reaction.

| Probe    | Dye        | Extinction       | Purpose (compare MM 2.1.5)  |
|----------|------------|------------------|---|
| ngf      | Hex/ BHQ-1 | 535 nm           | Normalization   |
| lacZ/neo | FAM/ BHQ-1 | 492 nm<br>(SYBR) | GT specific probe at the lacZ/neo border within the integrated gene trap vector (compare to Fig. 3.5) |

The annealing efficiency for the specific primers for ngf and lacZ/neo was measured with the linear increase (slope) of amplification. This was calculated with  $E = 10(1/\text{slope})$  (Pfaffl-method). The difference between having one or two alleles should be approximately 1  $\Delta Ct$ .

The following reaction was prepared (qPCR Core kit for SYBR® Green I (Eurogentec)):

5  $\mu$ l 10x Reaction Buffer  
2  $\mu$ l 50x dNTPs [5 mM]  
3.5  $\mu$ l MgCl<sub>2</sub> [50 mM]  
2  $\mu$ l Primer Mix 1 [10  $\mu$ M]  
2  $\mu$ l Primer Mix 2 [10  $\mu$ M]  
0.5  $\mu$ l Probe 1 [20  $\mu$ M]  
0.5  $\mu$ l Probe 2 [20  $\mu$ M]  
0.25  $\mu$ l Hot GoldStar enzyme  
31.25  $\mu$ l H<sub>2</sub>O  
3  $\mu$ l blastocyst gDNA (MM 2.2.2.6)

The qPCR reaction was run in the “Quantitative PCR (multiple standards)” modus.

PCR program (40 cycles):

95°C 10 min  
95°C 15 s  
60°C 1 min

### 2.2.2.13. Southern Blot with Radioactively Labeled Probes

#### DNA Preparation

Approximately 10  $\mu$ g gDNA were incubated with the desired restriction endonuclease o/n. The following day this gDNA was separated by electrophoresis in a thin 0.6% agarose gel at 60 Volt for about 5-6 h. To document the fragment sizes the gel was photographed with an UV-sensitive ruler laid alongside the gel.

#### Gel Treatment

The gel was treated as follows, completely covered with liquid and shaking at RT: first rinsed in H<sub>2</sub>O and incubated in Southern buffer I for 30 min (until the bromphenol blue of the loading buffer turned yellow); second rinsed in H<sub>2</sub>O and incubated in Southern buffer II for 20 min; third rinsed in H<sub>2</sub>O and incubated in Southern buffer III for 20 min (the bromophenol blue returned to its blue color); finally rinsed in H<sub>2</sub>O.

#### Set up of the Blotting Stack

To equilibrate, the nylon membrane (Hybond N+) was rinsed with H<sub>2</sub>O and incubated in 20x SSC for 10 min. The blotting stack was assembled onto a dish filled with 20x SSC with a bridge of Whatman paper (Fig. 2.1). As blot 3-5 Whatman sheets, the agarose gel, the equilibrated membrane, several Whatman sheets and a 5-10 cm stack of paper towels were assembled. Each layer was soaked in 20x SSC and air bubbles were removed with a plastic pen, rolling over the surface. On top of the stack was a glass plate with a ~0.25 kg weight arranged. The stack was left o/n. The next day, the membrane was recovered and the position

of the gel pockets was marked on the membrane. The membrane was rinsed in 6x SSC and air dried. The DNA transfer was controlled with an UV-lamp.

The membrane, DNA side up, was incubated in the UV-Stratalinker, program C-3 [150 mJ] to cross-link the DNA. This way it can be stored dry and dark in a plastic bag until usage.

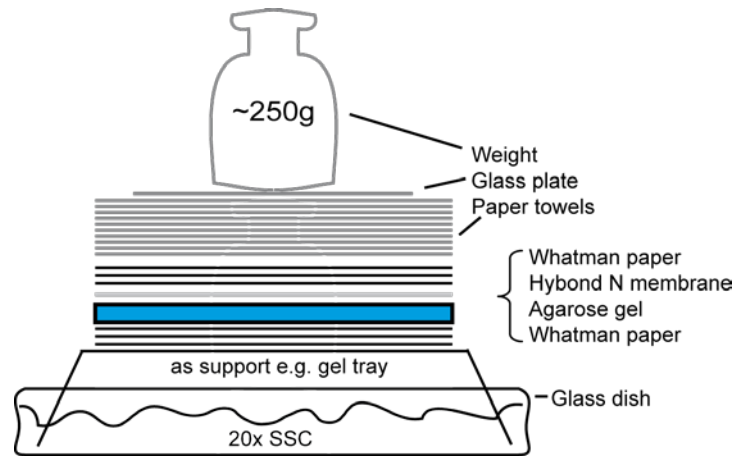


**Fig. 2.1: Set up of the blotting stag for Southern blot.**

## Pre-Hybridization

For pre- and hybridization, the hybridization solution ExpressHy™ (Clonetechn) was used. The membrane was pre-hybridized with 10 ml hybridization solution at 60°C for 1-2 h, on a rotating wheel.

## Labeling

To generate probes, either PCR products or isolated plasmid fragments were used and labeled with Random Primer DNA Labeling Kit (Invitrogen). 25 ng of DNA fragments were labeled with  $^{32}\text{P}$  dCTP [ $\sim 50 \mu\text{Ci}$ ] for 1 h at RT, according to the manufacturer's manual.

To remove the unincorporated labeled nucleotides ProbeQuant™ G-50 Micro Columns (Amersham) were used. The column resin was resuspended by vortexing and prepared by centrifuging for 2 min at 2700 rpm. The column was placed in a new screw-cap tube and the labeled sample was applied. The columns were centrifuged for 2 min at 2700 rpm to collect the sample.

The labeled probe was measured in the scintillation counter (Aim:  $1-2 \times 10^7$  cpm/ml; recommended final DNA probe concentration was 2-10 ng/ml or  $1-2 \times 10^6$  cpm/ml).

### Hybridization

First the radioactively labeled probe was denatured at 95°C for 5 min, then directly added to the membrane and incubated for 2 h at 60°C. Next the membrane was rinsed for several times with Southern Wash Buffer I at RT, incubated for 15 min at 60°C; followed by several washes in Southern Wash Buffer II at RT and two subsequent incubations for 30-45 min at 60°C. Finally the membrane was rinsed and washed in Wash Buffer III at RT, until the radioactive counts were below ~10-20 cpm/sec.

The membrane was transferred onto plastic wrapped Whatman and folded into plastic. This set up was exposed to x-ray film at -80°C with an intensifying screen for 1 to 2 days and developed.

## 2.2.3 Immunohistochemical Methods

### 2.2.3.1. Preparation of Paraffin Sections

#### Embedding of Embryos in the Uterus (5.5 to 7.5 dpc)

To orientate the embryos and to make serial sections, the uterine horns were dissected with the oviducts and the cervix. The uterus was spread onto a small index card and fixed with pins. The card with the uterus was fixed in 4% PFA and embedded in paraffin. By this approach the embryonic placenta should be orientated towards the mesometrial pole (according to (Papaioannou, 2005)).

#### Fixation

The following steps were proceeded in RNase free conditions (DEPC). Fixation was performed in 4% PFA, o/n at 4°C. The following day, the tissue was incubated at RT, twice in PBS for 10 min and in 0.9% NaCl<sub>2</sub> for 10 min. The subsequent isopropanol series, starting with 30%, 50%, 70% and 95% was incubated for 1-3 h. The last incubation took place o/n at 4°C. Next the tissue was transferred into 100% isopropanol twice for 2-3 h at RT. Followed by 2 h incubation in isopropanol/ethanol (1:1), 2 h CHCl<sub>3</sub>, and finally CHCl<sub>3</sub>/paraffin (1:1) o/n at 60°C. The next day, the paraffin was changed twice, and incubated for several days until embedding. The small paraffin blocks were stored 4°C.

#### Sectioning

The paraffin blocks were sectioned with a manual Mikrotom (Leica). The sections were about 4-8 µm thick. The sections were floated in a 42°C water bath, containing H<sub>2</sub>O. Next, they were transferred onto Superfrost Plus slides and dried on a heating plate at 42°C for ~30 min. After incubation at 60°C o/n, the slides were stored at 4°C until use.

### 2.2.3.2. HE Staining

The slides were first deparaffinized with two 10 min incubations in xylene. Next an ethanol series was performed, starting with 100% for 5 min, 90%, 70% and 50% for 3 min each. Rehydration took place in H<sub>2</sub>O for 5 min. After an incubation in Hämalaun (according to Mayer) for 10 min, the slides were transferred into H<sub>2</sub>O and rinsed with running tap water for 10 min, to develop the blue staining. To counterstain, the slides were incubated for 3 min in 0.1% Eosin solution and rinsed with H<sub>2</sub>O. The Eosin staining will be differentiated through incubation in 96% ethanol for 3 min, followed by a dehydration series through ethanol. After two additional 10 min incubations in xylene, the slides were mounted with Roti®-Histokitt.

### 2.2.3.3. TUNEL Staining

The terminal deoxynucleotidyltransferase-mediated dUTP-biotin nick end labeling (TUNEL) assay of embryonic sections was performed according to the manufacturer's manual (In-Situ Cell Death Detection Kit, POD; (Roche)). The following options were applied: paraffin-embedded tissue sections were deparaffinized in xylene, re-hydrated and protease treated. Additionally a 10 min Quenching (to block endogenous peroxidase activity) with 3% H<sub>2</sub>O<sub>2</sub> in methanol was performed and the sections were permeabilized with Citrate buffer pH 6.0 and microwave irradiation, before the TUNEL reaction mixture was added (Label and Enzyme solution). After the signal was transformed with a Converter-POD, the DAB substrate (DAB with Metal Enhancer; (Sigma)) was applied to stain the samples. Apoptotic cells were analyzed with bright field microscopy.

### 2.2.3.4. *In situ* Hybridization of Sections

#### Preparation of DIG-labeled Riboprobes

To generate riboprobes, linearized plasmid DNA (MM 2.1.6) was isolated and labeled with DIG RNA Labeling Mix (Roche). 10 µg plasmid DNA was restricted with 20 Units of the adequate restriction endonuclease, in a final volume of 50 µl for 3 h at 37°C, comparable with the standard preparative set up (MM 2.2.2.8). Next, a Phenol/CHCl<sub>3</sub> extraction with equal volumes, followed by a classical ethanol precipitation was performed (similar to MM 2.2.2.7). The DNA pellet was solved in 20 µl H<sub>2</sub>O (DEPC).

The subsequent steps were proceeded in RNase free conditions (DEPC). The following set up was mixed:

4  $\mu$ l linearized plasmid DNA  
2  $\mu$ l Transcription buffer (Roche)  
10.5  $\mu$ l H<sub>2</sub>O

& incubated for 15 min at RT

1.5  $\mu$ l DIG-labeling Mix (Roche)  
0.8  $\mu$ l RNase-Inhibitor  
1.2  $\mu$ l RNA-Polymerase (T3/T7/Sp6)

& incubated for 2 h at 37°C

1.0  $\mu$ l DNase I

& incubated for 15 min at 37°C.

To check the amount of probes labeled, 2  $\mu$ l samples were withdrawn and quantified on a MOPS RNA Gel (runtime 90 min at 100 V). The labeled riboprobes were ethanol precipitated twice with 7  $\mu$ l NH<sub>4</sub>Ac [7.5 M]. The final pellet was solved in 10 to 100  $\mu$ l H<sub>2</sub>O (estimated with the MOPS Gel Quantification) and diluted 1:10 with Hybridization Buffer Solution (HBS). The riboprobes were stored at -20°C until use.

### Tissue Recovering

The following steps were proceeded in RNase free conditions (DEPC). Prior to deparaffinization, the slides were placed in a 68°C oven for 30 min, to melt the paraffin. To deparaffinize the slides were treated as follows: twice CHCl<sub>3</sub> for 10 min, once 100%, 95%, 90%, 80%, 70%, 50% and 30% ethanol for 5 min each. Next, they were incubated in succession: twice PBS for 5 min, 4% PFA/PBS for 30 min, twice PBS for 5 min, Proteinase K/PK-buffer [10  $\mu$ g/ml] for 10 min (130  $\mu$ l PK [10 mg/ml] in 130 ml PK-buffer), PBS for 5 min, 4% PFA/PBS for 30 min, twice PBS for 5 min, twice 2x SSC for 2 min and twice Tris/Glycine buffer for 15 min. The sections were drained and transferred into Quadriperms (Greiner Bio-One).

### Hybridization

The desired DIG labeled RNA probes were diluted 1:100 with HBS Mix (HBS + 100  $\mu$ g/ml tRNA) and denaturated at 95°C for 4 min, and then cooled on ice. Per section 60  $\mu$ l denaturated HBS Mix was applied and the samples were covered with plastic stripes (e.g. autoclave bag). The sections were incubated in Quadriperms, in an airtight box with paper towel drenched in 5x SSC, at 70°C o/n.



## Post-Hybridization

The following day the sections were incubated 3 times in 5x SSC for 20 min at RT and once in preheated 20% Formamid (0.5x SSC) for 40 min at 60°C. The Formamid solution was exchanged and cooled approx. 15 min in a 37°C water bath. The slides were treated as follows at 37°C: NTE for 15 min, RNaseA/NTE [10 µg/ml] for 30 min and NTE for 15 min at 37°C. Then a transfer in 20% Formamid (0.5x SSC) for 30 min at 60°C and a final incubation in 2x SSC for 30 min at RT were carried out. For the subsequent treatment with antibody, the slides were drained, laid upside down and incubated in 1% Blocking/MABT for 1 h at RT. In parallel, the antibody (Anti DIG-AP conjugate (Roche)) was diluted 1:5000 in 1% Blocking/MABT and blocked for 1 h at 4°C. The slides were drained and finally incubated in a humid chamber with the blocked antibody, at 4°C o/n.

## Staining

The slides were washed in TBST for 4 times 10 min and 3 times 20 min each, followed by incubations in NTMT twice for 10 min and in NTMT/Levamisol [2 mM] once for 10 min. The staining solution was prepared before use as follows: first, centrifugation of BM-Purple (Roche) for 5 min at 3000 rpm, 4°C; second transfer of supernatant into a new falcon tube, third addition of 2 mM Levamisol and 0.1% Tween 20. The slides were drained and incubated with 1.5 ml staining solution for several days in the dark (incubation time depends on the riboprobe).

To stop the reaction, the slides were washed twice in NTMT for 15 min and once in PBS for 10 min. In parallel, the Kaisers Glygeringelantine was melted at 42°C. Finally the sections were embedded with several drops of Kaisers Glygeringelantine and mounted with coverslips. The sections were analyzed with bright field microscopy.

### 2.2.3.5. Whole Mount *in situ* Hybridization of Embryos (WISH)

#### Tissue Recovering & Fixation

The protocol is similar to the previously described *in situ* protocol on sections (MM 2.2.3.4). The following protocol was proceeded in RNase free conditions (DEPC). Each step at RT or 4°C was performed gently shaking.

The dissected embryos were rinsed several times in PBS. First the embryos were fixed in 4% PFA at 4°C o/n. The next day, an increasing methanol series was performed as follows: incubation twice in PBT for 15 min at RT, 25%, 50%, 75%, 100% methanol for 15 min each and 100% methanol at 4°C o/n. The fixed embryos were stored at -20°C until use or directly

processed the following day. Therefore a decrease methanol series was performed, each incubation for 10 min and the slides were washed twice with PBT for 10 min at RT.

### Pre-Hybridization & Hybridization

To prepare the embryos, they were first bleached with 6% H<sub>2</sub>O<sub>2</sub>/PBT for 1 h at 4°C. Next the samples were washed with PBT 3 times, then with RIPA buffer and again with PBT, for 5 min each at RT. For refixation the embryos were incubated for exactly 20 min in 0.2% Glutaraldehyd/4% PFA. This was followed by three additional PBT steps and a transfer into Hybridization Buffer Solution (HBS) mixed with PBT (1:1), for 10 min. The mixed HBS/PBT was exchanged with HBS and incubated for 10 min, followed by a pre-hybridization incubation in HBS Mix (HBS + 100 µg/ml tRNA) for 2-3 h at 70°C. In parallel HBS Mix was incubated at 70°C and prior to the hybridization mixed 1:10 with labeled riboprobe, which was denatured for 3 min at 80°C and then cooled on ice. The pre-hybridized embryos were transferred into glass tubes and incubated in the HBS/riboprobe at 70°C o/n.

### Post-Hybridization

The following day, the hybridization solution was taken off and stored at -20°C for reuse. The embryos were proceeded as follows: washed 3 times with preheated HBS for 30 min at 70°C and incubated in NTE for 15 min at RT. The RNase treatment was performed with 20 µg/ml RNase A in preheated NTE for 1 h at 37°C. After a 15 min wash with NTE at RT, the samples were incubated in preheated HBS for 30 min at 70°C, diluted HBS/TBST (1:1) for 20 min at RT, and rinsed twice in TBST. Next two incubation steps in MABT for 30 min at RT were followed by incubation in Blocking solution (MABT + 2% Blocking reagent + 20% goat serum) for 1 h at RT. At the same time the antibody (Anti DIG-AP conjugate (Roche)) was diluted 1:2000 in 1% Blocking/MABT and blocked for 1 h at 4°C. Finally the embryos were incubated with the blocked antibody, at 4°C o/n.

### Staining

The embryos were washed in MABT 10 times for 30 min each at RT. Moreover, the MABT was changed several times for the next 1-2 days, at 4°C. For the staining the embryos were transferred into NTMT, washed twice for 10 min at RT and incubated in 2 mM Levamisol/NTMT for 10 min. In parallel, the staining solution was prepared before use as follows: first, centrifugation of BM-Purple (Roche) for 5 min at 3000 rpm at 4°C; second transfer of supernatant into a new falcon tube, third addition of 2 mM Levamisol and 0.1% Tween 20. The embryos were incubated in staining solution for several hours in the dark (incubation time depends on the riboprobe).

To stop the reaction, the embryos were washed several times in TBST, until the solution was no longer colored. Finally they were re-fixed with 4% PFA at 4°C o/n and stored in methanol at -20°C. The embryos were analyzed with a binocular.

### 2.2.3.6. WISH of Blastocysts

The original protocol adapted from Yoshikawa was modified as follows: blastocysts were transferred with mouth pipetting and glass needles instead of a WISH chamber system (Yoshikawa et al., 2006). The following procedure was performed in RNase free conditions.

#### Embryo Collection & Fixation

Blastocysts were harvested 3.5 or 4.5 dpc by rinsing the uterus with PBS. These blastocysts were transferred through 3-4 drops of PBS. The following steps were performed in a 24-well plate, each well filled with 0.5 ml of the indicated buffer. For fixation, blastocysts were incubated in 4% PFA/PBT cautiously shaking at 4 °C o/n.

The following morning blastocysts were washed once with PBT for 2 min, and twice for 5 min. Next they were incubated with 2.5 µg/ml Proteinase K/PBT for 15 min and rinsed with PBT for 2 min. To post-fix, the blastocysts were incubated in 0.2% glutaraldehyde/4% PFA/PBT for 20 min at RT and rinsed with PBT, once for 2 min and twice for 5 min.

#### Pre-Hybridization & Hybridization

In parallel, the blastocysts and 50 µl labeled riboprobe were pre-hybridized in 450 µl Hybridization Buffer Solution Mix (HBS + 100 µg/ml tRNA) at 60°C for 3 h. The riboprobe was denaturated for 3min at 80°C, and then cooled on ice. Blastocysts were incubated with the denaturated hybridization solution at 60°C o/n (temperature according to the riboprobe).

#### Post-Hybridization

The post-hybridization washes were carried out at the same temperature as the hybridization. The blastocysts were rinsed with preheated Post-Hybridization Wash Buffer (PHWB) once for 2 min, 3 times for 25 min and a final wash gradually cooling the samples to RT.

Next two incubation steps in MABT, one for 20 min and one for 10 min, were followed by a 2 min and a subsequent 30 min incubation in Blocking solution (MABT + 2% Blocking reagent + 20% goat serum) at RT. At the same time the antibody (Anti DIG-AP conjugate (Roche)) was diluted 1:2000 in 1% Blocking/MABT and blocked for 30 min at 4°C. Finally the blastocysts were incubated with the blocked antibody, at 4°C o/n.

## Staining

The blastocysts were rinsed with MABT for 2 min and for 10 min, followed by incubations in NTMT and in NTMT/Levamisol [2 mM], both for 10 min. The staining solution was prepared before use as follows: first, centrifugation of BM-Purple (Roche) for 5 min at 3000 rpm, 4°C; second transfer of supernatant into a new falcon tube, third addition of 2 mM Levamisol and 0.1% Tween 20. The blastocysts were incubated in 0.5 ml staining solution for several hours in the dark gently shaking (incubation time depends on the riboprobe).

To stop the reaction, the blastocysts were rinsed several times in PBT, and additionally incubated 3 times for 5 min each. Blastocysts were stored in PBS at 4°C. Analysis was performed with an inverted bright field microscope.

## 2.2.4 Mouse

All animal studies were carried out according to the guidelines of the "Regierung von Unterfranken" and the University of Würzburg. The generations of the chimeras were performed by BayGenomics (<http://BayGenomics.ucsf.edu/>) and PolyGene Transgenetics (<http://www.polygene.ch/>).

### 2.2.4.1. Mouse Husbandry

#### Mouse Facility

All users changed their shoes and wore coats, caps, masks and gloves, before were entering the mouse facility. All incoming materials were treated with disinfectants. Mice were fed with standard rodent diet and filtered water, ad libitum. The mice were housed in type II polycarbonate cages. Health monitoring was carried out with sentinel mice every 3-6 months.

#### Breeding & Weaning

For simple strain maintenance and backcrossing (for congenic strain), we required 2-3 mating cages and 2-3 additional cages to hold weaned pups. To breed, we placed the animals in pairs of one male and two females, aged 8-12 weeks. We steadily replaced old breeders after 6-8 litters. To backcross, each time the new descendants were set up with new male or female to the recipient inbred strain, for more than 10 generations (F10+).

The cages were checked at least once each week to mark pregnant females and record the approximate birth dates of litters. The pups were weaned at 3-4 weeks of age and separated from the female. They were separated by gender, with no more than 5 mice per cage, tagged with metal ear tags and tail cuts were carried out to subsequently genotype them. All animals

were registered with identity number, gender, genotype, day of birth, and generation. To minimize fighting, weaned males were only grouped with littermates. Males that were breeders were always separately caged or sacrificed (sac). Females were grouped depending on their use.

Timed pregnancies were carried out, depending on the experimental needs. Therefore the presence of a vaginal plug, in the morning after mating (mating 4-6 pm, plug check 7-10 am) was used as sign that fertilization occurred and counted as 0.5 days post coitus (dpc).

## Dispatch Animals

We used two different approaches to sacrifice the animals, carbon dioxide inhalation (CO<sub>2</sub>) or cervical dislocation. For all animals sacrificed in the mouse facility CO<sub>2</sub> was used for euthanasia. CO<sub>2</sub> was administered in a special container to apply the correct dosage and to avoid behavioral distress for the animals. This approach has some disadvantages for histological preparations; it is likely to induce capillary hemorrhages in certain tissues, e.g. in lung and brain. To avoid these defects, we applied cervical dislocation. It is the quickest, most effective and humane way to ensure the death of an animal. Hence, cervical dislocation of un-anesthetized animals was only performed to prepare histological samples and for MEFs.

## 2.2.5 Biochemical methods

### 2.2.5.1. Whole Cell Lysates

MEFs cells were scraped with PBS, pelleted and resuspended with 10 times of their volume in TNN + protease inhibitors (PI 1:100 + PMSF 1:200) by pipetting up and down for 20 times and incubation on ice for 20 min. Lysates were centrifuged at full speed to remove the cell debris. The supernatant was immediately used for immunoprecipitation or boiled in 3x ESB for 5 min and frozen at -20°C.

### 2.2.5.2. Tissue Extract

The mouse was sacrificed and the organs of interest dissected. The tissue was washed in PBS and transferred into a cell strainer (Falcon), which was put onto a falcon tube. The sample was rinsed with 3 ml PBS and homogenized with forceps or spatula, pressing the tissue through the nylon mesh. Next the mesh was washed with 7 ml PBS and the resulting cell suspension was centrifuged at 1200 rpm for 5 min at RT. The cell pellet was resuspended in 3 ml ACK-lysis buffer and incubated for 3-5 min at RT (to lyse the erythrocytes). After adding 15 ml PBS and an additional centrifugation for 10 min at 1200 rpm, the supernatant was discarded and the cells resuspended in 1 ml PBS. The cell suspension was transferred into a new tube and

centrifuged at 1200 rpm for 10 min at 4°C. Finally, the supernatant was discarded and the cell pellet was immediately used for immunoprecipitation or frozen at -20 °C.

### 2.2.5.3. Determination of Protein Concentration (Bradford)

The protein concentration was determined with the method described by Bradford (Bradford, 1976). Therefore 2 µl of whole cell lysate were mixed with 1 ml of Bradford solution. The extinction at 595 nm was measured and compared to a standard BSA dilution series.

### 2.2.5.4. IP-Western Blot

The incubation steps at 4°C and at RT were all either performed on a rotating wheel or horizontal shaker.

#### Immunoprecipitation

Whole cell lysate [1-2 mg] was incubated with the preferred antibody at 4°C o/n (MM 2.1.7). The following day, 30 µl of protein A- or G-sepharose (for polyclonal or monoclonal antibodies) was added and incubated for 1 h at 4°C. The beads were washed 5 times with 1 ml TNN, centrifuged at 3000 rpm for 1 min at 4°C. After the last wash, the supernatant was removed completely, the beads were resuspended in 3x ESB and incubated at 95°C for 5 min. The samples were either directly used for electrophoresis or stored at -20°C.

#### SDS-polyacrylamide Gel Electrophoresis (SDS-PAGE)

The SDS-PAGE analysis was performed using a discontinuous method (Laemmli, 1970). First the separating gel (ranging from 8-14%) was prepared. Second after polymerization, the stacking gel was poured onto the separating gel. The electrophoresis was carried out in 1x SDS running buffer for approx. 1 h, at 35 mA/gel. The gels were either used for immunoblotting or stained for 30 min with Coomassie blue to visualize the proteins.

Set up for a standard 10% SDS-PAGE:

| Separating gel              | Stacking gel                  |
|-----------------------------|-------------------------------|
| 6.1 ml H <sub>2</sub> O     | 6.9 ml H <sub>2</sub> O       |
| 3.7 ml 1.5 M Tris pH 8.8    | 1.4 ml 0.5 M Tris pH 6.8      |
| 5 ml Acrylamid/Bisacrylamid | 1.6 ml Acrylamid/Bisacrylamid |
| 75 µl 20% SDS               | 50 µl 20% SDS                 |
| 100 µl 10% APS              | 50 µl 10% APS                 |
| 20 µl TEMED                 | 20 µl TEMED                   |

## Immunoblotting

Proteins were transferred onto a PVDF membrane with electro blotting. The membrane was pre-incubated for 1 min with 100% methanol and rinsed with Blotting buffer. The blot was assembled as follows: a wet sponge, a Whatman paper, the membrane, the SDS-PAGE followed by a second Whatman paper and a sponge. This blot was placed in Blotting buffer, in a cooled blotting tank (Biorad). The transfer occurred at 300 mA for 90 min. Successful and equal transfer of proteins was visualized by staining the membrane for 1 min with Ponceau S solution and rinsing in H<sub>2</sub>O.

To detect specific proteins with the respective antibodies (MM 2.1.7), the membrane was blocked with Blocking solution (3% milk powder in TBST) for 1-2 h, and then incubated with the primary antibody diluted in Blocking solution at 4°C o/n. The following day, the membrane was washed 3 times with TBST for 10 min each and incubated with the appropriate secondary antibody (MM 2.1.7) for 1 h at RT. After 3 washes with TBST for 10 min each, the specific bands were detected using a Luminol solution. The membrane was wrapped in plastic foil and exposed to an ECL-film.

## 3 RESULTS

### 3.1 Expression of *Lin* in Mouse

#### 3.1.1 Molecular Analysis of *Lin* mRNA Expression

To deeper investigate the role of *Lin9*, in cell cycle and differentiation, its expression was first analyzed in mice. Thus RNA from different wild type (wt) mouse organs (C57BL/6 males and females aged 6-8 weeks) was prepared. In these organs, mRNA expression of *Lin9* and of three other members of the human LINC core complex, namely *Lin52*, *Lin54* and *Lin37*, were analyzed by quantitative RT-PCR (qRT-PCR) (Schmit et al., 2007). Highest levels of *Lin9* mRNA were detected in thymus, testis and spleen. These are highly proliferative tissues. *Lin9* expression was also observed in all other tested tissues, although in lower amounts, e.g. in the brain, liver, lung and intestine (Fig. 3.1 A). An analogous expression pattern was observed for *Lin52*, *Lin54* and *Lin37*. In addition to its ubiquitous expression *Lin52* expression was notably higher in muscle tissue and in the lung while increased expression of *Lin37* was detected in the ovary (Fig. 3.1 A). Several different animals were tested.

Additionally, *Lin* expression was analyzed during mouse development. For this reason RNA from embryos 7.5 dpc (days post coitus) to 16.5 dpc was prepared. Stage 7.5 dpc represents the embryo right after gastrulation, where major proliferation, cell migration and differentiation take place to form three germ layers (Fig. 1.2). Next the cup-shaped gastrula is turned and the germ layers are orientated at stage 8.5 dpc. The embryogenesis per se is finished at 9.5 dpc. Afterwards, mainly organogenesis takes place, with massive proliferation and differentiation in all organs. For example, the CNS highly differentiates in stage 13.5 dpc and in general the size of each organ increases up to stage 16.5 dpc. Here *Lin9* as well as *Lin52*, *Lin54* and *Lin37* were again ubiquitously expressed throughout development. Only *Lin52* expression was notably higher in E12.5 and E14.5, so mainly in the phase of organogenesis and differentiation (Fig. 3.1 B).

*A-Myb*, *B-Myb* and *C-Myb* mRNA expression was analyzed in parallel and served as control (data not shown). The *Mybs*, especially *B-Myb*, another important member of the LINC complex, were as expected ubiquitously expressed throughout development and in adult organs (Latham et al., 1996; Sitzmann et al., 1996).



*Lin9* mRNA was also expressed in mouse ES cells and blastocysts as later mentioned in more detail (Fig. 3.10 & Fig. 3.13). Taken together these results show that *Lin9* as well as *Lin52*, *Lin54* and *Lin37* are ubiquitously expressed in adult mouse organs and throughout embryonic development.

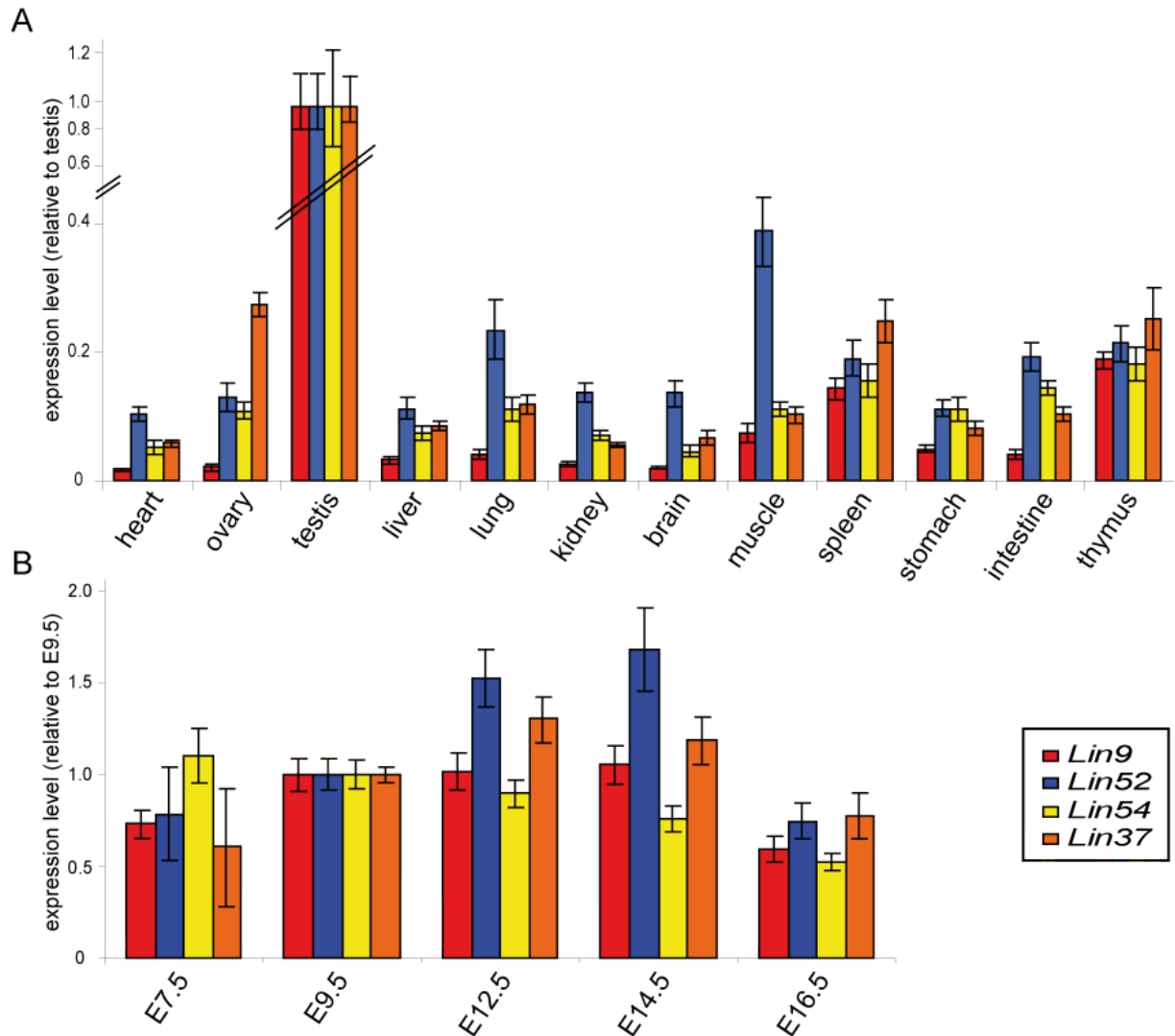


**Fig. 3.1: Relative expression of *Lin9*, *Lin52*, *Lin54* & *Lin37* mRNA in the mouse.** Expression of *Lin9*, *Lin52*, *Lin54* and *Lin37* mRNA in the indicated wt mouse organs and different stage embryos were analyzed by qRT-PCR. Expression was normalized to *Hprt1*. (A) Expression in adult mouse organs. Level is shown relative to testis expression. (B) Expression in different embryonic stages. Level is shown relative to E9.5. The different *Lin* mRNAs are ubiquitously expressed.

### 3.1.2 Histological Analysis of *Lin* mRNA Expression

To confirm the molecular data and further characterize *Lin9*, *Lin52*, *Lin54* and *Lin37* mRNA expression in mouse development, whole mount preparations and histological sections were analyzed.

First E9.5 whole-mount wt embryos were examined by *in situ* hybridization. *Lin9*, *B-MYB*, *Lin52*, *Lin54* and *Lin37* DIG-labeled *in situ* hybridization probes were generated by *in vitro* transcription from vectors containing the appropriate cDNAs (MM 2.1.5 & MM 2.2.2.11). Similar to the qRT-PCR data with mRNA from 9.5 dpc embryos, all investigated *Lins* and *B-Myb* were expressed throughout the entire embryo. Strongest expression was detected in the limb buds and in the head (Fig. 3.2), which are tissues that are highly proliferative and cell dense. No staining was seen in control hybridizations, with sense probes, indicating that the staining is specific (Fig. 3.2). The *B-Myb in situ* hybridization included in this experiment served as a positive control, since its ubiquitous expression is already well characterized (Latham et al., 1996; Sitzmann et al., 1996).

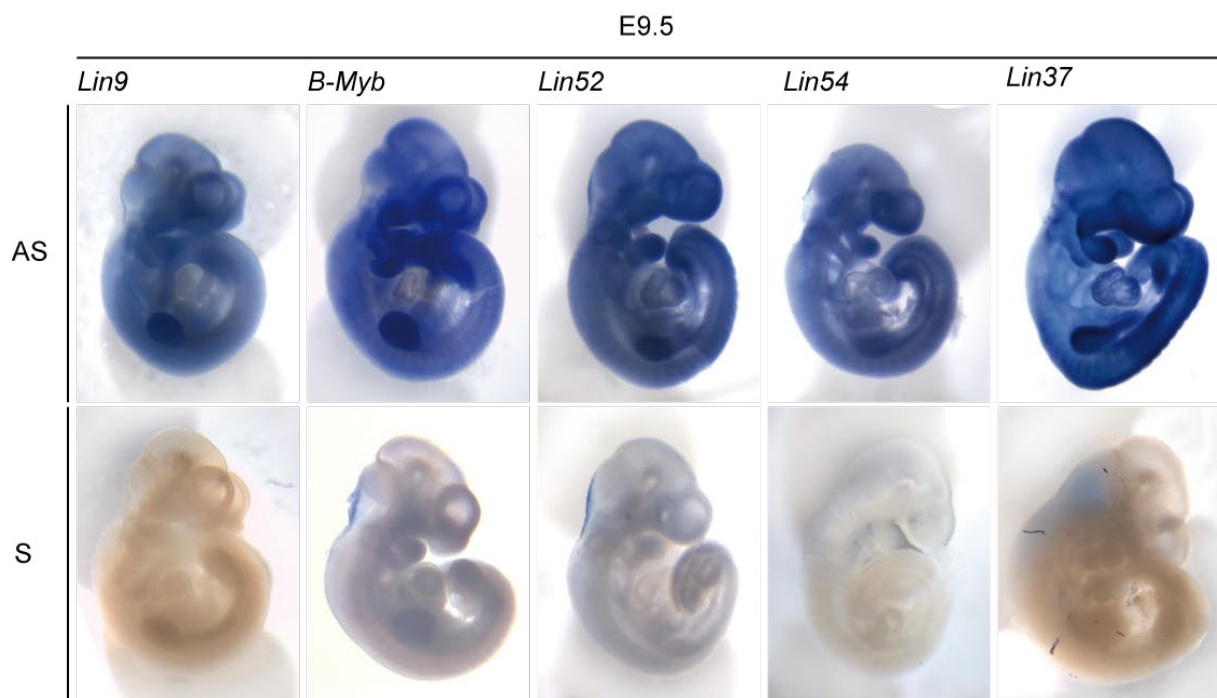


**Fig. 3.2: Expression of *Lin9*, *B-Myb*, *Lin52*, *Lin54* & *Lin37* mRNA in mouse embryos 9.5 dpc.** Whole-mount *in situ* hybridization in wt embryos E9.5. DIG-labeled probes for *Lin9*, *B-Myb*, *Lin52*, *Lin54* & *Lin37* were used. Expression of the *Lins* and *B-Myb* was seen throughout the entire embryo.

To further investigate the expression of *Lin9*, histological sections of 7.5, 9.5 and 14.5 dpc embryos were analyzed. Standard procedures were used for sectioning and *in situ* hybridization (MM 2.2.3.4). In figure 3.3 the haematoxylin and eosin (HE) staining is shown in parallel to the *in situ* data. At 7.5 dpc a distinct *Lin9* expression pattern was observed with

highest expression of *Lin9* in epithelial cells of the embryonic ectoderm and in the embryonic mesoderm. *Lin9* was weakly expressed in the embryonic visceral endoderm and the surrounding extraembryonic tissue, including trophoblast giant cells, extraembryonic ectoderm and ectoplacental cone (Fig. 3.3 A & C; Fig. 1.2). Trophoblast giant cells and parietal endodermal cells showed slightly more expression than the spongy layer of endometrial tissue consisting of decidual cells (Fig. 3.3 A). *Lin9* expression was also detected in the surrounding maternal tissue consisting of decidual cells, especially in the outer regions closer to the uteri wall (data not shown).

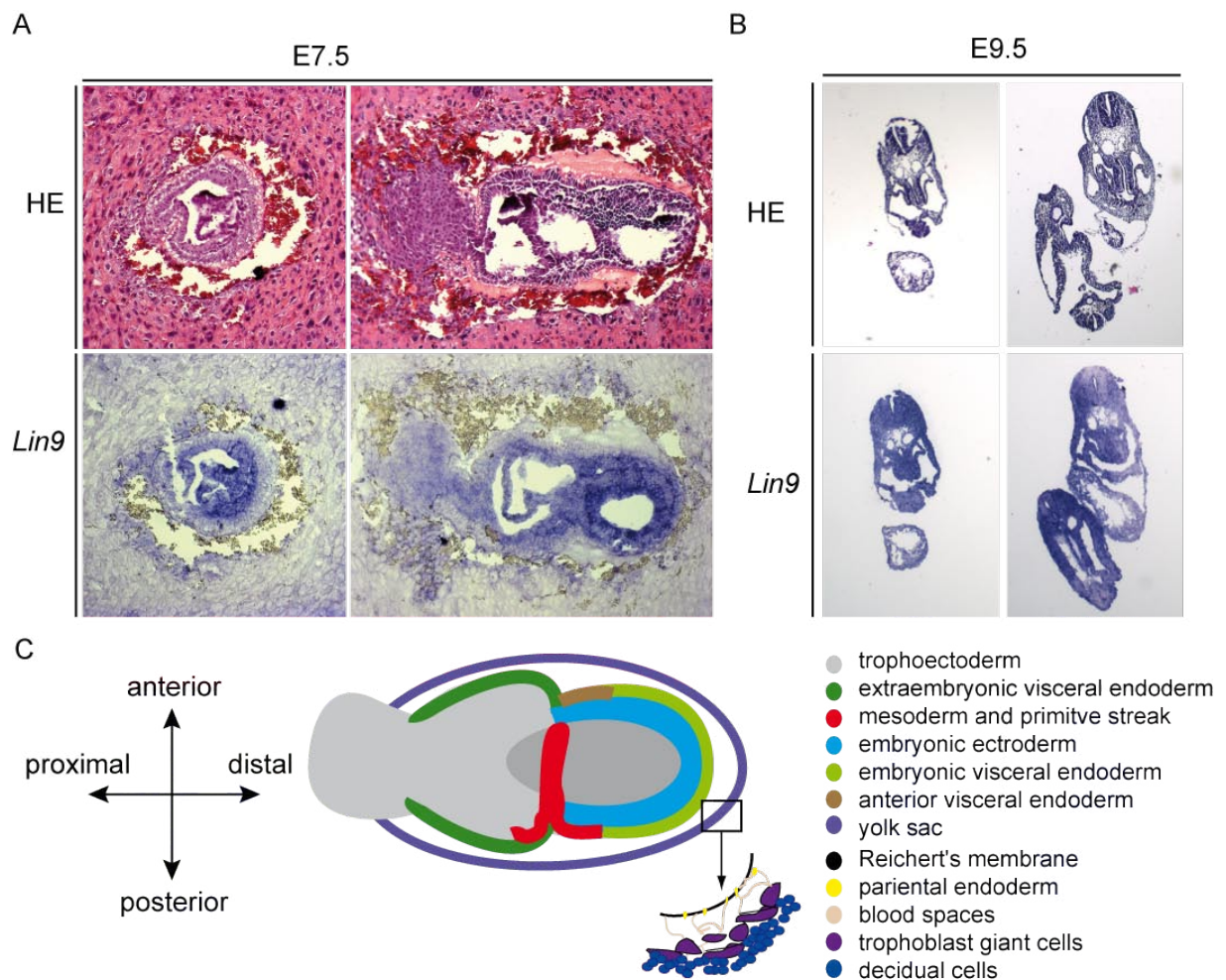


**Fig. 3.3: Expression of *Lin9* mRNA in mouse embryos 7.5 & 9.5 dpc.** Histological sections from wt embryos were stained with HE and RNA *in situ* hybridization was performed. A DIG-labeled probe for *Lin9* was used. (A) Sections of the whole decidual swellings at 7.5 dpc, transverse section left and sagittal on the right. The expression is detected strongest in the epiblast region. (B) Sections of 9.5 dpc. The expression appears to be ubiquitous. (C) Schematic drawing of an embryo ~6.5-7.5 dpc. Tissues are color labeled. The double-crossed arrows show the orientation of the proximal-distal and anterior-posterior embryonic axes. (based on (Pfister et al., 2007; Sutherland, 2003)).

Next, *Lin9* expression in sections of 9.5 dpc embryos was analyzed. Here the *Lin9* expression pattern was not restricted to a certain embryonic area. Rather *Lin9* mRNA was detected throughout the entire embryo (Fig. 3.3 B).

Furthermore, sagittal sections from embryos 14.5 dpc were analyzed for their *Lin9* mRNA expression. To facilitate orientation on the sections, HE staining was performed in parallel. *Lin9* was ubiquitously expressed at high levels in most organs (Fig. 3.4 A). Weaker expression of *Lin9* was detected in the heart and no *Lin9* mRNA was observed in the liver. All components of the heart are fully developed at this stage and it already has achieved its definitive prenatal configuration (Kaufman, 2004). The liver is by far the largest of the abdominal organs and has a fairly homogeneous histological appearance. This shows that it is the organ which is most developed at this stage of development. The rest of the organs still undergo structural changes (e.g. the brain) and are still highly proliferative at this stage to increase their size. In the brain the highest expression of *Lin9* was observed in the cortex. High levels of *Lin9* mRNA were also detected in the developing retina and lens (Fig. 3.4 A & data not shown).

To further investigate expression of *Lin9* in the developing brain, transverse brain sections of 14.5 dpc embryos were analyzed. *Lin9* expression was observed in the cortex, ventral in the telencephalon as well as in its lateral ventricular zone and the floor of the Diencephalon. Hence, the region of the subventricular zone of the developing cortex has been identified as the area with the highest *Lin9* expression (Fig. 3.4 B). The subventricular region of the developing brain is known to be a region of neuronal proliferation during embryogenesis. Staining specificity was confirmed with a sense probe in which case no staining is observed (Fig. 3.4 A & B on the right).

Additionally *Lin9* mRNA is expressed in ES cells and blastocysts as later mentioned in more detail (data not shown & Fig. 3.11). Taken together these histological results show that *Lin9* is ubiquitously expressed throughout embryonic development confirming the molecular analysis.

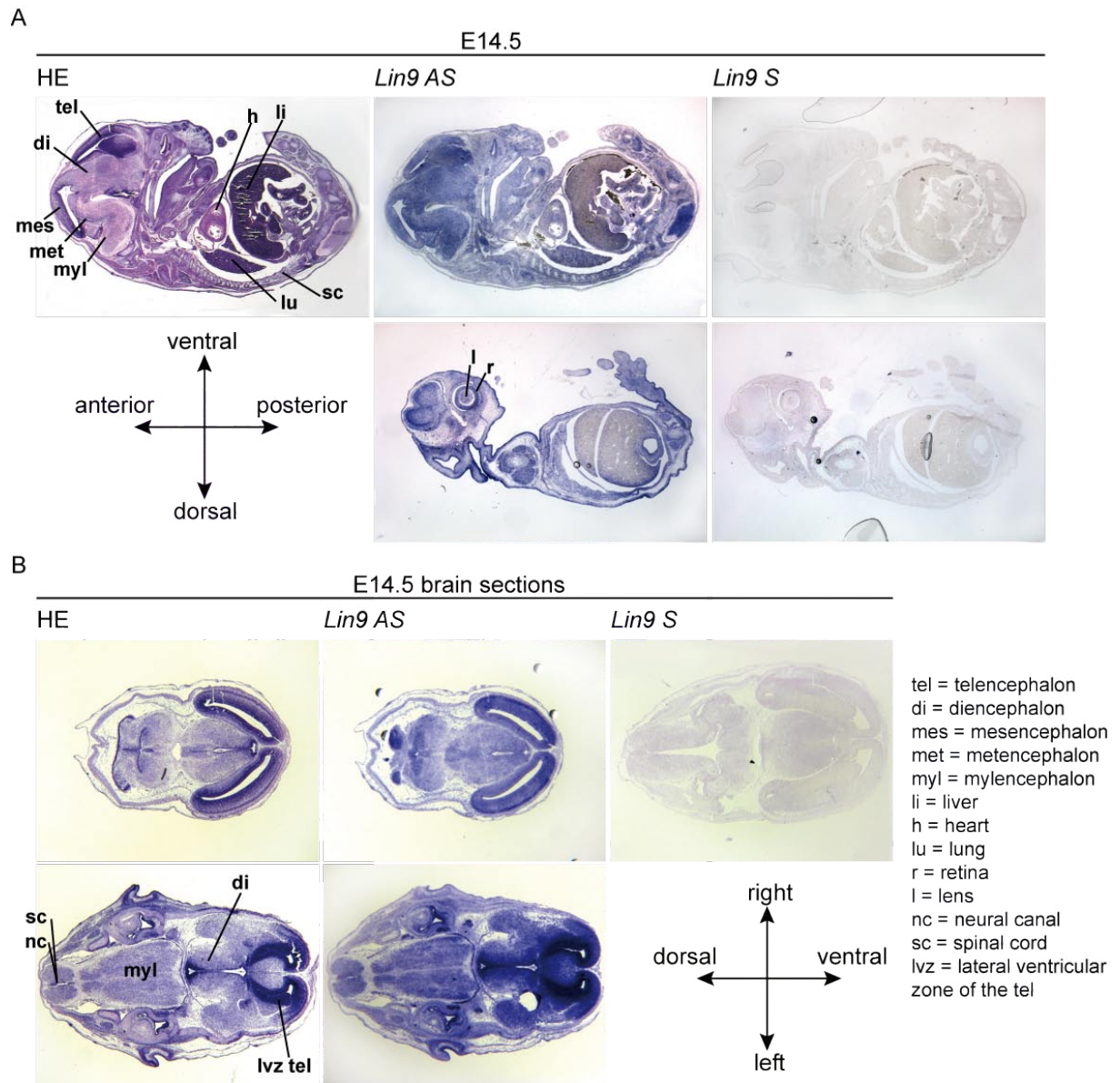


**Fig. 3.4: Expression of *Lin9* mRNA in mouse embryos 14.5 dpc.** Histological sections from wt embryos were stained with HE and a *Lin9* mRNA *in situ* hybridization was performed. The double-crossed arrows show the orientation of the embryonic axes. For inscriptions see figure legend. (A) Sagittal sections of the whole E14.5. The HE staining is depicted on the left, two sagittal examples of *Lin9 in situ* in the middle and for comparison a sense control on the right. The expression appears to be ubiquitous. The strongest expression is detected in the developing brain. (B) Transverse brain sections of E14.5. The sense probe as a control does not give any signal. (AS = AntiSense & S = Sense)



## 3.2 Lin9 Gene Trap Mouse Model (GT)

To understand the physiological role of Lin9, its role in development and to unravel a possible role in cell cycle *in vivo*, we used a Lin9 knockout mouse model.

### 3.2.1 Location of the Gene Trap in the Lin9 Allele

We identified a commercially available ES cell line in which one allele of Lin9 has been disrupted by a retroviral gene trap vector (pGTOLXf; BayGenomics: ES-clone # RRI306). The used gene trap vector contains a splice-acceptor site (SA) upstream of a promoter-less  $\beta$ -geo resistance gene ( $\beta$ -geo = fusion of  $\beta$ -galactosidase and neomycin phosphotransferase). After insertion into an intron, splicing generates a chimeric transcript that confers resistance to neomycin. In many cases, the resulting fusion protein is unstable and thus the insertion results in a complete knockout. This ES cell line was used by BayGenomics to create chimeric animals, using standard methods.

Chimeras were crossed with C57BL/6 wt animals and the resulting progenies were analyzed. Southern blots showed that the gene trap vector inserted near the Bgl II restriction site present in intron 11 close to exon 12 of the Lin9 gene. The detected wt Lin9 fragment is ~6 kb long, after Bgl II restriction and analysis with probe C (MM 2.1.5 & MM 2.2.2.13). The integrated gene trap vector did not carry a Bgl II site which then resulted in a longer fragment of ~12 kb (Fig. 3.5 C). The mutant allele, the so called Lin9 GT, was successfully transmitted to the germline.

Since the gene trap vector randomly inserts into the genome, the exact insertion site had to be located first. Based on original information from BayGenomics as well as on data gathered by Southern blotting, PCR primers were designed. PCR products obtained by long-distance PCRs were cloned and sequenced (data not shown). These experiments showed the exact insertion site of the gene trap vector in intron 11 of Lin9 (Fig. 3.5 A). A PCR strategy to genotype the Lin9 wt and GT allele in mice was designed based on this insertion site (Fig. 3.5 D).

The insertion of the gene trap vector should result in a truncated Lin9 fusion transcript, consisting of the Lin9 coding region including exon 11 and the  $\beta$ -geo resistance. Translation of the fused mRNA should result in a truncated LIN9  $\beta$ -geo protein, lacking conserved Box B of LIN9 (Fig. 3.5 B). To analyze this *in vivo*, testis lysates of wt and heterozygous animals were prepared and immunoprecipitated with antisera against human LIN-9. Bound mouse wt and GT LIN9 protein was detected by immunoblotting. In heterozygous mutant testis lysate,

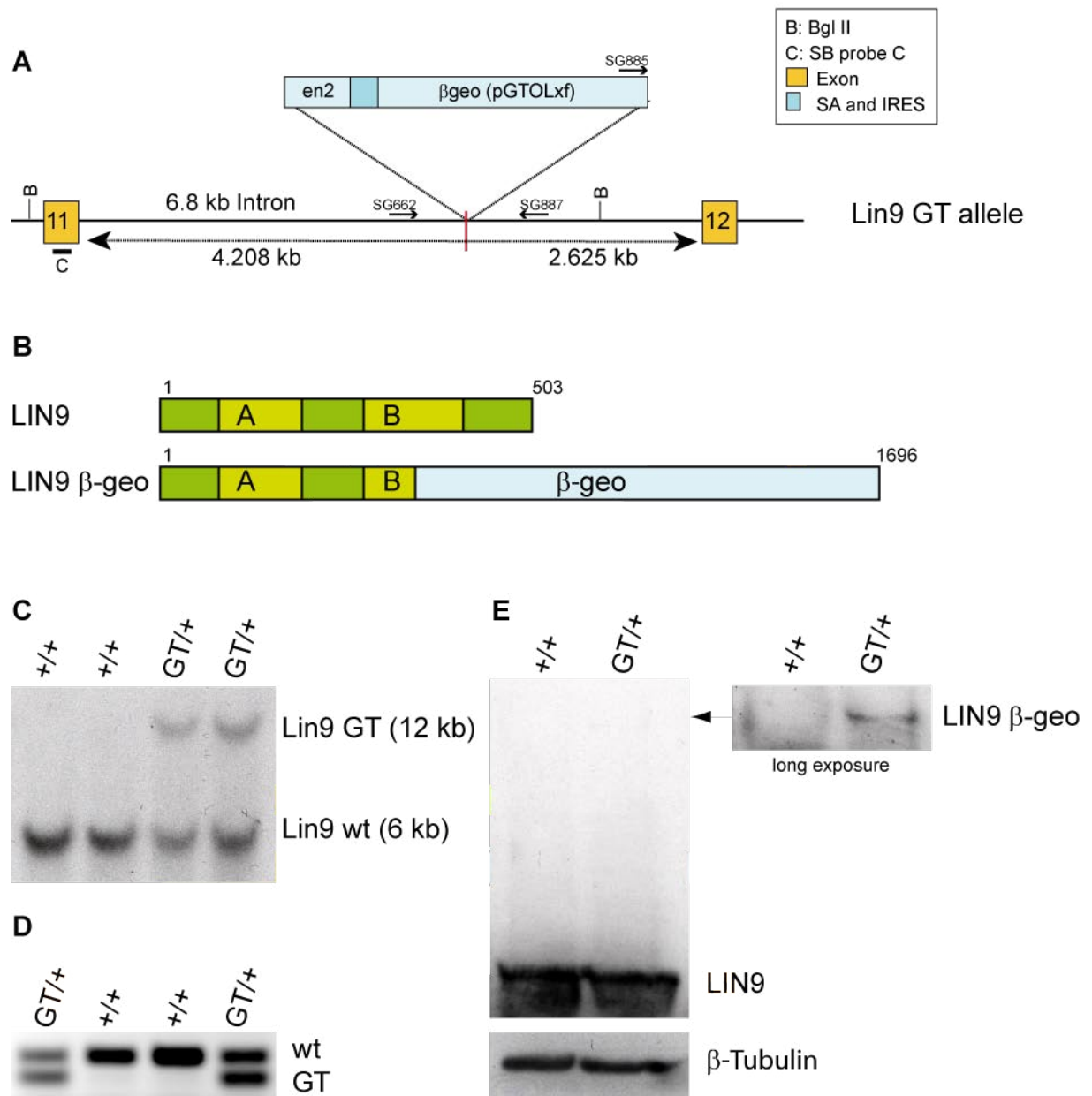


**Fig. 3.5: Generation of a *Lin9* knockout mouse.** (A) Scheme of the *Lin9* GT allele which is interrupted by the insertion of a gene trap vector ( $\beta$ -geo). The distances from the exons to the insertion and the positions of the Southern probes as well as the PCR primers are indicated. (B) Scheme of the wt versus the truncated LIN9 protein fused to  $\beta$ -geo shows the disrupted Box B. (C) Southern blot analysis of tail gDNA restricted with Bgl II and detected with labeled probe C. The alleles and their size are indicated on the right. (D) 3 primer based PCR to detect the wt (302 bp) and GT (215 bp) *Lin9* alleles in tail DNA, the products are mentioned on the right. The position of the primers is indicated in A (also see MM primer list). (E) Testes of wt and het animals were lysed and precipitated with human LIN-9 antisera and detected by immunoblotting. The right inlay represents the detection of the LIN9 GT protein upon longer exposure, about 15 min.

the level of GT LIN9 protein was very low compared to the endogenous LIN9 protein, whereas the GT fusion protein was detected only upon prolonged exposure of the western blot (Fig. 3.5 E). The amount of endogenous LIN9 protein was not altered. The Lin9/ $\beta$ -geo fusion mRNA was also detectable by RT-PCR (data not shown).

Taken together the 129-derived ES cell line from BayGenomics was successfully used to create knockout mice, which were further analyzed.

### 3.2.2 Analysis of Lin9 in Early Mouse Development

A cohort of heterozygous Lin9 animals (GT/+; 129 x C57BL/6) was established. Until now the Lin9<sup>GT/+</sup> animals develop and behave inconspicuous. Lin9<sup>GT/+</sup> males and females are healthy, fertile and born in a normal gender ratio. The oldest sacrificed animals, circa 1 1/2 years old, were not prone to tumors compared to wt Lin9 mice (+/+). From the beginning the mice were bred into the congenic mouse strain C57BL/6 (MM 2.1.10 & MM 2.2.4). This was achieved by backcrossing Lin9<sup>GT/+</sup> male and female descendants to the recipient inbred strain C57BL/6, for more than 10 generations (F10+). Backcrossing was also performed with C57BL/6 males to assure that the Y chromosome of the inbred strain was adopted into the GT Lin9 strain.

| Stage      | Total                 | Genotype |          |        | Fail. <sup>d</sup> | DF | Value  | Prob. |
|------------|-----------------------|----------|----------|--------|--------------------|----|--------|-------|
|            |                       | +/+      | + /GT    | GT/GT  |                    |    |        |       |
| Weanling   | 166 <sup>ab</sup>     | 52       | 114      | 0      | 6                  | 2  | 55.735 | 0.000 |
| E13.5      | 29 <sup>a</sup> (10R) | 6        | 13       | 0      | 10 (10R)           | 2  | 7.621  | 0.022 |
| E9.5       | 45 <sup>b</sup> (14R) | 12       | 30 (12R) | 2 (2R) | 1 (1R)             | 2  | 10.156 | 0.006 |
| E7.5       | 86 <sup>b</sup> (21R) | 19 (1R)  | 59 (13R) | 8 (6R) | 5 (1R)             | 2  | 14.72  | 0.001 |
| Blastocyst | 80 <sup>c</sup>       | 21       | 39       | 20     | 7                  | 2  | 0.075  | 0.963 |

**Tab. 3.1: Early lethality of Lin9-deficient embryos.** Genotypes were determined by Southern Blot<sup>a</sup>, PCR<sup>b</sup> or TaqMan qPCR<sup>c</sup>. Embryos genotyped as Lin9<sup>GT/GT</sup> at 9.5 and 7.5 dpc were partially resorbed (R). Lin9<sup>GT/GT</sup> blastocysts at 3.5 dpc were morphologically normal. PCR and Southern failures<sup>d</sup> were not counted for the level of significance. The Chi Square test was applied with two degrees of freedom (DF) to calculate the probability of the Mendelian segregation.

To analyze whether LIN9 is essential for mouse development, Lin9<sup>GT/+</sup> mice were intercrossed. Their progenies were genotyped as weanlings by Southern blot or PCR of tail samples (Fig. 3.5 C & D). Of 166 weanlings tested, about 70% were heterozygous (114), 30% wild type (52) and 0% homozygous mutant. These intercrosses of Lin9<sup>GT/+</sup> animals revealed that no live homozygous mutant weanlings were detected. This suggested that LIN9 is required for embryonic development in the mouse (Tab. 3.1).



To determine the stage of embryonic lethality of LIN9-deficient embryos, embryos from  $\text{Lin9}^{\text{GT}/+}$  mating were dissected and genotyped. To address various points in embryonic development, 13.5, 9.5 and 7.5 dpc embryos were examined. Neither at 13.5 dpc nor at 9.5 dpc were normal embryos, homozygous for GT Lin9 (GT/GT) detected. At stage 7.5 dpc, a high proportion of resorbed or embryos of abnormal histology could be detected. PCR genotyping confirmed that some resorbed embryos were knockout Lin9 (Tab. 3.1). Preparation of these partially resorbed embryos was difficult because of apoptotic or necrotic cells and the adjacent maternal decidual tissue. The Chi Square test was used to calculate the probability that  $\text{Lin9}^{\text{GT}/\text{GT}}$  embryos are not present in the expected Mendelian frequency. The number of weanlings at stage 9.5 and 7.5 dpc analyzed was sufficient to be statistically significant (probability below 1% level) and emphasized that the genotypes detected do not display the Mendelian ratio.

Taken together these data indicated that LIN9 is required for embryonic development in the mouse. The important question then was when and why the mutant embryos die. To investigate this in more detail, further analyses of E7.5 and E6.5 with specific lineage markers was performed.

### 3.2.3 Early Embryonic Lethality of $\text{Lin9}^{\text{GT}/\text{GT}}$ Embryos

To better characterize the cause of embryonic lethality, histological sections of decidual swellings at 7.5 and 6.5 dpc from  $\text{Lin9}^{\text{GT}/+}$  intercrosses were analyzed. Histological sections were prepared from whole decidual swellings and first stained with HE (MM 2.2.3.2).

With HE staining the abnormal implants were first visualized. The presumable  $\text{Lin9}^{\text{GT}/\text{GT}}$  embryos had no organized cell structures and lacked distally the distinct epithelial cells which are typical for the epiblast and therefore the embryo (Scheme: Fig. 1.2 & Fig. 3.3 C). The implants showed no amniotic cavity and extraembryonic coelomic cavity nor the ectoplacental cavity in the proximal region. Only in some implants was the yolk sac cavity visible. In general, the unstructured remains are smaller compared to their  $\text{Lin9}^{+/+}$  or  $\text{Lin9}^{\text{GT}/+}$  counterparts (Fig. 3.6 A).

Genotyping some of the 7.5 dpc old embryos was possible by scratching the embryonic remains off the slides, isolating gDNA from the paraffin fixed tissue and genotyping with TaqMan qPCR (Fig. 3.8 & data not shown). The embryos depicted in the following figure were genotyped. When counting the presumable  $\text{Lin9}^{\text{GT}/\text{GT}}$  embryos, 10 out of 48 embryos were found to be abnormal.

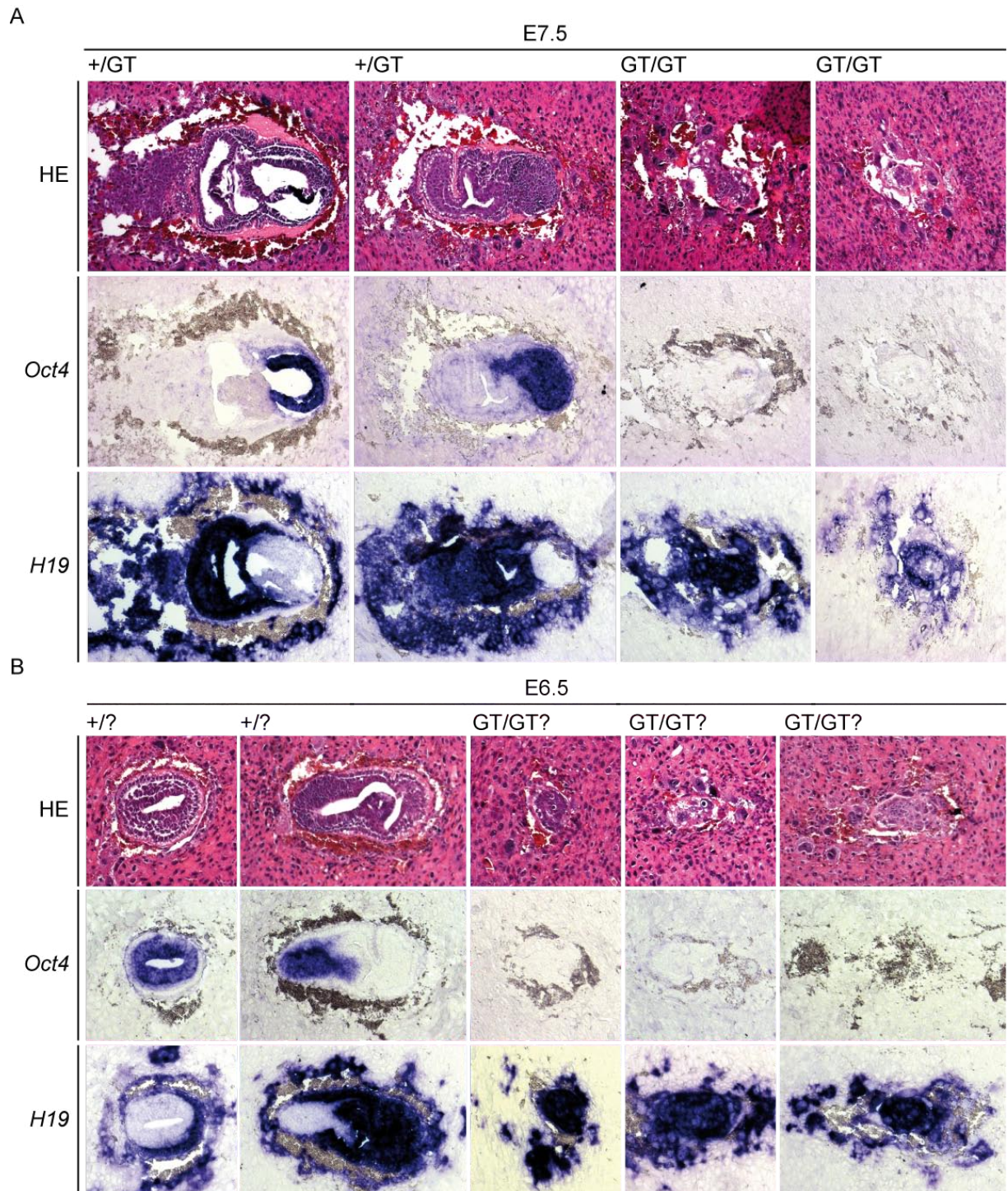


**Fig. 3.6: E7.5 & E6.5 Lin9-deficient embryos lack epiblast.** Histological sections from whole decidual swellings at 7.5 and 6.5 dpc resulting from  $\text{Lin9}^{\text{GT/+}}$  intercrosses were stained with HE and RNA *in situ* hybridization was performed. DIG-labeled probes for *Oct4* and *H19* were used, as indicated on the left. (A) The first 2 columns show sagittal sections through genotyped  $\text{Lin9}^{\text{GT/+}}$  embryos as mentioned on top. The next 2 columns depict sections from genotyped  $\text{Lin9}^{\text{GT/GT}}$  implant. The epiblast is clearly *Oct4* positive and the adjacent tissue is positive for *H19* in the  $\text{Lin9}^{\text{GT/+}}$  embryos. However, there is no expression for *Oct4* detected in the abnormal  $\text{Lin9}^{\text{GT/GT}}$  implants, only *H19* expression. (B) The first column depicts transverse, the second sagittal sections through  $\text{Lin9}^{\text{+/?}}$  or  $\text{Lin9}^{\text{GT/+}}$  embryos. The next 3 columns show sections from presumed  $\text{Lin9}^{\text{GT/GT}}$  implant. The epiblast is clearly *Oct4* positive and the adjacent tissue is positive for *H19* in the  $\text{Lin9}^{\text{+/?}}$  embryos. However, there is no expression for *Oct4* detected, only *H19* expression in the abnormal presumed  $\text{Lin9}^{\text{GT/GT}}$  implants. There is no structure equivalent to the epiblast detectable (Scheme: Fig. 1.2).

The result for the examined embryos stage 6.5 dpc was very similar concerning the disorganized phenotype, the lack of the epithelial cell structures as well as the missing cavities and the frequency of abnormal implants (Fig. 3.6 B). About one quarter of implantation sites were empty or contained resorbed embryos (12 out of 59 embryos analyzed in total). This frequency correlates with the expected Mendelian ratio. Although in both cases the abnormal implantation sites contained no clear epiblast structures, trophoblast giant cells were present, suggesting that implantation had indeed occurred (Fig. 3.6 A & B).

To further characterize this phenotype, RNA *in situ* hybridization was used to analyze the cell types present in the abnormal structured Lin9<sup>GT/GT</sup> implants. Therefore *Oct4*, a well studied epiblast marker, was applied to detect the developing embryo (Nichols et al., 1998; Pelton et al., 2002; Pesce and Scholer, 2000). First a part of *Oct4* cDNA was cloned into an expression vector and transcribed (MM 2.1.6). *Oct4 in situ* hybridization gave a strong signal in the epiblast, located in the distal region, of Lin9<sup>+/+</sup> and/or Lin9<sup>GT/+</sup> embryos, in stage 7.5 and 6.5 dpc. Interestingly, *Oct4* was completely absent in the presumed 6.5 dpc and genotyped 7.5 dpc Lin9<sup>GT/GT</sup> (Fig. 3.6). The visible disturbed structures could be remains of implanted extraembryonic tissue e.g. trophoblast giant cells. To emphasize the lack of the epiblast and to confirm the existence of only extraembryonic cells, *H19* was used as a hybridization probe (MM 2.1.6). *H19* gives the reciprocal pattern of expression to *Oct4* and is positive in all extraembryonic cell types in the early post-implantation embryo (Poirier et al., 1991). In normal implants, *H19* was expressed in the proximal region, as well as posterior and anterior throughout the adjacent areas to the epiblast. However, in the Lin9<sup>GT/GT</sup>, *H19* was expressed throughout the entire area corresponding to the implantation site (Fig. 3.6).

Consequently, there is no structure equivalent to the epiblast existing in the knockout Lin9 implants comparing *in situ* hybridizations with the HE staining.



### 3.2.4 Analysis of Apoptosis in $\text{Lin9}^{\text{GT/GT}}$ Embryos

Embryos which do not develop properly, will be quickly resorbed by the surrounding maternal tissue in the deciduas. TUNEL staining was performed to examine apoptosis on sections (MM 2.2.3.3). Apoptosis in the  $\text{Lin9}^{\text{GT/+}}$  and  $\text{Lin9}^{+/+}$  embryos stage 7.5 dpc was minor. Some positive cells are due to normal restructuring in the evolving embryonic tissue, which will be accomplished by the surrounding trophoblasts (Pampfer and Donnay, 1999). The TUNEL staining in the  $\text{Lin9}^{\text{GT/GT}}$  implants showed signs of apoptosis (Fig. 3.7 & Section 3.2.2). Many of the abnormal implants as well as surrounding cells were TUNEL positive, these areas could be the beginning of the resorption process. There are clear signs for apoptosis in the  $\text{Lin9}^{\text{GT/GT}}$  at stage 7.5 dpc.

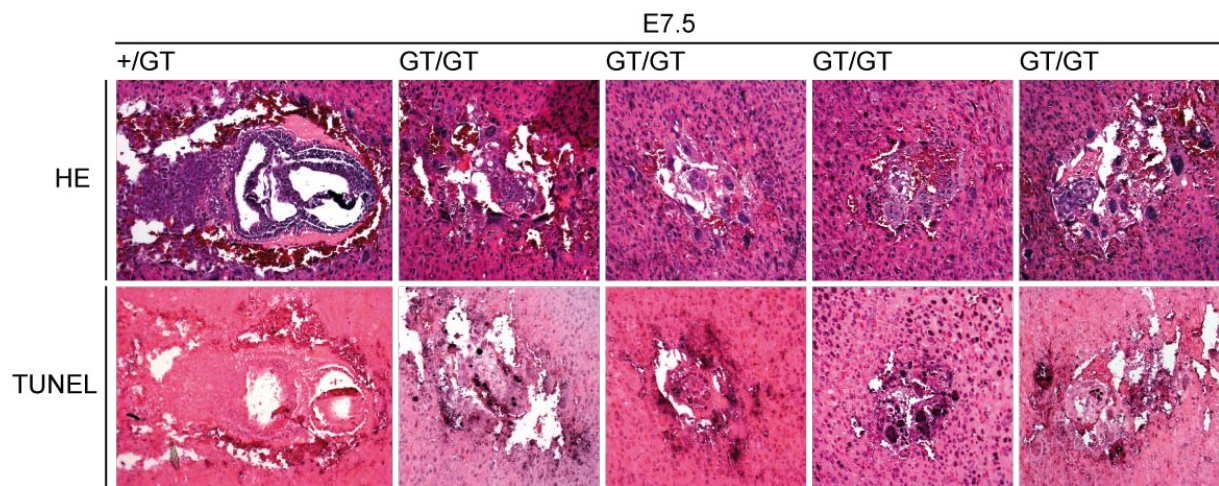


**Fig. 3.7: Apoptosis in  $\text{Lin9}$ -deficient embryos 7.5 dpc.** Histological sections from whole decidual swellings at 7.5 dpc resulting from  $\text{Lin9}^{\text{GT/+}}$  intercrosses were stained with HE and the TUNEL assay was performed, as indicated on the left. The first column shows sagittal sections through genotyped  $\text{Lin9}^{\text{GT/+}}$  embryos as mentioned on top. The next 4 columns depict sections from genotyped  $\text{Lin9}^{\text{GT/GT}}$  implant. Many of the  $\text{Lin9}^{\text{GT/GT}}$  implants were positive for apoptosis, stained in black.

### 3.2.5 Analysis of $\text{Lin9}^{\text{GT/GT}}$ Peri-implantation Phenotype

The presence of resorbed embryos implied that  $\text{LIN9}$ -deficient embryos are able to implant and then die shortly after implantation, which indicates a peri-implantation phenotype. To test whether the frequency of  $+/+$ ,  $\text{GT}/+$  and  $\text{GT}/\text{GT}$   $\text{Lin9}$  blastocysts obey the Mendelian ratio, first blastocysts derived from  $\text{Lin9}^{\text{GT/+}}$  crosses were genotyped (Tab. 3.1). As blastocysts consist of only 60-100 cells, a more sensitive TaqMan qPCR protocol was developed to genotype the  $\text{GT}$   $\text{Lin9}$  allele.

Therefore, one probe specific for *ngf* (nerve growth factor) to normalize with and another one specific for the  $\text{GT}$  allele at the *lacZ*/*neo* border within the integrated gene trap were designed (Fig. 3.5 A & MM 2.2.2.12). Both probes were labeled with different fluorescent dyes, which made it possible to run the TaqMan qPCR in one reaction. To establish this approach,

TaqMan PCRs were performed with  $\text{Lin9}^{\text{GT}/+}$  gDNA. Figure 3.8 A and B shows linear slope, which represents the annealing efficiency for the specific primers for *ngf* and *lacZ/neo*. The TaqMan PCR should be sensitive enough to detect differences of approximately 1 Ct, to be able to distinguish between GT/+ and GT/GT allelic situation in blastocysts. To verify this,  $\text{Lin9}^{\text{GT}/+}$  gDNA was mixed 1:1 with wt gDNA to dilute the GT allele relative to *ngf* (Fig. 3.8 C). The difference observed corresponded to the approximate 1  $\Delta\text{Ct}$  (*ngf* Ct - *lacZ/neo* Ct).

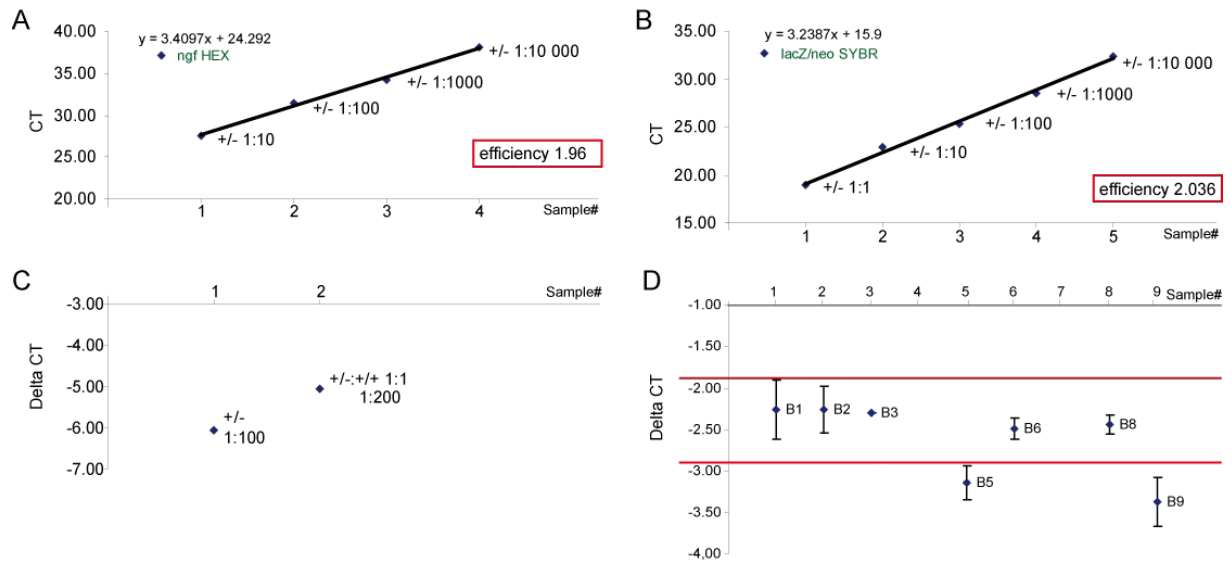


**Fig. 3.8: TaqMan qPCR approach to genotype blastocysts.** (A) & (B) Dilution of  $\text{Lin9}^{\text{GT}/+}$  gDNA to evaluate the primer annealing efficiency for *ngf* and *lacZ/neo*. Graph shows the linear slope. The efficiency was calculated  $E = 10^{(1/\text{slope})}$  (Pfaffl-method). To be sufficient this should be  $\sim 2$ . The efficiency is depicted in the boxes. (C) The difference of the two alleles should be 1  $\Delta\text{Ct}$  (*ngf* Ct - *lacZ/neo* Ct). Therefore  $\text{Lin9}^{\text{GT}/+}$  gDNA was mixed 1:1 with wt gDNA and the distance shows  $\sim 1 \Delta\text{Ct}$ . (D) Example of an evaluation with 9 blastocysts. The red bars indicate  $\sim 1 \Delta\text{Ct}$  distance to distinguish between the two populations.

To genotype blastocysts, they were flushed out of the uterus of pregnant mice at day 3.5. The blastocysts were washed carefully in several PBS drops and incubated for 2 hours at  $65^\circ\text{C}$  in 2  $\mu\text{l}$  of Tail buffer with Proteinase K. Next, the TaqMan qPCR was set up in triplicate. The example depicted in figure 3.8 D shows a typical result. Here 5 blastocysts (B1-3, 6 & 8) were genotyped as GT/+, 2 as GT/GT (B5 & B9) and 2 as +/+ *Lin9* (B4 & B7). Wt *Lin9* is not detectable since the *lacZ/neo* probe only hybridizes with the *lacZ/neo* locus in the GT allele.

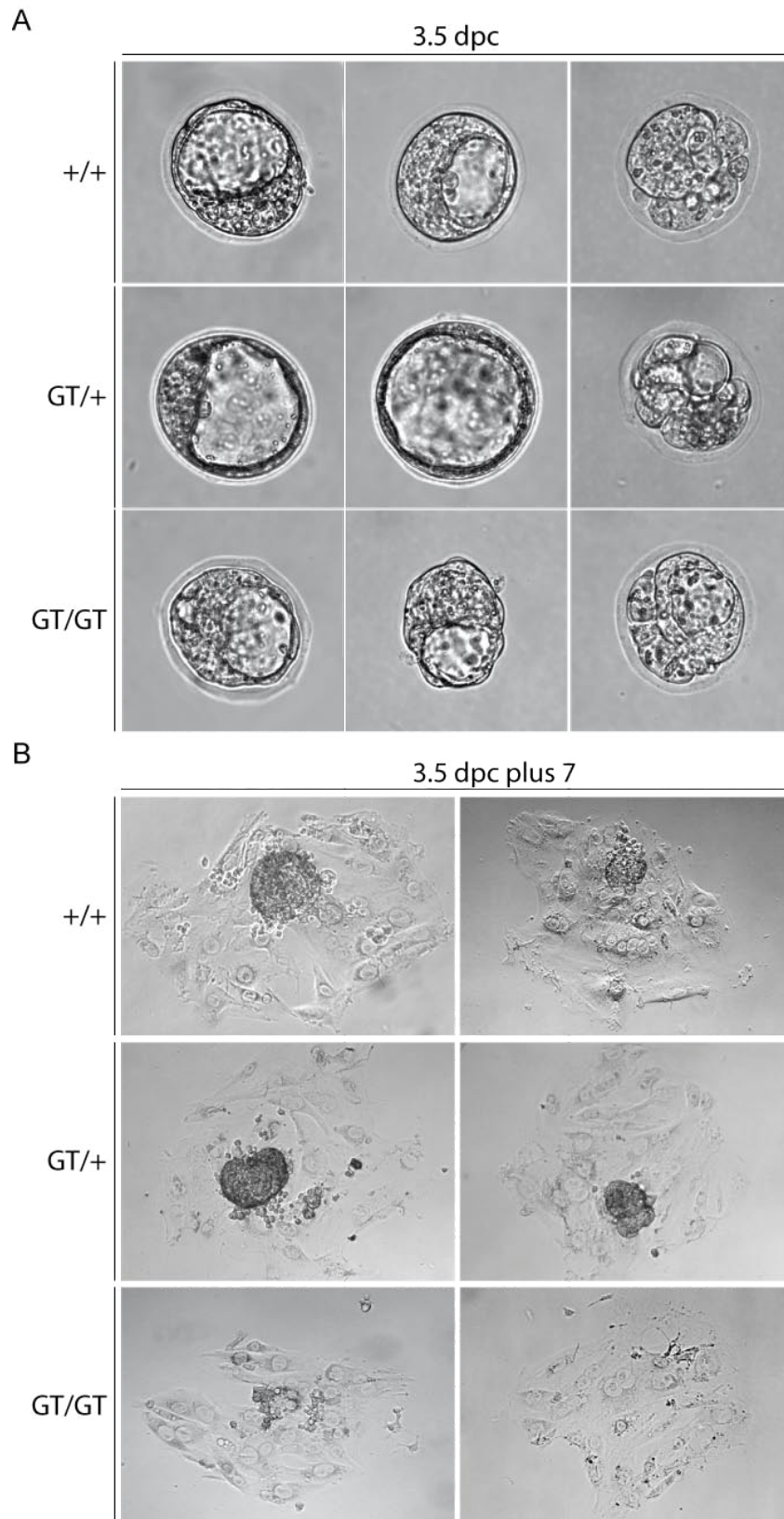


**Fig. 3.9: Phenotypical examination of blastocysts.** Images of blastocysts harvested at day 3.5 from  $\text{Lin9}^{\text{GT/+}}$  crosses. (A) Blastocysts at 3.5 dpc were documented and directly genotyped with TaqMan qPCR. The  $+/+$ ,  $\text{GT}/+$  and  $\text{GT}/\text{GT}$   $\text{Lin9}$  blastocysts looked indistinguishable (40X magnification). (B) Phase contrast images of blastocysts isolated at 3.5 dpc and cultured in vitro for 7 days (10X magnification). They were genotyped with TaqMan qPCR, as indicated.  $\text{Lin9}^{\text{GT}/\text{GT}}$  blastocysts showed no robust ICM upon the layer of trophoblast cells.

The analysis of 80 blastocysts, stage 3.5 dpc, from  $\text{Lin9}^{\text{GT}/+}$  crosses showed that roughly one quarter were  $\text{Lin9}^{\text{GT}/\text{GT}}$ . The Mendelian frequency reached nearly 100% (96.3% probability) (Tab. 3.1). These  $\text{Lin9}^{\text{GT}/\text{GT}}$  blastocysts are indistinguishable from  $\text{Lin9}^{+/+}$  blastocysts (Fig 3.9 A). Although some isolated blastocysts looked disorganized or smaller, this phenotype did not correlate with the knockout genotype.

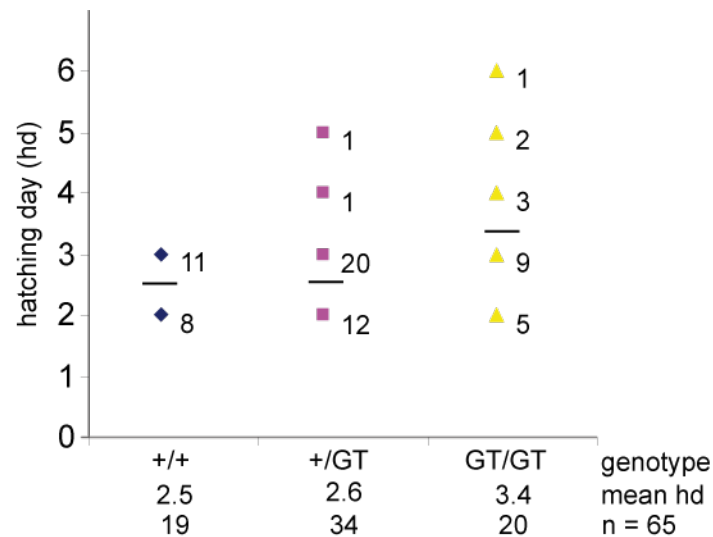


**Fig.3.10: Analyses of hatching behavior of blastocysts cultured *in vivo*.** Blastocysts harvested at day 3.5 from  $\text{Lin9}^{\text{GT}/+}$  crosses were monitored and documented each day. After several days of growing in culture, they were genotyped with TaqMan qPCR. The chart depicts the mean (black bar) and the individual (boxes) day of hatching, in comparison to the genotype. The number of individuals hatched at the indicated day is labeled (total  $n = 65$ ). ( $n = \text{number} \ \& \ \text{hd} = \text{hatching day}$ )

More blastocysts were harvested and cultured in ES-cell media for several days. The growth of the inner cell mass (ICM) and trophoblast layer was documented every 24 hours. The blastocysts hatched and attached to the dish. After growing up to 10 days in culture, the outgrowth was harvested and genotyped with TaqMan PCR.  $\text{Lin9}^{\text{GT}/+}$  and  $\text{Lin9}^{+/+}$  blastocysts displayed a relative robust growing ICM on a layer of trophoblasts (Fig. 3.9 B). In contrast, from  $\text{Lin9}^{\text{GT}/\text{GT}}$  blastocysts only trophoblast cells remained and no obvious ICM was left. In total, 65 blastocysts were successfully genotyped after monitoring them *in vitro*. However,  $\text{Lin9}^{\text{GT}/\text{GT}}$  blastocysts hatched on average one day later (at day 3.4) than their  $\text{Lin9}^{\text{GT}/+}$  and  $\text{Lin9}^{+/+}$  counterparts (at day 2.5), from their zona pellucida (Fig. 3.10).

In summary, all the data presented above suggests that the loss of  $\text{Lin9}$  leads to embryonic lethality at peri-implantation, and indicates that  $\text{LIN9}$  is required for proper formation of the epiblast (Tab. 3.1, Fig. 3.6 & Fig. 3.9).



### 3.2.6 Analysis of *Lin9* mRNA Expression in Blastocysts

The presence of resorbed embryos indicated that LIN9-deficient embryos are able to implant, but die shortly after implantation. One question remaining is whether *Lin9* is expressed in blastocysts and therefore could be involved in establishing the well regulated evolving cell lineage of the epiblast. To test this I examined *Lin9* mRNA expression in wt blastocysts 3.5 dpc. *Oct4* a well studied epiblast marker was applied as a positive control (Section 3.2.3). The blastocysts were flushed out of the uterus of 3.5 and 4.5 dpc pregnant mice, fixed and incubated with DIG-labeled probes. *Lin9* mRNA was evident in the entire ICM of 3.5 and 4.5 dpc blastocysts. Additionally it is expressed in the trophoectodermal cell in late blastocysts (Fig. 3.11).

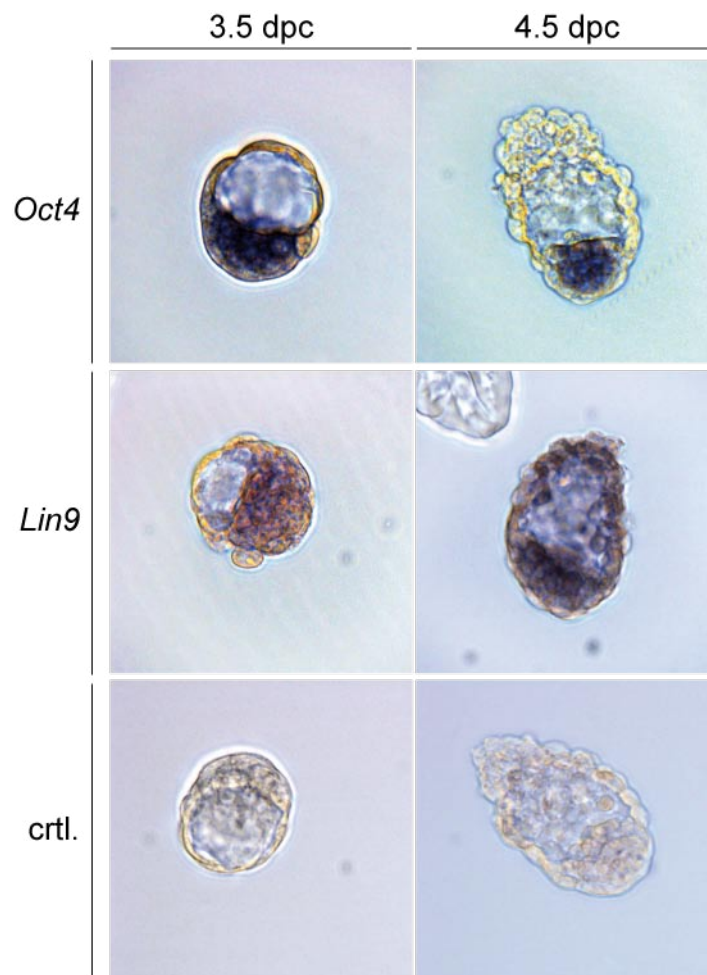


**Fig. 3.11: *Lin9* expression in blastocysts is ICM-predominant.** Blastocysts stage 3.5 and 4.5 dpc from wt crosses were prepared and *in situ* hybridization with *Oct4* and *Lin9* DIG-labeled probes was performed (stage and probe as mentioned in the panel). As a control untreated blastocysts are shown. *Oct4* probe was used to compare *Lin9* to a known ICM-predominant expression. The *Lin9* probe shows a very similar expression pattern in the early blastocysts and even higher expression in the trophoectoderm in the later stages 4.5 dpc.



### 3.2.7 Analysis of GT Lin9 Heterozygous MEFs

To further analyze LIN9 function in the mouse, an *in vitro* cell culture system was utilized. Primary murine embryonic fibroblasts (MEFs) were prepared from 13.5 dpc embryos (MM 2.2.1.1). Since Lin9-deficient embryos are lethal at peri-implantation stages, only Lin9<sup>+/+</sup> and Lin9<sup>GT/+</sup> MEFs could be established. From previous experiments in our lab in human cell lines, it is known that human LIN-9 is involved in the regulation of genes that ensure the progression through G2/M phase of the cell cycle (Osterloh et al., 2007). To monitor if this is also the case in Lin9<sup>+/+</sup> and Lin9<sup>GT/+</sup> MEFs, their flow cytometry profiles (FACS) of asynchronously growing MEFs at passage 4 were compared. Lin9<sup>GT/+</sup> cells show no alteration of the cell cycle (Fig. 3.12 A). Late passage MEFs (P6 shortly before they undergo crisis) were also monitored but no differences occurred (data not shown).

The proliferation ability of the Lin9<sup>+/+</sup> and Lin9<sup>GT/+</sup> MEFs was analyzed. MEF were plated  $1 \times 10^4$  in triplicates in 24-well plates and fixed at different time points as indicated in figure 3.11 B. The plotted growth rate revealed no significant difference in proliferation ability between Lin9<sup>+/+</sup> and Lin9<sup>GT/+</sup> cells.

Next Lin9<sup>+/+</sup> and Lin9<sup>GT/+</sup> MEF lysates were prepared to compare their level of LIN9 protein. The wt lysate was diluted to compare to 100% lysate from Lin9<sup>GT/+</sup> cells. The lysates were immunoprecipitated with antisera against human LIN-9. Bound mouse wt LIN9 was detected by immunoblotting (Fig. 3.12 C). LIN9 protein levels are only slightly reduced (75-100%) in GT heterozygous MEFs compared to LIN9 in wt MEFs. Additionally *Lin9* expression was examined by qPCR with primers that exclusively detect the GT or wt mRNA. Moreover it was analyzed whether these Lin9<sup>GT/+</sup> MEFs display any effects on known target gene expression, such as *cdc2a* and *Birc5*. However, only a marginal decrease in *Lin9* mRNA was observed and no alteration in *cdc2a* and *Birc5* expression (MM 2.1.5; data not shown).

In summary, examination of the *in vitro* characteristics of Lin9<sup>GT/+</sup> MEFs relative to their Lin9<sup>+/+</sup> counterparts revealed no significant differences neither in cell cycle profiles, growth rates, protein levels nor in RNA expressions.

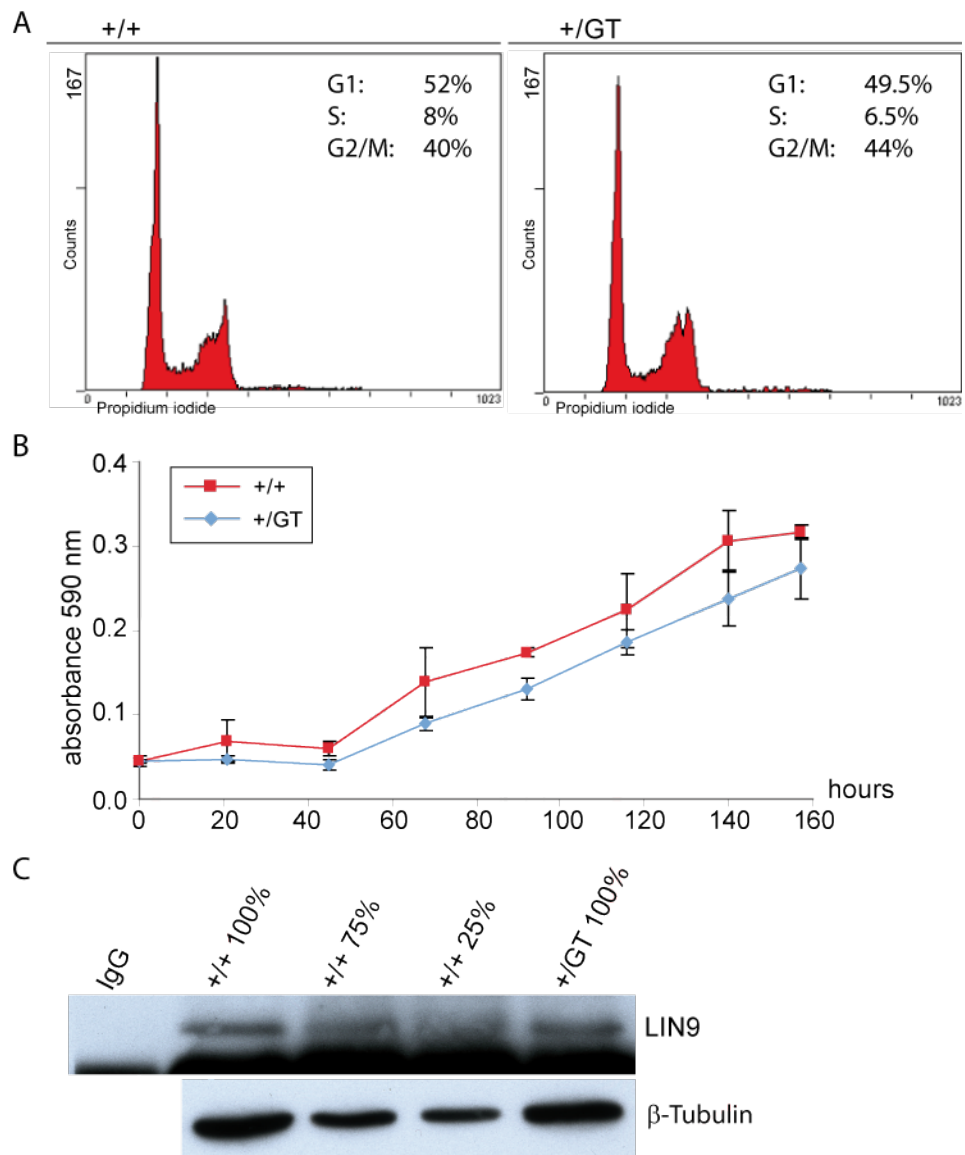


**Fig. 3.12: Analysis of Lin9<sup>GT/+</sup> MEFs.** (A) FACS analysis of Lin9<sup>+/+</sup> and Lin9<sup>GT/+</sup> MEFs are indistinguishable. MEFs asynchronously growing in passage 4 were compared. DNA content was determined by intensity of intercalated PI (Propidium iodide). Percentage of cells within each cell cycle phase is indicated. (B) Population growth rates of Lin9<sup>+/+</sup> and Lin9<sup>GT/+</sup> MEFs. (D) Immunoblot showing that LIN9 protein levels are only slightly reduced in Lin9<sup>GT/+</sup> MEFs as compared to LIN9 in wt. IgG was used as a negative control for the IP,  $\beta$ -Tubulin as loading control, dilution as indicated above.

### 3.3 Generation of a Conditional Lin9 Knockout Mouse Model

From these analyses of the  $\text{Lin9}^{\text{GT}/+}$  intercrosses, we knew that no embryos with Lin9 knockout are detectable at 9.5 dpc or stages beyond (Section 3.2). Due to this early embryonic lethality around peri-implantation, these mice are only of limited use for defining the functional role of LIN9 in adult mice *in vivo*. Furthermore in *in vitro* studies,  $\text{Lin9}^{\text{GT}/+}$  MEFs showed no significant differences and due to the peri-implantation phenotype, it is not possible to obtain  $\text{Lin9}^{\text{GT}/\text{GT}}$  MEFs. For this reason, a conditional knockout mouse model was designed and generated.

#### 3.3.1 Construction of the Conditional Lin9 Knockout

A targeting vector was created to "floxed" exon 7 of the Lin9 gene. This vector contained a  $\beta$ -geo selection cassette flanked by site-specific FRT recombination sites in intron 7 (Fig. 3.13 A). To clone the left and right homologous recombination regions, genomic Lin9 sequences were obtained by PCR of gDNA from 129-derived ES cells (129/OlaHsd). Exon 7 and its flanking regions were step-wise inserted into a vector backbone already containing the appropriate loxP recombination sites (pBS246 (loxP)). Next the  $\beta$ -geo selection cassette flanked by FRT sites was first excised from pBS-2FRT-IRES/ $\beta$ -geo and inserted into the right homologous recombination region, intron 7 (Suppl. Fig. 7.1 A, B & C).

After integration into the Lin9 locus, this construct will give rise to a bicistronic mRNA that is transcribed from the endogenous Lin9 promoter. Thus the expression of the neomycin selection gene will depend on the endogenous expression of *Lin9* in ES cells. Lin9 expression in ES cells was confirmed by RT-PCR (Fig. 3.14 A). The selection cassette can be removed *in vivo* from the conditional allele (co) with the site-specific recombinase FLPe by crossing animals harboring the modified conditional Lin9 allele with a FLPe expression deleter strain (Fig. 3.13 B & (Farley et al., 2000)). This *in vivo* approach was administered to avoid an additional transient transfection with FLP-recombinase, followed by a second round of selection to screen for ES cell clones with the desired deletion. Additional manipulations of the ES cells would have been very time consuming and are risky, concerning their capacity to later contribute to the germ line in resulting chimeras (Schwenk et al., 1995). After the correct removal of the  $\beta$ -geo selection cassette, exon 7 will be flanked by only the loxP sites and one remaining FRT site in intron 7; termed floxed allele (fl). The final site-specific Cre-mediated excision of exon 7, delta-floxed allele ( $\Delta$ fl), (either in mice or in MEFs) will be accompanied

with a frame shift, which will lead to a termination codon in exon 8 and a truncated protein of 195 amino acids, so that no functional LIN9 will be produced beyond exon 7 (Fig. 3.13 C).

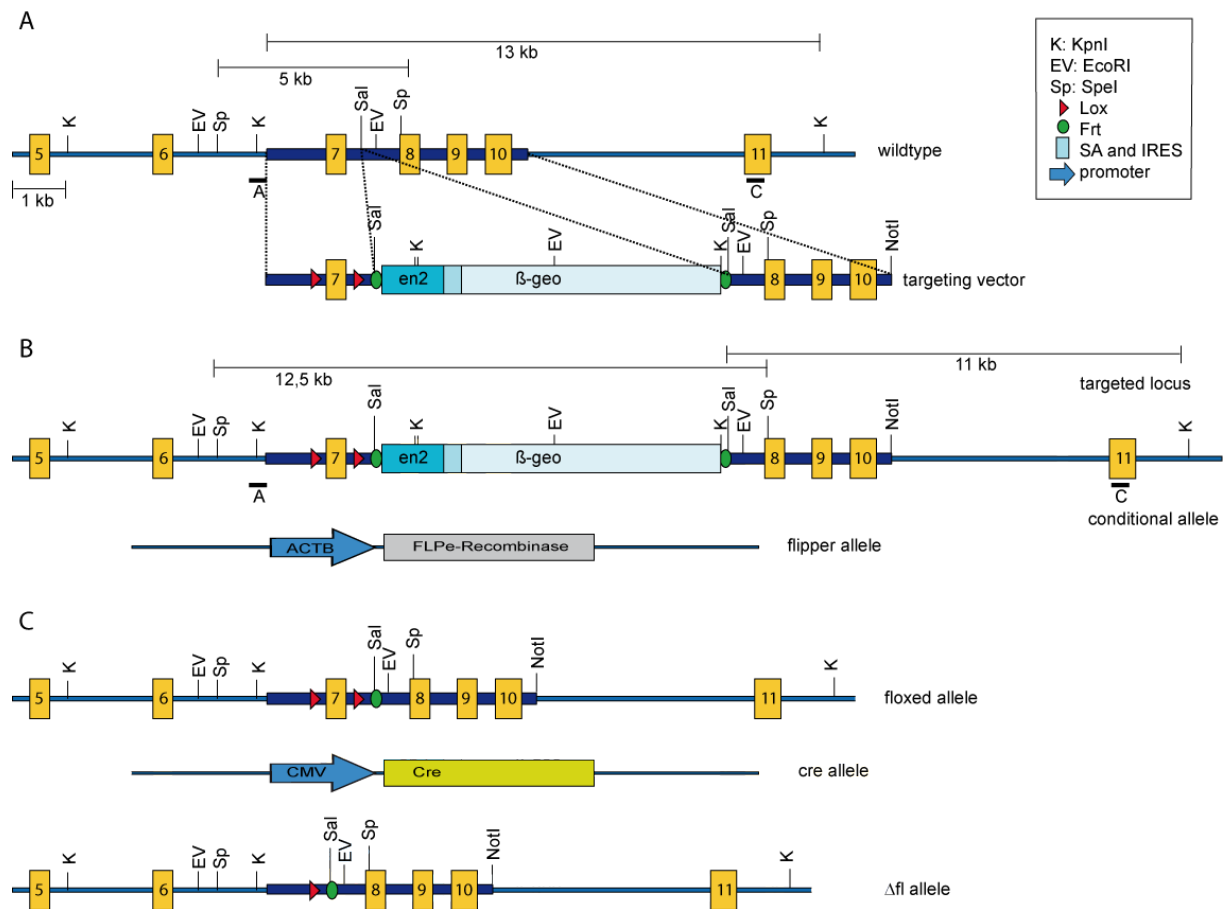


**Fig. 3.13: Generation of a conditional Lin9 knockout mouse.** Scheme of the conditional Lin9 targeting strategy. (A) Wt Lin9 allele and targeting vector are illustrated. The dashed lines represent the regions for homologous recombination. The targeting vector consists of 2 Lin9 homologous regions (dark thick blue), the floxed exon 7 and the FRT flanked  $\beta$ -geo selection cassette (light blue). (B) The recombination results in the conditional allele. The selection cassette can be excised with e.g. FLPe recombinase. The fragment sizes of the alleles are indicated in the above scheme, if restricted with Spe I or Kpn I for Southern blot probe A or C, respectively. The position of the Southern probes as well as the restriction sites are indicated. (C) Only the loxP sites flanking exon 7 and one FRT site remained in the floxed allele. The exon can be deleted by the Cre recombinase *in vivo* and *in vitro* (here illustrated with a cre-deleter allele e.g. under the control of the CMV promoter).

### 3.3.2 Generation of Conditional Knockout Mice

129-derived ES cells were transfected with the targeting vector, selected with neomycin and grown in culture (PolyGene). Positive ES cell clones were identified by Southern blot, using two different probes located upstream and downstream of the integration site, probe A and C, respectively (probe A; Suppl. Fig.7. 1 D). Probe C detects a fragment of ~13 kb in ES cell gDNA, restricted with Kpn I corresponding to the wt allele. In correctly targeted ES cell clones, probe C detects an additional band ~11 kb (Fig. 3.14 B).

Next, a properly targeted ES cell clone was injected in C57BL/6 blastocysts to generate chimeras (PolyGene). Several chimeric males were obtained and crossed with C57BL/6

females. Genotyping of their agouti progenies with Southern blot and PCR showed that the mutant allele was successfully transmitted to the germ line. A Southern blot example from tail gDNA with probe C is depicted in Fig.3.14 C. The Co-PCR detects the conditional and the wt allele (Fig. 3.14 D; Suppl. Fig. 7.2 & 7.3).

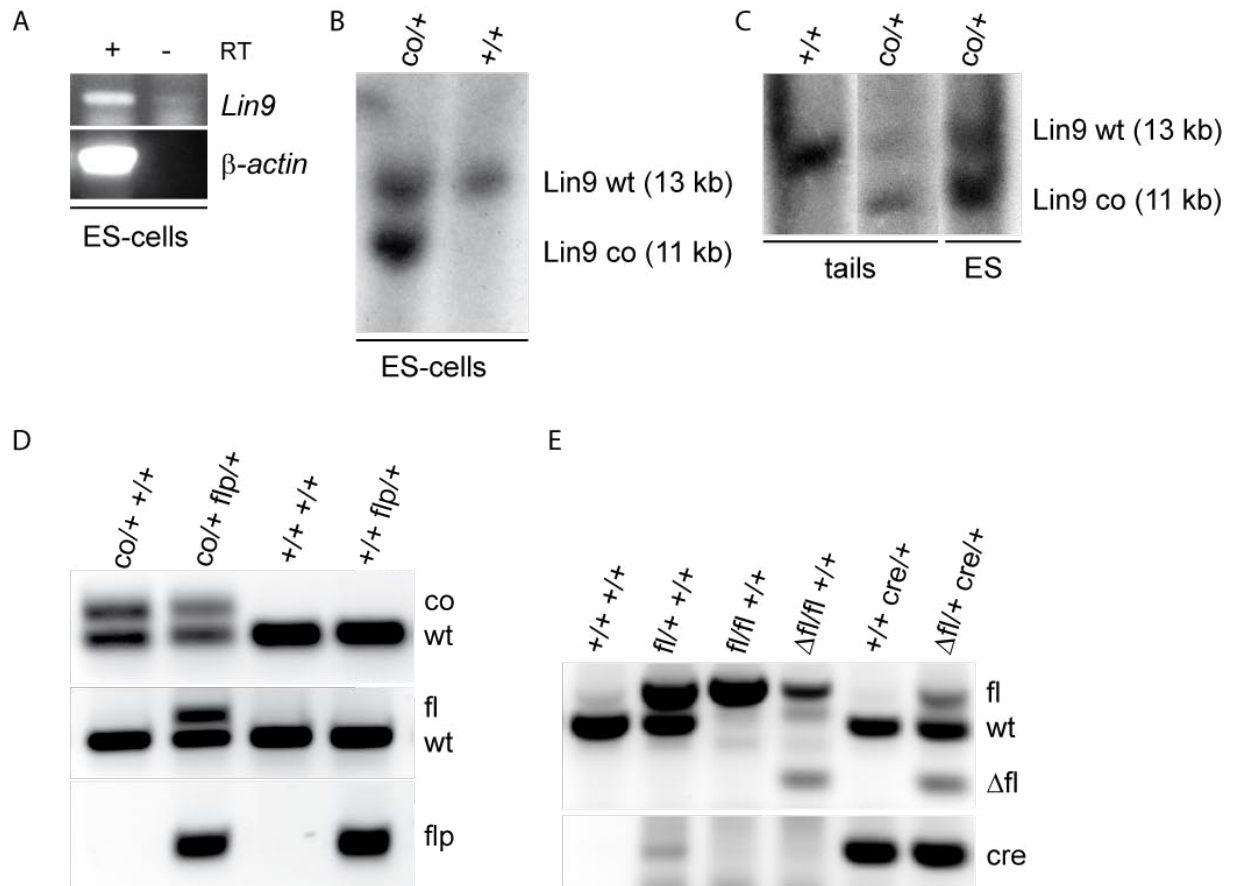


**Fig. 3.14: Generation of a conditional *Lin9* knockout mouse *in vivo*.** (A) RT-PCR result for *Lin9* expression in ES cells.  $\beta$ -actin was used as a loading control (B) Southern blot analysis of ES cell gDNA which was restricted with Kpn I and detected with radioactive labeled probe C. The alleles and their sizes are indicated on the right. (C) Southern blot analysis of tail gDNA which was restricted with Kpn I and detected with probe C. ES gDNA was used as a control. The alleles and their sizes are indicated on the right. (D) PCRs for tail lysates: 1<sup>st</sup> row the Co-PCR detected the *co* (298 bp) and *wt* (192 bp) *Lin9* allele, 2<sup>nd</sup> row FRT-PCR for *fl* (624 bp) and *wt* (498 bp) and 3<sup>rd</sup> row Flp-PCR detected the *flp* (725 bp) allele. (E)  $\Delta$ FI-PCR example for the 2 primer based strategy with the possibility to detect all 3 different products, the *wt* (541 bp), the *fl* (770 bp) and the  $\Delta$ *fl* (289 bp) allele. Bottom row shows Cre-PCR (~400 bp). (The position of all the primers is depicted in the sequence cutout shown in Suppl. Fig. 7.2 & 7.3; MM 2.1.5.)

To remove the  $\beta$ -geo selection cassette, animals carrying the *Lin9*<sup>*co/+*</sup> allele were bred with FLPe expressing deleter mice (Rodriguez et al., 2000). The progenies were genotyped by FRT-PCR, to detect the *fl* and the *wt* allele. In addition, a PCR for the FLPe allele was performed (Fig. 3.14 D, bottom row). The sequence of the *fl* *Lin9* allele was confirmed by cloning the PCR product and sequencing. As expected, exon 7 is flanked by loxP sites and a single FRT site remains in intron 7. The *Lin9*<sup>*fl/+*</sup> animals were intercrossed and bred to homozygosity (*fl/fl*). These *Lin9*<sup>*fl/fl*</sup> mice are phenotypically normal and fertile, indicating that the loxP sites do not interfere with the normal processing of the *Lin9* mRNA.

Next it was very important to prove that exon 7 can be deleted by introducing Cre recombinase *in vivo*. Therefore  $\text{Lin9}^{\text{fl/fl}}$  mice were bred with an early Cre expressing deleter strain, which is under the control of the CMV promoter and located on the X-chromosome (Schwenk et al., 1995). The Cre-mediated excision of exon 7 results in deletion of the exon 7 ( $\Delta\text{fl}$  allele), as shown by  $\Delta\text{Fl}$ -PCR (Fig. 3.14 E; Suppl. Fig. 7.2 & 7.3). Additionally a PCR for the Cre allele was performed (Fig. 3.14 E, bottom row).

To test whether removal of exon 7 results in a null allele, animals heterozygous for the  $\Delta\text{fl}$  allele ( $\text{Lin9}^{\Delta\text{fl}/+}$ ) were intercrossed. Genotyping indicated that no  $\text{Lin9}^{\Delta\text{fl}/\Delta\text{fl}}$  animals were born (Tab. 3.2). Thus deletion of exon 7 by Cre-recombinase results in embryonic lethality. It can be concluded that deletion of exon 7 disrupts the function of LIN9 in a comparable manner to the GT allele described above (Section 3.2.8).

| Stage    | Total           | Genotype |                       |                                   | Fail. <sup>b</sup> | DF | Value  | Prob.  |
|----------|-----------------|----------|-----------------------|-----------------------------------|--------------------|----|--------|--------|
|          |                 | fl/fl    | fl/ $\Delta\text{fl}$ | $\Delta\text{fl}/\Delta\text{fl}$ |                    |    |        |        |
| Weanling | 61 <sup>a</sup> | 26       | 57                    | 0                                 | 4                  | 2  | 24.158 | 0.0006 |

**Tab. 3.2: Genotypic analysis of  $\text{Lin9}^{\Delta\text{fl}/+}$  intercrosses.** Genotypes were determined by  $\Delta\text{Fl}$ -PCR<sup>a</sup> on tail biopsies. PCR failures<sup>b</sup> were not counted. The Chi Square test was applied with two degrees of freedom (DF).

To briefly summarize these findings, a conditional  $\text{Lin9}$  mouse model was generated. The selection cassette was successfully removed *in vivo*. Animals homozygous for the floxed  $\text{Lin9}$  allele ( $\text{Lin9}^{\text{fl/fl}}$ ) develop normally, which indicates that the loxP sites do not interfere with the function of  $\text{Lin9}$ . Floxed exon 7 can be deleted *in vivo* by crossing with early Cre-deleter mice. No homozygous  $\Delta\text{fl}$   $\text{Lin9}$  animals ( $\text{Lin9}^{\Delta\text{fl}/\Delta\text{fl}}$ ) could be observed. This proves that the excision of exon 7 disrupts the function of LIN9. Finally we had the tool to overcome the early embryonic lethality, and to further study the role of LIN9 *in vivo* and *in vitro*.

### 3.3.3 Analysis of $\text{Lin9}^{\text{fl/fl}}$ MEFs with Cre-Infection

First a cohort of  $\text{Lin9}^{\text{fl}/+}$  animals was established. All the experiments mentioned in this part and the following section were conducted in animals and MEFs resulting from a mixed genetic background, in F1 or F2 (129 x C57BL/6). To generate MEFs homozygous for the floxed  $\text{Lin9}$  allele, timed pregnancies of  $\text{Lin9}^{\text{fl}/+}$  intercrosses were prepared. With this set up,  $\text{Lin9}^{\text{fl/fl}}$  MEFs as well as  $\text{Lin9}^{+/+}$  control MEFs from the same litter were generated.

To delete  $\text{Lin9}$  in MEFs, retroviral infections with recombinant virus carrying a Hit and Run Cre-recombinase (HR-Cre; (Silver and Livingston, 2001)) were performed. To exclude any toxic effects Cre expression may have, this particular HR-Cre will self-excite once the critical

level of expression required is reached. Passage 3  $\text{Lin9}^{\text{fl/fl}}$  and  $\text{Lin9}^{+/+}$  MEFs were infected with HR-Cre viral supernatant, parallel to a control infection with H2B-GFP. Exon 7 was successfully deleted in the HR-Cre infected cells after double infection and ~48 h recovery, confirmed with  $\Delta\text{fl}$ -PCR (Fig. 3.15 A; MM 2.2.1.4).

Next the protein level as well as the RNA expression of *Lin9* was examined in these MEFs. First, to compare their LIN9 amount and visualize the knockout effect on protein level, protein lysates from the infected MEFs were prepared, after a ~48 h recovery period post infection. The lysates were immunoprecipitated with antisera against human LIN-9. Bound mouse wt LIN9 was detected by immunoblotting (Fig. 3.15 B). LIN9 protein levels are significantly reduced in the HR-Cre infected  $\text{Lin9}^{\text{fl/fl}}$  MEFs compared to their  $\text{Lin9}^{+/+}$  counterparts and control infections.

Second RNA from these MEFs was prepared and RT-PCR was performed. The expression for *Lin9* was analyzed by qPCR with primers specific for the undeleted exon 7 (Fig. 3.15 C, Suppl. Fig. 7.2; MM 2.1.5). There was a decrease of about 80% in *Lin9* expression in the HR-Cre treated  $\text{Lin9}^{\text{fl/fl}}$  MEFs compared to control cells.

Finally these MEFs were further monitored and their proliferation ability was analyzed. The infected MEFs were replated  $1 \times 10^4$  in triplicate in 24-well plates. The population growth rates revealed only slight differences in proliferation ability between the HR-Cre infected  $\text{Lin9}^{\text{fl/fl}}$  MEFs and the control cells (data not shown). Hence, in repeated experiments there was a tendency for the *Lin9*-deficient cells to proliferate slower, but in the end these knockout cells seemed to recover and were nearly as dense as the control cells. Thus it is possible that retroviral expression of HR-Cre was not as efficient enough to delete LIN9 in the whole cell population.

To test this idea,  $1 \times 10^4$  MEFs were plated onto 10 cm dishes. gDNA was isolated at different time points after Cre-mediated deletion of exon 7 (24 hours, 7 days and 3 weeks). The genotype was determined by  $\Delta\text{fl}$ - and Cre-PCR (Fig 3.15 D). In the initial cell population, deletion of exon 7 was detected. At later time points the floxed allele returned and the deleted exon 7 disappeared and was nearly undetectable in PCRs from cells harvested 3 weeks post-infection. This indicates that the  $\text{Lin9}^{\Delta\text{fl}/\Delta\text{fl}}$  MEFs have a growth disadvantage, and that, over time, they are overgrown by the cells still harboring the intact *Lin9* allele.

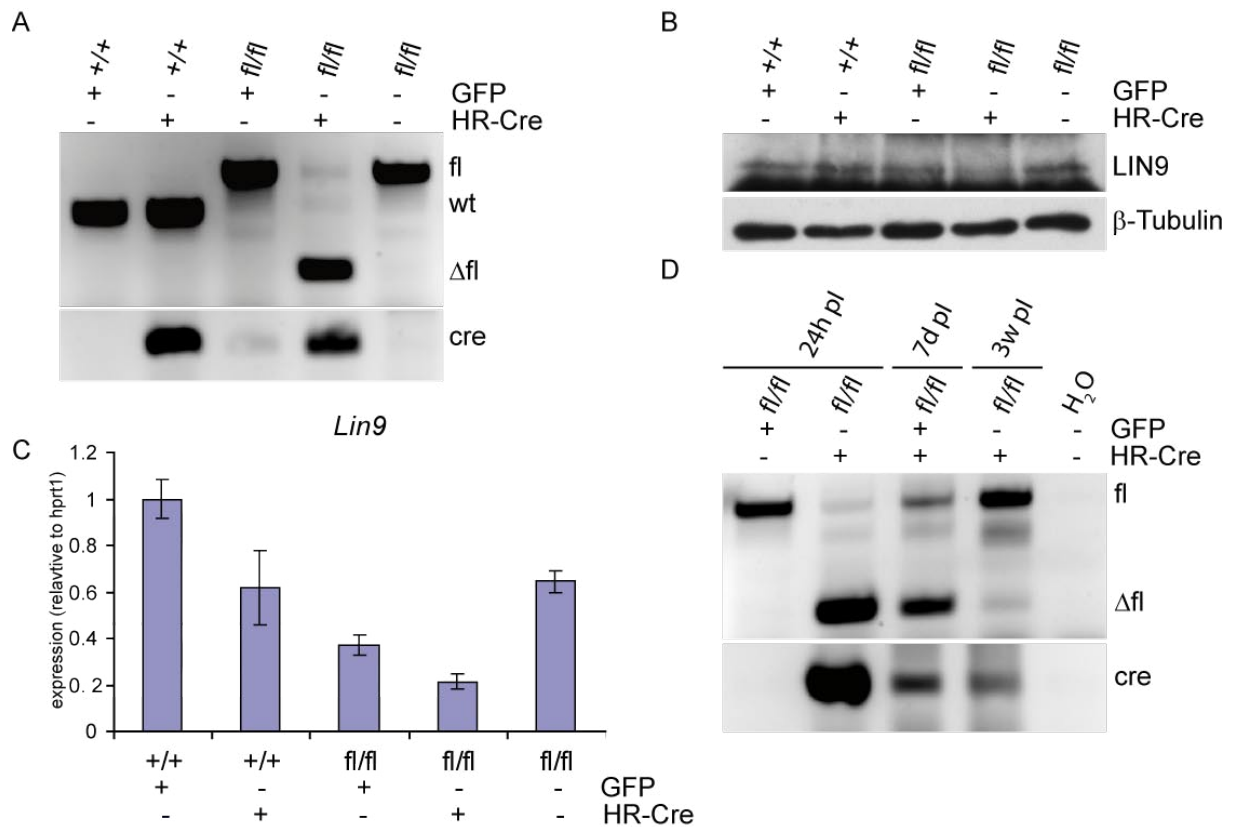


**Fig. 3.15: Analysis of  $Lin9^{fl/fl}$  MEFs infected with HR-Cre.** MEFs were treated twice with HR-Cre viral supernatant. Experiments were performed ~48 h post-infection. H2B-GFP was used as control infection. (A)  $\Delta$ FI-PCR which detects all 3 different alleles, wt (541 bp), fl (770 bp), and  $\Delta$ fl (289 bp). Bottom row shows Cre-PCR (~400 bp). (B) Immunoblot showing that LIN9 protein level is reduced in HR-Cre positive cells.  $\beta$ -Tubulin used as a loading control. (C) Expression of *Lin9* was analyzed with RT-PCRs in asynchronously growing MEFs. The wt control infected cells were set to one. (D)  $\Delta$ FI-PCR at 3 different time points indicated above. Bottom row shows Cre-PCR. (The position of all primers is shown in Suppl. Fig. 7.2; MM 2.1.5.)

Taken together, these experiments showed that the generation of  $Lin9^{fl/fl}$  MEFs was successful and that exon 7 can also be deleted *in vitro*. The deletion seemed very efficient and the  $Lin9$ -deficient MEFs displayed a growth defect. Since these  $Lin9^{\Delta fl/\Delta fl}$  MEFs were overgrown by  $Lin9^{fl/fl}$  cells which remained after infection, a different system to more effectively delete exon 7 was established.



### 3.3.4 Analysis of $\text{Lin9}^{\text{fl/fl}}$ $\text{Cre-ER}^{\text{T2}}$ MEFs

$\text{Lin9}^{\text{fl/fl}}$  mice were crossed with mice harboring inducible  $\text{Cre-ER}^{\text{T2}}$ . These transgenic mice express Cre-recombinase that has been fused to a mutated ligand-binding domain of the mutant human estrogen receptor ( $\text{ER}^{\text{T2}}$ ) resulting in a tamoxifen-inducible Cre-recombinase. The  $\text{Cre-ER}^{\text{T2}}$  allele is located in the ROSA26 locus and is more efficiently induced in cell culture than the classical  $\text{Cre-ER}^{\text{T}}$  allele ((Feil et al., 1997; Hameyer et al., 2007), Fig. 3.13 C).  $\text{Cre-ER}^{\text{T2}}$  is activated by administering 4-hydroxytamoxifen (4-OHT/tamoxifen) (MM 2.2.1.6).

To generate  $\text{Lin9}^{\text{fl/fl}}$  MEFs harboring  $\text{Cre-ER}^{\text{T2}}$ , timed pregnancies of  $\text{Lin9}^{\text{fl/+}}$  and  $\text{Cre-ER}^{\text{T2}}$  intercrosses were set up. Thereby  $\text{Lin9}^{\text{fl/fl}}$  as well as  $\text{Lin9}^{\text{+/+}}$  MEFs were received which carried one  $\text{Cre-ER}^{\text{T2}}$  allele. The MEFs were plated in passage 3, at a density of  $5.5 \times 10^5$  cells per 10 cm dish, 1 day prior to the 48 h treatment with 1  $\mu\text{M}$  tamoxifen. After ~60 h recovery in fresh media the cells were harvested to perform PCR. Exon 7 was successfully deleted, compared to control MEFs (Fig. 3.16 A).

Next, *Lin9* mRNA expression was examined in these MEFs. The level of *Lin9* was measured with primers specific for the undeleted exon 7 (Suppl. Fig. 7.2; MM 2.1.5). A reduction of about 95% on mRNA level was detected (data not shown).

To analyze the proliferation ability of 4-OHT induced compared to uninduced cells, MEFs were treated as mentioned above and plated, after ~8 h recovery, at a density of  $1 \times 10^4$  in triplicate in 24-well plates. The triplicates were harvested at the indicated time points. The population growth rates revealed a significant proliferative arrest for the  $\text{Lin9}^{\Delta\text{fl}/\Delta\text{fl}}$  MEFs (Fig. 3.16 B). They proliferated only minimally compared to the control cells. Importantly, 4-OHT treatment had no effect on the growth of  $\text{Lin9}^{\text{+/+}}$  MEFs.

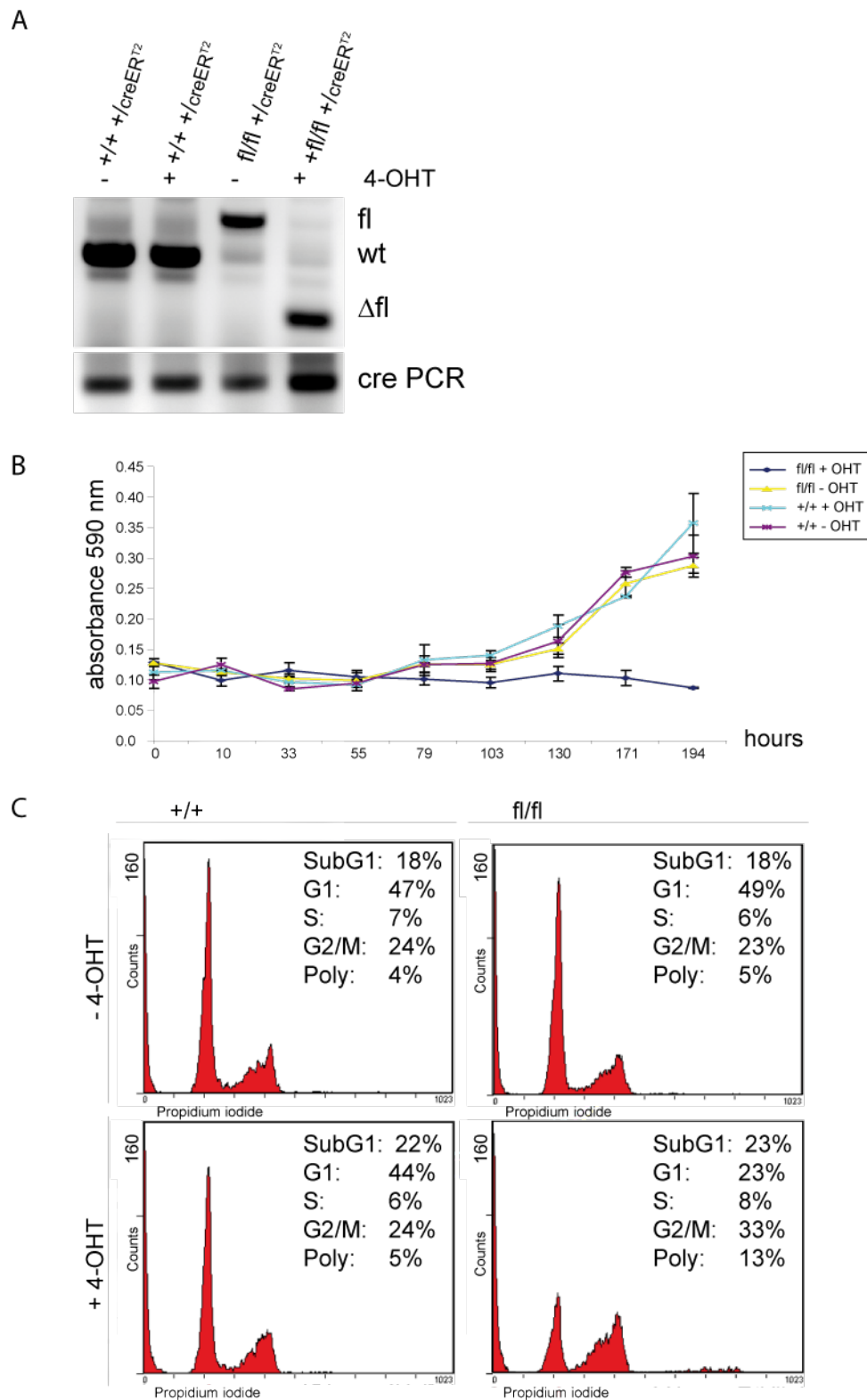


**Fig. 3.16: Analysis of  $Lin9^{fl/fl}$  Cre-ERT2 MEFs.** MEFs in P3 were treated with  $1\mu\text{M}$  4-OHT for 48 h and recovered for 60 h, if not mentioned otherwise. (A)  $\Delta\text{fl}$ -PCR detected all 3 alleles, the wt, fl and  $\Delta\text{fl}$ . Bottom row shows Cre-PCR, all cells are as expected CreER<sup>T2</sup> positive. (The position of all the primers is depicted in Suppl. Fig. 7.2 & MM 2.1.5) (B) Population growth rates of  $Lin9^{fl/fl}$  and  $Lin9^{+/+}$  MEFs, in passage 4, treated and untreated. The cells were plated in 24-wells 8 h after treatment. (C) FACS analyzes of the un- and induced  $Lin9^{fl/fl}$  and  $Lin9^{+/+}$  MEFs were asynchronously growing. The DNA content was determined by intensity of intercalated PI. The numbers indicate the percentage of cells in each phase of the cell cycle and additionally the SubG1 and polyploidy cells.

To monitor the cell cycle of these *Lin9*-deficient MEFs, their flow cytometry profiles compared to untreated and *Lin9*<sup>+/+</sup> cells were analyzed. Therefore MEFs were grown asynchronously and treated with 4-OHT as mentioned above. Cells were collected after ~60 h recovery, fixed, stained with propidium iodide, and analyzed by flow cytometry. *Lin9*<sup>Δfl/Δfl</sup> MEFs showed an obvious accumulation in G2/M phase of the cell cycle, 33% versus 23% in control cells (Fig. 3.16 C). This is accompanied by changes for the G1 phase and the S phase, from 49% to 23% and 6% to 8%, respectively, in untreated versus treated *Lin9*<sup>fl/fl</sup> cells. Additionally, the counts for cells in SubG1, which marks apoptotic cells, as well as polyploidy, clearly increased. The alteration for SubG1 is due to the 4-OHT treatment, 23% in the *Lin9*<sup>Δfl/Δfl</sup> cells compared to 22% in *Lin9*<sup>+/+</sup> MEFs. However, the increase in polyploid cells is solely seen in 4-OHT treated floxed MEFs, from 5% in uninduced to 13% in induced cells.

In summary, deletion of the floxed *Lin9* allele, created with a tamoxifen inducible Cre-recombinase (Cre-ER<sup>T2</sup>), was highly efficient. On RNA levels, it lead to an almost complete knockout of *Lin9*. The examination of the *in vitro* characteristics of these *Lin9*<sup>Δfl/Δfl</sup> MEFs, relative to the controls, revealed a significant impact upon cell cycle distribution and growth rates. Why the *Lin9*<sup>Δfl/Δfl</sup> MEFs arrest in G2/M and whether they will overcome the loss of their proliferation ability remains unclear and needs further investigation.

## 4 DISCUSSION

### 4.1 Expression of *Lin* mRNA in the Mouse

There are numerous *in vivo* analyses contributing to our understanding of transcriptional regulation in different cells, tissues and in the development of whole organisms, such as pRB and E2F4 knockout mouse models. Similar to these proteins, the newly identified LINC complex was first mainly analyzed in cell culture based model systems. LIN9 is one of the most interesting components of the LINC core module, but so far nothing is known about its function *in vivo*. LIN9 is not only involved in transcription, but in association with pRB it may also promote differentiation. Therefore, the aim of this study was to analyze the role of Lin9 in mouse development.

First, *Lin9* mRNA expression was analyzed in mice. *Lin9* is ubiquitously expressed in all tested adult mouse organs and throughout embryogenesis (7.5 to 16.5 dpc). Its expression is highest in thymus, testis and spleen, which are highly proliferative tissues (Fig. 3.1). *B-Myb*, *Lin52*, *Lin54* and *Lin37*, other members of the human LINC complex, are also ubiquitously expressed in adult organs, with highest expression in the testis. Only *Lin52* mRNA has higher expression in muscle tissue and in the lung; and *Lin37* was additionally detected in the ovary. Interestingly, *Lin52* expression is highest during embryonic stages 12.5 and 14.5 dpc, which are the main phases of organogenesis and differentiation. These LINC members may have an additional role in these tissues.

Moreover, *Lin* and *B-Myb* expression was examined in more detail in whole mount preparations and histological sections of different developmental stages. *in situ* hybridizations for *Lin9*, *B-MYB*, *Lin52*, *Lin54* and *Lin37* were analyzed in whole-mount embryos 9.5 dpc (Fig. 3.2). The examined *Lins* and *B-Myb* are expressed throughout the entire embryo. Highest expression was detected in the highly proliferative and cell dense limb buds and head region.

When histological sections of 7.5, 9.5, and 14.5 dpc embryos were analyzed by *in situ* hybridization, a distinct *Lin9* mRNA expression pattern was observed (Fig. 3.3 A). *Lin9* mRNA is detected in epithelial cells of the embryonic ectoderm and in the embryonic mesoderm. These tissues mainly constitute to the later embryo. A weaker *Lin9* expression was observed in the embryonic visceral endoderm and the surrounding extraembryonic tissue, including the trophoblast giant cells, the extraembryonic ectoderm and the ectoplacental cone. This indicates that *Lin9* is expressed in lower levels in cells that will later contribute to the extra placental tissues, and may be less relevant in this particular tissue at this stage of development. Still the trophoblast giant cells and the parietal endodermal cells directly

enveloping the embryo show to some extent higher *Lin9* expression than the decidual cells of the spongy layer of the endometrial tissue. These cells are important for the restructuring of the surrounding maternal tissue to ensure blood supply and proper embryonic development.

Later in development *Lin9* expression is no longer restricted to certain embryonic regions. In embryos 9.5 dpc, *Lin9* mRNA was detected throughout the entire embryo (Fig. 3.3 B). This ubiquitous expression was also observed in most organs of sectioned embryos 14.5 dpc (Fig. 3.4 A), although *Lin9* mRNA levels were lower in the heart and liver. This may be due to the developmental stage of the heart, which has already achieved its definitive prenatal arrangement at 14.5 dpc, similar to the liver (Kaufman, 2004). Maybe reduced *Lin9* expression is sufficient for these organs at the examined stage. At this developmental stage, other organs undergo further structural changes and are still highly proliferative to increase their size. Further analysis of *Lin9* mRNA in transverse brain sections revealed high expression in the entire cortex and a particularly high expression in the subventricular zone (Fig. 3.4 B). This region of the developing cortex is known to be a region of extensive neuronal proliferation during this stage of development. The mRNA expression for the other *Lins* and *B-Myb* is similar. Expression is ubiquitously distributed in the entire embryo and in the developing cortex (data not shown).

Taken together, the molecular as well as the histological analysis of *Lin9*, *Lin52*, *Lin54*, *Lin37*, and *B-Myb* mRNA expression *in vivo* in adult organs and throughout embryogenesis revealed that all of them are ubiquitously expressed and similarly distributed. This is the first examination of *Lin* expression in mice. The expression pattern observed for *Lin9* mRNA indicates that it is highly expressed in tissues and regions which undergo massive proliferation, structural rearrangements and specification underlined by differentiation. This correlates with the ubiquitous *B-Myb* expression pattern, which was previously described and associated with cellular proliferation (Latham et al., 1996; Sitzmann et al., 1996).

Moreover the similar distribution of the *Lins* indicates that they all function in the same cells, therefore most likely also in the same pathways and as a complex. Colamonici's group recently identified some of the LINC homologues in murine NIH-3T3 cells. They found that LIN9, B-Myb, E2F4, p130 and p107 interact with each other and form a context-dependent mammalian dREAM-like complex in mice (Pilkinton et al., 2007). This complex behaves similar to LINC, except that it contained p107 in its repressive state in G0. Nevertheless, this suggests, combined with the observed expression pattern of *Lin9* and *B-Myb* which correlate with the other *Lins*, that a complex like LINC also exists *in vivo* in the mouse.

## 4.2 Lin9 Gene Trap Mouse Model

### 4.2.1 Establishment of the Lin9 GT Knockout Model

To understand the physiological role of LIN9 *in vivo*, a Lin9-deficient mouse model was generated. We identified a commercially available ES cell line in which one allele of Lin9 was disrupted by a retroviral gene trap vector (BayGenomics). The used gene trap vector carried a promoter-less  $\beta$ -geo resistance gene (Fig. 3.5). Chimeras were generated and germ line transmission of the Lin9 GT allele occurred.

The truncated LIN9  $\beta$ -geo fusion protein lacks the conserved Box B of LIN9 (Fig. 3.5). This Box B encodes the so called DIRP region (Domain in Rb-related pathway). The DIRP domain is known to be essential for the association of pRB and LIN-9 (Gagrica et al., 2004) and may also be important for the binding to the other pocket proteins. Therefore the only so far known important domain of LIN-9 is eliminated by the gene trap insertion. The Lin9/ $\beta$ -geo fusion protein was detected in testis lysate of Lin9<sup>GT/+</sup> mice, with western blot, upon long exposure whereas the amount of wild type LIN9 protein was not altered. This indicates that the LIN9 fusion protein is unstable and rapidly degrades *in vivo*. Taken together Lin9 was successfully trapped and the knockout mice were further analyzed.

### 4.2.2 Early Embryonic Lethality of Lin9<sup>GT/GT</sup> Embryos

With this GT Lin9 mouse model, we are able to analyze the role of LIN9 *in vivo*, for the first time. Lin9<sup>GT/+</sup> mice were intercrossed and their progenies were genotyped as weanlings. The genotyping quickly revealed that no live homozygous mutant weanlings are obtained. Moreover, while determining the stage of embryonic lethality of Lin9-deficient embryos, neither at stage 13.5 nor at stage 9.5 dpc, were Lin9<sup>GT/GT</sup> embryos found. Lin9-deficient embryonic remains are first detected at stage 7.5 dpc (Table 3.1). This suggested that LIN9 is required for embryonic development in the mouse.

To further analyze the embryonic lethality, histological sections of decidual swellings of Lin9<sup>GT/+</sup> intercrosses were examined in more detail, comparing HE staining and *in situ* hybridization with specific lineage markers. The results of the examined embryos in stage 6.5 and 7.5 dpc are over all similar. Lin9<sup>GT/GT</sup> embryos display no organized cell structures and lack the distinct epithelial cells which are typical for the epiblast and therefore the embryo. Furthermore, the analyzed smaller abnormal implants display no obvious amniotic nor extraembryonic and ectoplacental cavity, compared to their Lin9<sup>+/+</sup> or Lin9<sup>GT/+</sup> littermates (Fig. 3.6). In both stages, the abnormal implantation sites contain no clear epiblast structure,

but trophoblast giant cells are present. 7.5 dpc embryonic remains could be genotyped and were confirmed as  $\text{Lin9}^{\text{GT/GT}}$  embryos. These abnormal implants were observed in frequency of about 25%, this correlates with the expected Mendelian ratio.

Similar phenotypes are common in embryos deficient for genes which are necessary for cell lineage specificity such as *Oct4* or *Sox2* (Avilion et al., 2003; Nichols et al., 1998). These cell lineage markers should supply us with further information about the epiblast development in abnormally structured  $\text{Lin9}^{\text{GT/GT}}$  embryos. *In situ* hybridization studies with *Oct4*, as an epiblast marker, and *H19*, as an extraembryonic cell marker, were performed (Nichols et al., 1998; Pelton et al., 2002; Pesce and Scholer, 2000; Poirier et al., 1991). *Oct4* which gives a strong signal solely in the epiblast in control embryos was completely missing in the  $\text{Lin9}^{\text{GT/GT}}$  implants. *H19* displays the expected reciprocal pattern in wild type and heterozygous embryos, with a positive staining only in extraembryonic cells. Interestingly, the entire disturbed structure in the  $\text{Lin9}^{\text{GT/GT}}$  implants is strongly *H19* positive. This suggests that these structures are the remains of implanted extraembryonic tissue e.g. trophoblast giant cells (Fig. 3.6). Further experiments analyzing the expression of additional lineage specific factors could define the epiblast loss in more detail, such as *Gata6*, which is a well studied factor involved in the formation of the primitive endoderm (Chazaud et al., 2006; Morrisey et al., 1998).

TUNEL staining of the  $\text{Lin9}^{\text{GT/GT}}$  embryos at 7.5 dpc revealed apoptotic cells surrounding as well as being part of the unstructured extraembryonic tissue, compared to control embryos (Fig. 3.7), suggesting that apoptosis contributes to the elimination of abnormal *Lin9*-deficient embryos.

In summary, these data suggests that *Lin9*-deficient embryos fail to develop proper epiblast structures after implantation.

### 4.2.3 Peri-implantation Lethality of $\text{Lin9}^{\text{GT/GT}}$ Embryos

If *Lin9* deficiency indeed results in lethality at the peri-implantation stage, blastocysts should be distributed with normal Mendelian frequency, which was confirmed by PCR genotyping (Fig. 3.8 & Tab. 3.1).

Peri-implantation phenotypes are known for several LINC regulated genes involved in G2/M transition, such as *Survivin*, *Bub1*, *CENP-E*, and *Cyclin A2* (Tab. 1.3). For example, homozygous *Survivin* (*Birc5*) null mutants display an early embryonic lethality around 4.5 dpc. The *Survivin*-deficient blastocysts do not form a proper blastocoel and fail to hatch. The remaining blastomeres display deterioration and appear grossly atypical, developing

solely into giant cells. Most of these cells exhibit abnormal nuclei with aberrant mitotic spindles (Uren et al., 2000). Bub1 knockout embryos are also early embryonic lethal while implantation takes place. Their null blastocysts appear normal. Interestingly, cultured Bub1 knockout blastocysts do not develop a proper ICM and display no cells in mitosis (Perera et al., 2007). Similarly, homozygous CENP-E null mutants are early embryonic lethal around 4.5 dpc. The cultured CENP-E-deficient blastocysts have problems attaching to the dish. The cells that finally adhere do resemble ICM cells (Putkey et al., 2002). In addition this was also observed for cyclin A2-deficient embryos, which successfully develop until the blastocyst stage. Hence, they also die at peri-implantation 5.5 dpc (Murphy et al., 1997).

Lin9<sup>GT/GT</sup> blastocysts are indistinguishable from Lin9<sup>+/+</sup> and Lin9<sup>GT/+</sup> blastocysts. When they were cultured for several days, almost all blastocysts hatched and attached to the dish. Analysis of their hatching ability reveals that the Lin9<sup>GT/GT</sup> blastocysts hatched at an average about one day later from their zona pellucida. In addition, after several days in culture, the ICM of Lin9-deficient blastocysts, fails to grow and only a trophoblast cell layer remains (Fig. 3.9 & 3.10). This is similar to phenotypes observed for knockouts of LINC targets, such as Bub1 or CENP-E (mentioned above), and is also comparable to B-Myb knockout embryos, which also die between 4.5 to 5.5 dpc, due to defects in ICM formation (Tanaka et al., 1999).

Additional studies, for example the isolation and culturing of the ICM by immunosurgery, will be important to further analyze if LIN9 is required in ICM formation as opposed to the trophoectodermal lineage (Solter and Knowles, 1975). ICM cells kept in media containing LIF should remain as undifferentiated cell mass and endodermal cells. Hence ICM cells which carry a knockout in lineage specific genes such as Sall1 or Oct4 transdifferentiate into trophoectodermal cells (Elling et al., 2006; Nichols et al., 1998). With this approach we would be able to study the differentiation ability of the Lin9<sup>GT/GT</sup> ICM and whether it really is involved in lineage differentiation.

The question when and why exactly the LIN9-deficient embryos die still remains. Given that LIN9 is required for expression of mitotic genes, Lin9<sup>GT/GT</sup> embryos could exhibit defects in progression into or through mitosis. Experiments such as live video microscopy and phospho-histone H3 (PH3) staining of blastocysts harvested at day 3.5 or 4.5 and in blastocyst outgrowth could help to further analyze the role of LIN9 in cell cycle regulation of the ICM.

Consistent with a role for LIN9 in the ICM, is its expression in this tissue at the blastocysts stages (Fig. 3.11). This ICM-predominant expression of *Lin9* appears similar to *B-MYB* mRNA distribution (Yoshikawa et al., 2006). Additionally, *Lin9* is expressed in mouse ES



cells (Fig. 3.14). The next question arose whether Lin9 is involved in establishing the well regulated evolving cell lineage of the epiblast or is involved in the early embryonic cell cycle.

#### 4.2.4 Possible Role in Early Embryonic Cell Cycle Regulation &/or Lineage Specification

Many knockout mouse models of cell cycle regulators were generated. Interestingly only a few knockout mice showed the previously expected early embryonic lethality. Embryonic cell cycle regulation is much more complex than expected from simple yeast and cell culture experiments. The embryogenesis starts with the pre-implantation phase which takes only about 72h to reach the early blastocyst stage with its first lineage and differentiation signs (Section 1.3). These two cell lineages, the TE and the ICM, separates after implantation into various cell lineages which continue to proliferate with different kinetics to start gastrulation and to contribute to all subsequent organs and tissues in the developing organism (Section 1.3.1). The factors essential for these early cell cycles of the pre- and peri-implantation phases are mostly unknown. All known major cell cycle regulators are present in these early cell cycles; however most of them seem not to be essential. For example, knockout studies of all three D-type cyclins, either individually knocked out or together, as well as CDK4- and CDK6-deficiency revealed that they are not as essential as previously expected for cell cycle progression. There is no general phenotype, at least in early embryonic development and throughout embryogenesis, since most knockout animals are viable. Only certain tissues and cell lineages display defects. In contrast, most organ and tissue development appears unaltered; which is also true for knockout mice of the pocket proteins as well as the E2F family members (Tab. 1.3 & Section 1.2.3; reviewed in (Ciemerych and Sicinski, 2005; Sherr and Roberts, 2004)).

Moreover mice can survive without interphase CDKs such as CDK2, CDK3, CDK4 and CDK6. Even quadruplicate knockout embryos, (also referred to as triple knockouts (TKO), since the naturally occurring mutation of CDK3 is very common in most mouse strains), undergo organogenesis and develop to midgestation (12-15 dpc). Expression levels of important cell cycle regulators like cyclins and CDK1 are not altered in these TKO embryos. Furthermore, CDK1 binds to all cyclins and in late G1 phosphorylates pRB, thereby freeing the E2Fs to precede to S phase. Recently, the group of Barbacid generated a CDK1 knockout mouse; which identified the first cell cycle regulator to be indispensable for embryonic cell cycle in the absence of interphase (Tab. 1.3 (Santamaria et al., 2007)). These knockout mice die prior to 1.5 dpc; the embryos do not even develop to the morula stage (16-64 cells) which indicates that CDK1 alone is sufficient for the cell division cycles in the early embryonic

development (Santamaria et al., 2007). This implies that the activity of CDK1 to precede cell cycle cannot be replaced by any of the interphase CDKs during development.

There are several possible explanations why a knockout of a cell cycle relevant gene may not result in an early lethality. First the relative survival may be due to maternal depositions of either protein and/or RNA, second to a possible redundancy, or third to a functional overlap that may interfere. Therefore, it is possible that an earlier Lin9<sup>GT/GT</sup> phenotype is masked by the presence of maternally deposited protein and mRNA. These maternal depositions may last long enough that Lin9-deficient embryos survive until the blastocyst stage and implant. To further investigate whether LIN9 is required for the earliest cell cycles, the conditional Lin9 mouse model combined with an oocyte-specific Cre-recombinase such as Gdf9 Cre could be used (Lan et al., 2004).

Knockout mice for several LINC target genes such as Survivin, Bub1, CENP-E, and Cyclin A2 produced a peri-implantation phenotype at an earlier stage than the so far examined classical cell cycle regulators (mentioned above, Tab. 1.3). This emphasizes that Lin9's role, probably as a member of the LINC core module, is essential for regulating important cell cycle factors that are known to be involved in G2/M transition. However, further experiments to unravel the exact mechanism concerning Lin9 function in early cell cycle regulation will be of great importance. This could be achieved by analyzing Lin9 knockout ES cell lines.

The high differentiation potential makes ES cells an ideal model to study early embryonic cell cycles, as well as cell lineage specificities *in vitro*. ES cells are generated from the ICM of blastocysts. They are pluripotent and can differentiate into all somatic lineages (Bradley et al., 1984; Evans and Kaufman, 1981; Martin, 1981). Several distinct features are known for ES cells: they have symmetrical self-renew, are immortal, show no contact inhibition and grow anchorage independently, never undergo crisis or senescence, and hence retain their diploid karyotype. ES cells behave autonomously, like cells that do not depend on adjacent cells for signals controlling growth and survival. These are all typical features of transformed cells, although ES cells are wild type. Still, they are tumorigenic since they can form benign tumors (teratocarcinomas) when introduced into adult tissue (Mummery et al., 1987; Orford and Scadden, 2008).

Moreover, ES cells and cells in the early embryo clearly function under a different cell cycle regulation. As previously mentioned ES cells have a very short G1 phase with reduced or no cell cycle controls (R point) and their cell cycle is very rapid (11-16 hours). Additionally, some cells will perform endoreduplication cycles in which S phases are not followed by mitosis (Section 1.1.1). Therefore, it seems logical that genes that progress and drive mitosis

are indispensable for rapidly cycling embryonic cells to form the basis of the embryo. On the other hand, it is not surprising that the knockout embryos of *Lin9* and *Lin9* target genes still form trophoblast cells and are able to implant since they basically only endoreduplicate. In contrast to the more classical cell cycle regulators which are mainly involved in G1/S transition.

Another striking feature is that ES cells constantly suppress differentiation during proliferation (Savatier et al., 1994). Notably, expression of the cyclins and CDKs as well as the pocket proteins and the E2Fs are not cell cycle-dependent. The exception is cyclin B1/CDK1 (Stead et al., 2002). The cyclin E1/CDK2 is constitutively active. D-type cyclins/CDK4 are only expressed at very low levels. In contrast to p107 and pRB, p130 is not expressed in ES cells (LeCouter et al., 1998b; Robanus-Maandag et al., 1998). However pRB is consequently inactivated by predominant hyperphosphorylation and therefore there is a constitutive active E2F signaling (Burdon et al., 2002).

Several studies examined the differentiation and cell cycle capability of various knockout situations. For example, triple knockout ES cells of p107, p130, and pRB show normal proliferation rates, but have very limited differentiation potential (Dannenberg et al., 2000; Sage et al., 2000). These observations indicate that ES cells do not necessitate pocket proteins for proliferation, but for differentiation (Dannenberg et al., 2000; Iwamori et al., 2002). In contrast, triple knockout MEFs display an increased proliferation rate and are unable to arrest. These MEFs make obvious that the pocket proteins are important for the cell cycle regulation of somatic cells (Dannenberg et al., 2000; Sage et al., 2000).

Interestingly, B-Myb is expressed in ES cells and it is not possible to produce B-Myb knockout ES cells, which suggests that B-Myb plays a crucial role in the maintenance of ES cells (Tanaka et al., 1999). Iwai and colleagues established an ES cell line with an inducible dominant Myb protein (MERT), which interferes with the normal B-Myb function. They showed that B-Myb plays an important role in regulating cell adhesion and cell cycle progression in ES cells (Iwai et al., 2001). Interestingly, the observed morphological alteration and G1/S arrest of the ES cells were not accompanied by expression of differentiation markers. Recently, B-Myb was identified to be necessary in ES cells for the correct mitotic spindle formation and maintenance of euploidy (Tarasov et al., 2008a). These are the first hints that B-Myb might be required not only for normal ES cell cycle progression, but also regulate lineage specific differentiation genes. This implied that B-Myb may play a role in either the maintenance of the undifferentiated stem cell state, or the early events of differentiation (Tarasov et al., 2008b).

From all the data gathered so far, this could also be true for Lin9 and needs to be further investigated, for example with a conditional Lin9 ES cell line. This approach would allow additional studies concerning LIN9's possible role in differentiation, since ES cells can evolve into embryonic bodies (EBs), which resemble the early differentiation events in embryogenesis *in vitro* (Kurosawa, 2007). It will be essential to understand whether LIN9 plays an important role in proliferation and/or survival of ES cells and if this function is associated with its cell cycle regulation potential and/or lineage specificity in mouse development. Taken together the ES cells will complement our understanding of LIN9 function *in vivo*.

#### 4.2.5 *In vitro* Analysis of LIN9's Role in Cell Cycle in MEFs

To further analyze LIN9 function in the cell cycle, Lin9<sup>+/+</sup> and Lin9<sup>GT/+</sup> primary MEFs from 13.5 dpc embryos were generated. These Lin9<sup>GT/+</sup> MEFs were monitored, but showed no significant differences neither in cell cycle phases, growth rates, protein levels nor in RNA expressions (Fig. 3.12). This suggests that the remaining Lin9 allele in heterozygotes is probably upregulated. Overall these results are not surprising since we never observed any alterations in the Lin9<sup>GT/+</sup> mice.

It is not unusual that heterozygous MEFs display no obvious phenotypes. For example, Cyclin A2 heterozygous MEFs also do not show any alterations. However it is also true that for most mutated MEFs once they are pushed and put under pressure, their behavior changes. For example, further analysis in CENP-E heterozygous MEFs, which show no obvious phenotype in the first place, revealed an increase in aneuploidy and chromosomal instability compared to control cells, depending on the passage and status. Moreover, aneuploidy in the heterozygous animals promotes tumorigenesis in some contexts, such as ageing. In other cases it inhibits tumor development, for example, liver tumor incidences decreased in 7,12-dimethyl-benz-(a)anthracene (DMBA) treated animals (Weaver et al., 2007).

It would be worth investigating similar alterations in Lin9<sup>GT/+</sup> animals. Preliminary analysis of a model of non-small-cell lung cancer in Lin9<sup>GT/+</sup> mice is currently being examined, in cooperation with Rudolf Götz and Ulf Rapp (Virchow Center, Würzburg). These so called SP-C C-Raf BxB mice express an oncogenic, constitutively active C-Raf kinase (Goetz et al., 2004). Preliminary results suggest that Raf-induced adenomas are larger and more vascularized in Lin9<sup>GT/+</sup> mice compared to the control BxB tumors. This would suggest that LIN9 may play a role in tumor suppression *in vivo*.

## 4.3 Conditional Lin9 Knockout

### 4.3.1 Generation of the Conditional Lin9 Knockout Model

To overcome the previously mentioned limitation of the classical gene trap knockout model, a conditional Lin9 mouse model was generated. Typically Cre-loxP mice are produced by using transgenic technology (Nagy, 2000; Sadowski, 1995; Sauer and Henderson, 1988). We used Cre-loxP and FLP-FRT system as a genetic tool to enable cell type specific and/or inducible deletion of Lin9. The loxP and the FRT sites were placed in cis (same DNA strand) and the same directional orientation. This is a common approach which results in a simple excision of the flanked element (Fig. 3.13). There are several advantages: First in comparison to shRNA or siRNA (short hair pin or small interfering RNA) experiments, the floxed gene will be completely deleted. Second, this model will provide an *in vivo* system, which is tissue and temporally specific. Many special Cre strains can be used, each containing a Cre-recombinase under different tissue-specific promoters. Moreover it will be possible to construct a variety of Cre-mediated mouse models and Cre-inducible mice. This will allow us to study various Lin9 effects in different tissues and models, *in vivo* and *in vitro*.

The targeting vector was constructed to flank exon 7 of the Lin9 gene with loxP recombination sites and to insert a  $\beta$ -geo selection cassette flanked by FRT sites (Fig. 3.13). We obtained chimeras and the mutated allele was successfully transmitted to the germ line. The selection cassette from the conditional allele was removed *in vivo*, with FLP-deleter mice (Fig. 3.14 & (Farley et al., 2000; Rodriguez et al., 2000)). The sequence of the floxed Lin9 allele was confirmed by sequencing. Lin9<sup>fl/fl</sup> animals are fertile and phenotypically normal. This suggests that the integrated loxP sites do not interfere with Lin9 transcription and translation.

### 4.3.2 Cre-mediated Excision *in vivo*

Deletion of the floxed exon 7 was achieved with Cre-recombinase *in vivo* and *in vitro*. This Cre-mediated excision was accompanied by a frame shift and resulted in a truncated protein. No functional LIN9 was produced and this led to a complete null phenotype. Lin9 was first deleted *in vivo* by crossing Lin9<sup>fl/fl</sup> animals with an early Cre expressing deleter strain (Schwenk et al., 1995). The deletion of exon 7 by the Cre-recombinase resulted in embryonic lethality; no live Lin9<sup>fl $\Delta$ /fl $\Delta$</sup>  weanlings were born. This proved that deletion of exon 7 disrupts the function of LIN9 in a comparable manner to the GT allele (Fig. 3.14 & Tab. 3.2).

### 4.3.3 Cre-mediated Excision *in vitro*

First  $\text{Lin9}^{\text{fl/fl}}$  MEFs as well as  $\text{Lin9}^{+/+}$  control cells were generated from the same litter to minimize background level. The floxed allele in MEFs was deleted with retroviral infections of the Hit and Run Cre-recombinase (HR-Cre; (Silver and Livingston, 2001). Excision of exon 7 in MEFs was successful, the protein level as well as the RNA expression of *Lin9* showed a considerable reduction in HR-Cre infected  $\text{Lin9}^{\text{fl/fl}}$  MEFs (Fig. 3.15). *Lin9*-deficient MEFs showed only a tendency to proliferate slower and they recovered in the end and are nearly as dense as the control cells. This recovery was due to an overgrowth of cells still harboring the intact *Lin9* allele. Thus these experiments suggest that the  $\text{Lin9}^{\Delta\text{fl}/\Delta\text{fl}}$  MEFs have a severe growth disadvantage.

### 4.3.4 Inducible Cre-mediated Excision *in vivo*

To overcome efficiency problems, resulting from the retroviral infection, MEFs which carry  $\text{Lin9}^{\text{fl/fl}}$  and a tamoxifen-inducible Cre-ER<sup>T2</sup> were generated (Feil et al., 1997; Hameyer et al., 2007). The deletion of exon 7 of *Lin9* created with inducible Cre-ER<sup>T2</sup> is highly efficient (Fig. 3.16). Most significantly, in  $\text{Lin9}^{\Delta\text{fl}/\Delta\text{fl}}$  MEFs cell cycle distribution and growth rate were majorly impacted. Their proliferation ability was only minimal in population growth rate experiments. Additionally, these *Lin9*-deficient MEFs displayed a clear accumulation in G2/M phase, accompanied by massive changes in G1 and S phase of the cell cycle, and an increase in polyploid cells (Fig. 3.16).

The reason how and why these  $\text{Lin9}^{\Delta\text{fl}/\Delta\text{fl}}$  MEFs arrest in G2/M and whether these cells will overcome the arrest remains unclear and needs to be further investigated. A similar growth disadvantage was recently discovered in conditional B-Myb knockout MEFs, by Ishii's research group. Deletion of B-Myb was generated with lentiviral infection with Cre-recombinase. They observed in B-Myb-deleted cells a comparable growth disadvantage and growth arrest in G2/M (Yamauchi et al., 2008). With time-laps recording and staining they showed that B-Myb-deficient MEFs display great difficulties to finish cytokinesis, which is probably due to defects in localization of clathrin at the mitotic spindle. Moreover they identified a complex containing B-Myb, clathrin and filamin, termed Myb-Clafi complex, which seems to be directly involved in spindle integrity and genomic stability. Interestingly, they observed in B-Myb-deleted MEFs a decrease of G2/M gene expression levels (Yamauchi et al., 2008). These seven candidates, cyclin A2, cyclin B1, aurora A, Survivin, Bub1, CENP-E and CDK1 are all well known targets of LINC (Osterloh et al., 2007; Schmit et al., 2007).

Comparing these recent findings and results concerning LINC, kinases such as Bub1 which regulate the spindle assembly checkpoint are of special interest. This checkpoint assures the exact partition of genetic material equally between the two daughter cells. It blocks the ubiquitin ligase activity of the APC or cyclosome (APC/C), stabilizes securin (an APC/C substrate), and inhibits the activation of separase and therefore the onset of anaphase, until the sister chromatids are correctly attached to the mitotic spindle. Bub1 is a main component of the spindle checkpoint, regulating the kinetochore localization of Mad2 and other checkpoint components (Yu and Tang, 2005). Severe defects in sister chromatid cohesion and the spindle assembly checkpoint were visible in Bub1-deficient MEFs. Moreover these conditional MEFs showed decreased proliferation ability (Perera et al., 2007). In parallel another group around van Deursen was able to generate a conditional knockout mouse with a gradient of reduced Bub1 expression. This approach made it possible to compare wild type, hypomorphic, haploinsufficient, and complete Bub1 knockouts. The analysis of these mice revealed that the dosage of Bub1 is critical to assure proper chromosomal segregation as well as to develop spontaneous tumors (Jeganathan et al., 2007). Moreover as mentioned previously the early lethality phenotype of knockout Bub1 is very similar to Lin9 and B-Myb knockouts (Perera et al., 2007).

Taken together it will be of great interest to further investigate the cause of the growth arrest in Lin9-deficient MEFs and to analyze in more detail whether the arrest is due to the newly identified Myb-Claf1 complex or if its basis is comparable to LINC and its target genes. Therefore, LIN9 regulated genes, in synchronized MEFs, will be systematically analyzed with cDNA micro-arrays. This will be followed by analysis of candidate target genes as well as known LINC target genes such as cyclin B1 and Bub1. Moreover it can be identified whether LIN9 directly regulates these genes with ChIP experiments. To study the phenotype in MEFs in more detail, it will be important to monitor single cells with time-lapse analysis and DAPI staining, to examine spindle assembly and chromosomal integrity.

#### 4.3.5 LIN9 Function in Tumorigenesis & Differentiation *in vivo*

The conditional knockout mouse is a powerful tool to study LIN9 function in differentiation and tumorigenesis *in vivo*. It is of great interest, since from previous studies in human cell culture, it is known that LIN-9 cooperates with pRB in differentiation. Additionally, it was observed that LIN-9 showed tumor suppressing properties *in vitro* (Gagrica et al., 2004). Moreover preliminary data, comparing adenoma development in SP-C C-Raf BxB mice wild type for Lin9 versus heterozygous GT Lin9 shows that these tumor suppressive activities

could be necessary *in vivo* (Section 4.2.5). To further characterize the role of LIN9 in tumorigenesis further inducible-Cre tumor models will be used.

### 4.3.6 Hypothesis

Taken together from previous studies in human cell culture it is known that LIN-9 is associated and cooperates with pRB in differentiation and senescence. Depletion of LIN-9 leads to transformation *in vitro* (Gagrica et al., 2004). LIN-9 is essential for transcriptional regulation of G2/M genes (Osterloh et al., 2007). Moreover LIN-9 is cell context-dependent, associated in a complex termed LINC with other essential cell cycle regulators, such as B-Myb and E2F4 as well as the pocket proteins p130 and p107 and the newly identified LINCs (Schmit et al., 2007). If this complex is disrupted, cell cycle progression is altered, as demonstrated previously in human cells (Schmit et al., 2007) and in MEFs in this study. This is probably due to genomic instability and chromosomal aberrations, followed by subsequent polyploidy, which compares to the deletion of B-Myb (Yamauchi et al., 2008) and CENP-E (Weaver et al., 2007). Moreover recent experiments have shown that decreased levels of Lin9 leads to senescence (Kathrin Schmitt unpublished data), which may interfere or oppose tumor development (Fig. 4.2), e.g. similar to Bub1 (Jeganathan et al., 2007). However, these cellular changes may also lead to tumor development (comparable with preliminary adenoma results), considering the tumor suppressive function of Lin9 in the pRB-pathway (Gagrica et al., 2004). This outcome could very well be dosage as well as cell type dependent, similar to observations in Bub1 knockout animals and moreover for the loss of CENP-E *in vitro* and *in vivo* (Weaver et al., 2007). However, we know that the loss of Lin9 leads to early embryonic lethality *in vivo* (this study). This is consistent with all the previously mentioned knockout models and underlines the necessity for Lin9 in development. Moreover with the generated conditional knockout model we now have the tool to unravel its exact function in the cell cycle or cell lineage of early embryogenesis. Additionally, this will help to reveal Lin9's role in differentiation.



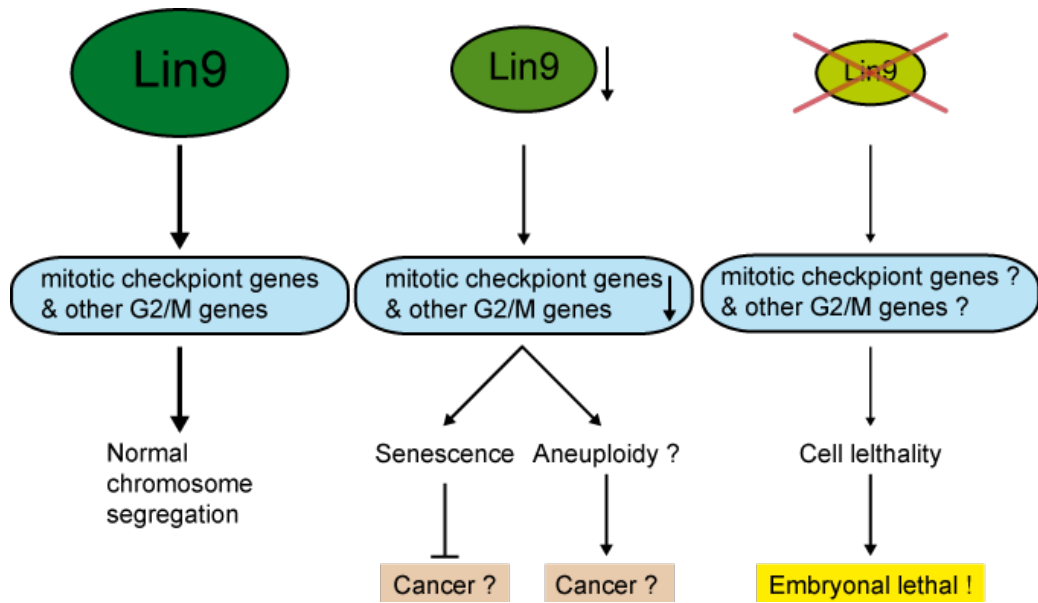


**Fig. 4.2: Hypothesis: LIN9 is a dosage dependent tumor suppressor and its complete loss leads to lethality.** Schematic of the levels of Lin9, indicated by the relative size of the oval. This resembles the context-dependent amount and therefore the dosage of Lin9, either reduced through e.g. shRNA depletion (middle panel) or a knockout approach (right panel). Further information is in the text.

## 5 SUMMARY

LINC, the human homologue of an evolutionary conserved complex, regulates the transcription of a set of genes essential during the G2/M transition (Osterloh et al., 2007; Schmit et al., 2007). One component of the LINC core module is LIN-9. LIN-9 is essential for the transcriptional activation of LINC target genes and also promotes differentiation in association with pRB (Gagrica et al., 2004). However, nothing is known about its function *in vivo*.

Histological and molecular analysis revealed that *Lin9* is ubiquitously expressed throughout embryonic development and in all examined adult organs. Additionally, *Lin9* mRNA is expressed in ES cells and blastocysts. Moreover the analogous distribution of the other LINC components suggested that they all function in the same cells and most likely in the same pathway.

To deeper investigate the role of LIN9 in cell cycle and differentiation *in vivo*, a *Lin9* gene trap mouse model (GT) was successfully generated and examined. Heterozygous *Lin9*<sup>GT/+</sup> mice were inconspicuous and develop normally. However, homozygous knockout embryos were never obtained. The *Lin9*<sup>GT/GT</sup> embryos die at peri-implantation, probably due to a defect in the development of the epiblast, which could be shown with *in situ* hybridization with specific lineage markers. *In vitro*, the ICM of *Lin9*-deficient blastocysts did not develop properly. These data suggest that the loss of *Lin9* leads to embryonic lethality at peri-implantation, and indicates that LIN9 is required for proper formation of the epiblast.

In parallel, the first conditional *Lin9* mouse model based on the Cre-loxP technology was generated. The *Lin9*<sup>fl/fl</sup> allele can be deleted by Cre-recombinase, *in vivo* and *in vitro*. Therefore an inducible system with *Lin9*<sup>fl/fl</sup> mice harboring Cre-ER<sup>T2</sup> was established. The MEFs generated from these transgenic mice carried a nearly complete knockout upon induction with tamoxifen. Deletion of LIN9 in MEFs had a major impact upon the cell cycle and growth rates. Specifically, they arrested in G2/M phase and stopped to proliferate.

Taken together, I was able to generate a *lin9* gene trap and a *lin9* conditional knockout mouse model. All results obtained so far demonstrate, that *Lin9* is an essential gene for embryonic development and cell cycle control. It will be of great interest to further investigate *Lin9*-deficiency to gain insights into the mechanism of cell cycle control in early embryonic development and cell differentiation.

## 6 ZUSAMMENFASSUNG

LINC, das humane Homolog eines evolutionär konservierten Komplexes, reguliert die Transkription von Genen, die essentiell für die G2/M Transition sind (Osterloh et al., 2007; Schmit et al., 2007). Eine Komponente des LINC Komplexes ist LIN-9. LIN-9 ist für die transkriptionelle Aktivierung LINC spezifischer Zielgene essentiell und kann, in Assoziation mit pRB, die Differenzierung humaner Zellen fördern (Gagrica et al., 2004). Bisher ist jedoch nichts über die *in vivo* Funktion LIN9s bekannt.

Histologische und molekulare Analysen der Maus machen deutlich, dass *Lin9* während der embryonalen Entwicklung und in allen untersuchten adulten Organen ubiquitär exprimiert wird. Zusätzlich wird *Lin9* mRNA in ES Zellen und in Blastocysten exprimiert. Außerdem legt die analoge Verteilung anderer LINC Komponenten nahe, dass sie sehr wahrscheinlich gemeinsam in den gleichen Zellen und Signalwegen agieren.

Um die Funktion des LIN9 Proteins im Zellzyklus und der Differenzierung *in vivo* genauer zu erforschen, wurde ein *Lin9* „Gene Trap“ Maus Modell (GT) generiert und untersucht. Heterozygote *Lin9*<sup>GT/+</sup> Mäuse sind unauffällig und entwickeln sich normal. Allerdings wurden keine *Lin9* knockout Embryonen erhalten. *Lin9*<sup>GT/GT</sup> Embryonen sterben in der peri-Implantationsphase, vermutlich auf Grund eines Entwicklungsdefekts des Epiblasten, was mit *in situ* Hybridisierung von Abstammungslinien spezifischen Markern gezeigt werden konnte. Die ICM *Lin9* defizienter Blastocysten entwickelte sich *in vitro* nicht richtig. Diese Daten machen deutlich, dass der Verlust von *Lin9* zu embryonaler Letalität im Peri-Implantationsstadium führt, und zeigt dass *Lin9* für die richtige Ausbildung des Epiblasten benötigt wird.

Gleichzeitig wurde das erste konditionelle *Lin9* Maus Modell, basierend auf der Cre-loxP Technologie, generiert. Das *Lin9*<sup>fl/fl</sup> Allele kann *in vivo* und *in vitro* mit der Cre-Recombinase deletiert werden. Deshalb wurde ein induzierbares System mit *Lin9*<sup>fl/fl</sup> Mäusen, die zusätzlich Cre-ER<sup>T2</sup> tragen, etabliert. Die MEFs dieser transgenen Mäuse trugen nach Induktion mit Tamoxifen einen kompletten *Lin9* Knockout. Die Deletion von LIN9 hat dramatische Auswirkung auf den Zellzyklus und die Wachstumsrate der MEFs. Neben der Akkumulation in der G2/M Phase des Zellzyklus kommt es zu einem vollständigen Proliferationsstopp.

Zusammenfassend war es möglich, ein *Lin9* „Gene Trap“ und ein konditionelles Knockout Maus Modell zu generieren. Beide Mausmodelle belegen, dass *Lin9* ein essenzielles Gen für die Embryonalentwicklung und die Kontrolle des Zellzyklus ist. Die weitere Erforschung der LIN9 Defizienz wird dazu beitragen, grundlegende Mechanismen der frühen Zellzykluskontrolle und der embryonalen Entwicklung zu verstehen.

## 7 APPENDIX

### 7.1 Supplementary Figures

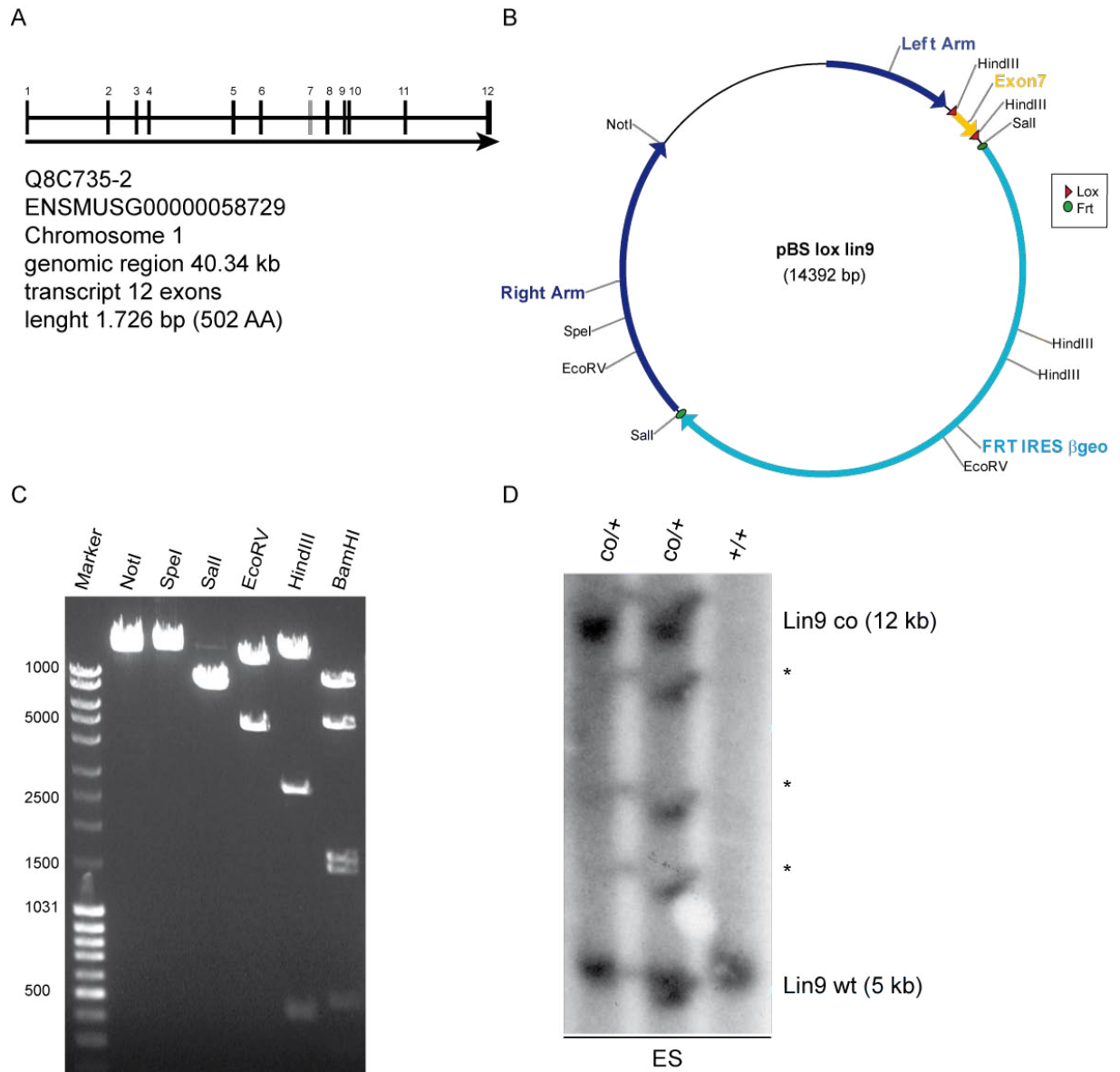


**Fig. 7.1: Conditional Lin9 knockout.** (A) Genomic organization of Lin9 gene, based on sequence information from ensembl genome browser. (B) Map of the conditional Lin9 targeting vector (plasmid #822). (C) Restriction analysis of the targeting vector. Restriction endonucleases lead to the following pattern: Hind III (11362 +2314 +367 +347 bp), EcoR V (4098 +10294 bp), Sal I (6931 +7461 bp), Spe I & Not I linearized (14392 bp). (D) Southern blot analysis of ES gDNA which was restricted with Spe I and detected with radioactive labeled probe A. The alleles and their size are indicated on the right. The asterisks mark unspecific background bands.

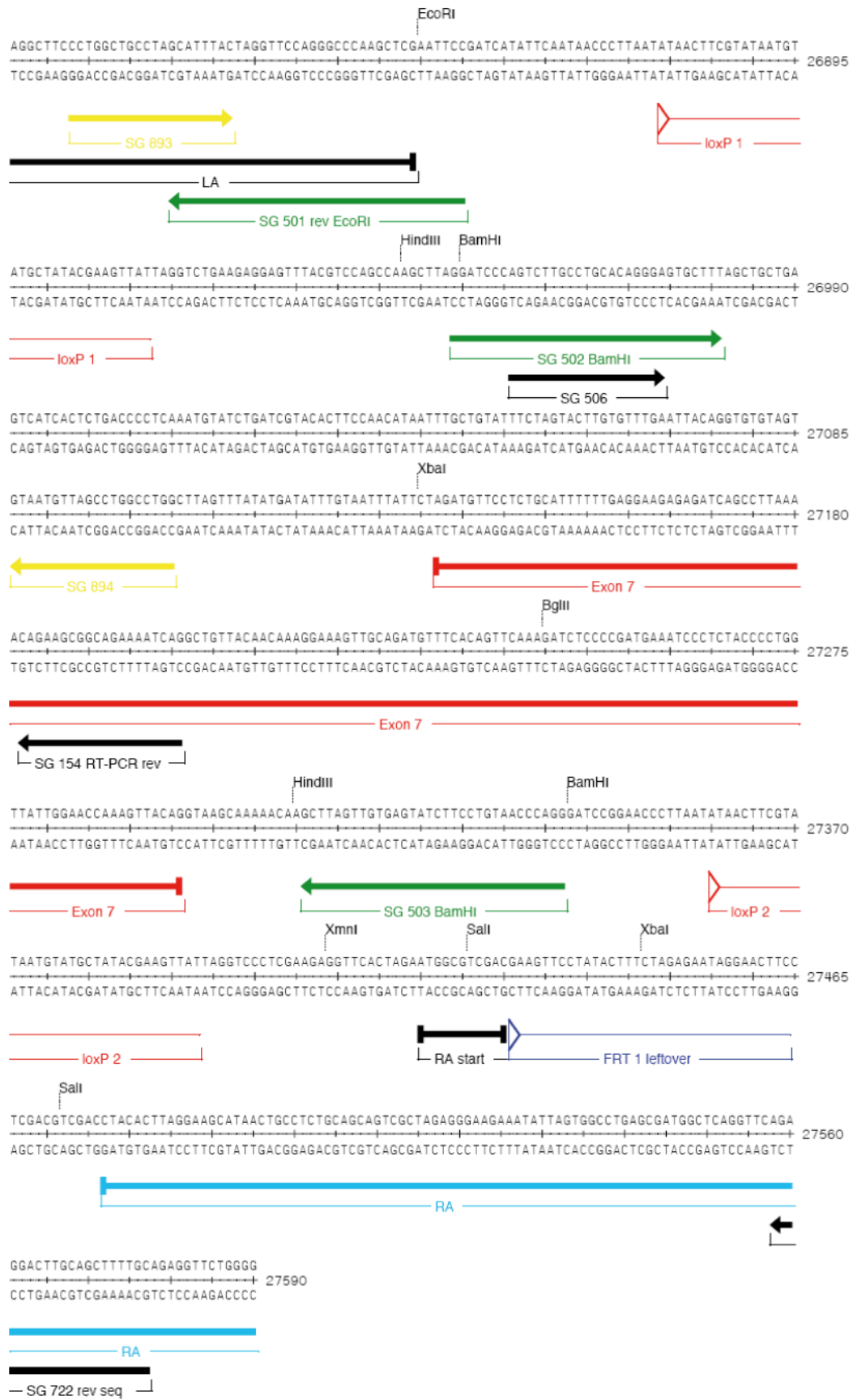


**Fig. 7.2: Sequence overview of the floxed Lin9 allele.** Position of all primers used is depicted in the sequence cutout, as well as the location of the LoXP/FRT sites. The primers are labeled with their internal numbers (MM 2.1.5). (LA = left arm; RA = right arm)

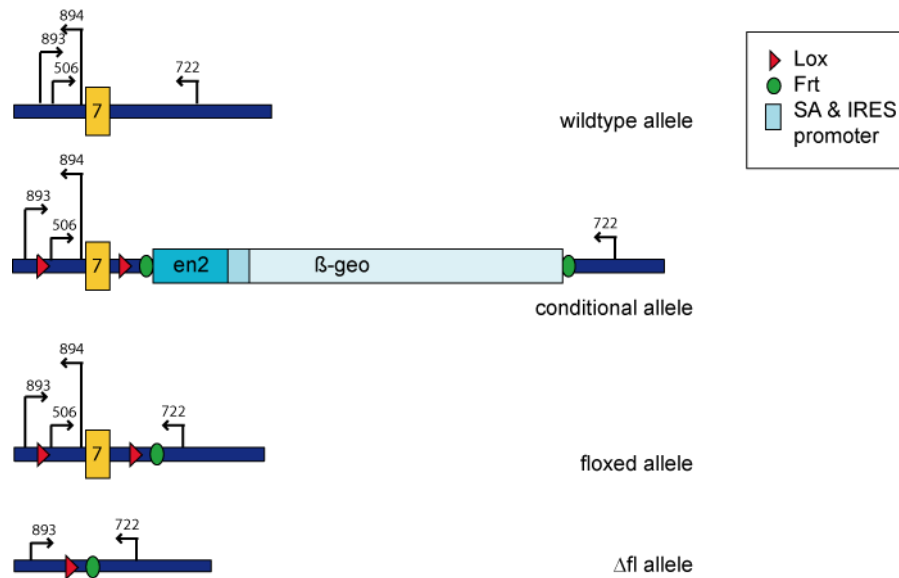


**Fig. 7.3: Primer scheme for the floxed targeting strategy.** Position of all primers used and location of exon 7 and the equivalent LoxP/FRT sites are indicated in the scheme. The primers are labeled with their internal numbers (MM 2.1.5).

## 7.2 Mouse Genome Informatics (MGI)

| Synonyms     | MGI         | Origin  |
|--------------|-------------|---|
| <b>Lin9</b>  | MGI:1919818 | lin-9 homolog ( <i>C. elegans</i> )<br>Synonyms 2700022J23Rik, TGS1 |
| <b>Lin37</b> | MGI:1922910 | lin-37 homolog ( <i>C. elegans</i> )<br>Synonyms 1810054G18Rik      |
| <b>Lin52</b> | MGI:3045391 | lin-52 homolog ( <i>C. elegans</i> )                                |
| <b>Lin54</b> | MGI:2140902 | lin-54 homolog ( <i>C. elegans</i> )                                |
| <b>C-myb</b> | MGI:97249   | Myb: myeloblastosis oncogene  |
| <b>A-myb</b> | MGI:99925   | Mybl1: myeloblastosis oncogene-like 1                               |
| <b>B-myb</b> | MGI:101785  | Mybl2: myeloblastosis oncogene-like 2                               |

## 7.3 Database

| <b>Tool</b>  | <b>Homepage</b>   |
|--|---|
| MGI_3.43-mouse genome informatics                                | <a href="http://www.informatics.jax.org/">http://www.informatics.jax.org/</a>   |
| National Center for Biotechnology Information (NCBI)             | <a href="http://www.ncbi.nlm.nih.gov/">http://www.ncbi.nlm.nih.gov/</a>   |
| Ensembl  | <a href="http://www.ensembl.org/index.html">http://www.ensembl.org/index.html</a>   |
| Primer3 v0.4.0   | <a href="http://fokker.wi.mit.edu/primer3/input.htm">http://fokker.wi.mit.edu/primer3/input.htm</a>   |
| Roche Applied Science Universal ProbeLibrary Assay Design Center | <a href="https://www.roche-applied-science.com/sis/rtPCR/ucpl/acenter.jsp?id=030000">https://www.roche-applied-science.com/sis/rtPCR/ucpl/acenter.jsp?id=030000</a> |
| Oligo calculator   | <a href="http://mbcf.dfc.harvard.edu/docs/oligoCalc.html">http://mbcf.dfc.harvard.edu/docs/oligoCalc.html</a>   |

## 7.4 Software

| <b>Program</b>             | <b>Program</b>      |
|----------------------------|---------------------|
| Microsoft Office 2007      | Adobe Acrobat 8.0   |
| Illustrator CS2            | Photoshop CS3       |
| ApE-A plasmid Editor v1.15 | DNASTAR Lasergene   |
| EndNote X2                 | Leica LAS AF v1.5.1 |

## 7.5 Abbreviations & Symbols

|              |   |              |                                      |
|--------------|---|--------------|--------------------------------------|
| <b>AS</b>    | anti sense  | <b>min</b>   | minutes                              |
| <b>β-geo</b> | Fusion of β-galactosidase & neomycin phosphotransferase | <b>MM</b>    | Material & Methods                   |
| <b>bp</b>    | Base pairs  | <b>MOPS</b>  | 3-(N-morpholino)propanesulfonic acid |
| <b>BSA</b>   | Bovine serum albumin                                    | <b>n</b>     | numbers                              |
| <b>CDK</b>   | Cyclin dependent kinase                                 | <b>NEAA</b>  | Nonessential amino acids             |
| <b>ChIP</b>  | Chromatin immunoprecipitation                           | <b>NP-40</b> | Nonylphenoxy polyethoxy ethanol      |
| <b>co</b>    | Conditional   | <b>o/n</b>   | over night                           |
| <b>DF</b>    | Two degrees of freedom                                  | <b>4-OHT</b> | 4-Hydroxytamoxifen                   |
| <b>DMEM</b>  | Dubecco's Modified Eagle Medium                         | <b>PBS</b>   | Phosphate buffered saline            |

|             |                                     |                 |                                      |
|-------------|-------------------------------------|-----------------|--------------------------------------|
| <b>DMSO</b> | Dimethylsulfoxid                    | <b>PCR</b>      | Polymerase chain reaction            |
| <b>DNA</b>  | Deoxyribonucleicacid                | <b>PFA</b>      | Paraformaldehyde                     |
| <b>DOC</b>  | Sodium deoxicholat                  | <b>PIPES</b>    | 1,4-Piperazinediethanesulfonic acid  |
| <b>dpc</b>  | Days post coitum                    | <b>PMSF</b>     | Phenylmethanesulfonylfluoride        |
| <b>EDTA</b> | Ethylene diamine tetraacetic acid   | <b>qPCR</b>     | Quantitative real time PCR           |
| <b>ES</b>   | Embryonic stem                      | <b>R</b>        | Resorbed                             |
| <b>FACS</b> | Fluorescence-Activated Cell Sorting | <b>RNA</b>      | Ribonucleic acid                     |
| <b>FCS</b>  | Fetal calf serum                    | <b>R point</b>  | Restriction point                    |
| <b>Fig.</b> | Figure                              | <b>RT</b>       | Room temperature                     |
| <b>gDNA</b> | Genomic DNA                         | <b>S</b>        | sense                                |
| <b>GT</b>   | Gene trap                           | <b>SDS</b>      | Sodium dodecyl sulfate               |
| <b>h</b>    | hours                               | <b>Suppl.</b>   | Supplementary                        |
| <b>hd</b>   | hatching days                       | <b>Tab.</b>     | Table                                |
| <b>HE</b>   | Haemotoxylin & Eosin                | <b>TBST</b>     | Tris buffered saline-Tween           |
| <b>HRP</b>  | Horseradish-peroxidase              | <b>TEMED</b>    | N'N'N'N'-tetramethylethylene-diamine |
| <b>ICM</b>  | Inner cell mass                     | <b>Tris</b>     | Tris(hydroxymethyl)aminomethane      |
| <b>IgG</b>  | Immunoglobulin G                    | <b>ubiquit.</b> | ubiquitous                           |
| <b>IP</b>   | Immunoprecipitation                 | <b>Wt</b>       | wild type                            |
| <b>ko</b>   | knock out                           | <b>+/+</b>      | Homozygous, wild type                |
| <b>LIF</b>  | Leukemia inhibitory factor          | <b>+/-</b>      | Heterozygous                         |
| <b>LINC</b> | LIN-Complex                         | <b>-/-</b>      | Homozygous, knock out                |
| <b>MABT</b> | Maleic acid buffer-Tween            | <b>Δ</b>        | Delta/Deletion                       |

## 7.6 List of Figures & Tables

### Table

Tab. 1.1: Summary of pRB/E2F complexes in different species.

Tab. 1.2: List of important LINC target genes.

Tab. 3.1: Early lethality of Lin9-deficient embryos.

Tab. 3.2: Genotypic analysis of Lin9<sup>Δfl/+</sup> intercrosses.



## Figures

- Fig. 1.1: Simplified representation of the mammalian cell cycle.
- Fig. 1.2: Mouse development from zygote to onset of primitive streak formation.
- Tab. 1.3: LINC member and target genes and their functions in mouse.
- Fig. 2.1: Set up of the blotting stag for Southern blot.
- Fig. 3.1: Relative expression of *Lin9*, *Lin52*, *Lin54* & *Lin37* mRNA in the mouse.
- Fig. 3.2: Expression of *Lin9*, *B-Myb*, *Lin52*, *Lin54* & *Lin37* mRNA in mouse embryos 9.5 dpc.
- Fig. 3.3: Expression of *Lin9* mRNA in mouse embryos 7.5 & 9.5 dpc.
- Fig. 3.4: Expression of *Lin9* mRNA in mouse embryos 14.5 dpc.
- Fig. 3.5: Generation of a *Lin9* knockout mouse.
- Fig. 3.6: E7.5 & E6.5 *Lin9*-deficient embryos lack epiblast.
- Fig. 3.7: Apoptosis in *Lin9*-deficient embryos 7.5 dpc.
- Fig. 3.8: TaqMan qPCR approach to genotype blastocysts.
- Fig. 3.9: Phenotypical examination of blastocysts.
- Fig.3.10: Analyses of hatching behavior of blastocysts cultured *in vivo*.
- Fig. 3.11: *Lin9* expression in blastocysts is ICM-predominant.
- Fig. 3.12: Analysis of *Lin9*<sup>GT/+</sup> MEFs.
- Fig. 3.13: Generation of a conditional *Lin9* knockout mouse.
- Fig. 3.14: Generation of a conditional *Lin9* knockout mouse *in vivo*.
- Fig. 3.15: Analysis of *Lin9*<sup>fl/fl</sup> MEFs infected with HR-Cre.
- Fig. 3.16: Analysis of *Lin9*<sup>fl/fl</sup> Cre-ERT2 MEFs.
- Fig. 4.2: Hypothesis: LIN9 is a dosage dependent tumor suppressor and its complete loss leads to lethality.
- Fig. 7.1: Conditional *Lin9* knockout.
- Fig. 7.2: Sequence overview of the floxed *Lin9* allele.
- Fig. 7.3: Primer scheme for the floxed targeting strategy.

## 7.7 Citations

- Aoki, F., Worrall, D. M., Schultz, R. M., 1997. Regulation of transcriptional activity during the first and second cell cycles in the preimplantation mouse embryo. *Dev Biol.* 181, 296-307.
- Arroyo, M., Raychaudhuri, P., 1992. Retinoblastoma-repression of E2F-dependent transcription depends on the ability of the retinoblastoma protein to interact with E2F and is abrogated by the adenovirus E1A oncoprotein. *Nucleic Acids Res.* 20, 5947-54.
- Avilion, A. A., Nicolis, S. K., Pevny, L. H., Perez, L., Vivian, N., Lovell-Badge, R., 2003. Multipotent cell lineages in early mouse development depend on SOX2 function. *Genes Dev.* 17, 126-40.
- Bates, S., Parry, D., Bonetta, L., Vousden, K., Dickson, C., Peters, G., 1994. Absence of cyclin D/cdk complexes in cells lacking functional retinoblastoma protein. *Oncogene.* 9, 1633-40.
- Beall, E. L., Bell, M., Georgette, D., Botchan, M. R., 2004. Dm-myb mutant lethality in *Drosophila* is dependent upon mip130: positive and negative regulation of DNA replication. *Genes Dev.* 18, 1667-80.
- Beall, E. L., Lewis, P. W., Bell, M., Rocha, M., Jones, D. L., Botchan, M. R., 2007. Discovery of tMAC: a *Drosophila* testis-specific meiotic arrest complex paralogous to Myb-Muv B. *Genes Dev.* 21, 904-19.
- Beall, E. L., Manak, J. R., Zhou, S., Bell, M., Lipsick, J. S., Botchan, M. R., 2002. Role for a *Drosophila* Myb-containing protein complex in site-specific DNA replication. *Nature.* 420, 833-7.
- Bender, T. P., Kremer, C. S., Kraus, M., Buch, T., Rajewsky, K., 2004. Critical functions for c-Myb at three checkpoints during thymocyte development. *Nat Immunol.* 5, 721-9.
- Benetti, R., Gonzalo, S., Jaco, I., Munoz, P., Gonzalez, S., Schoeftner, S., Murchison, E., Andl, T., Chen, T., Klatt, P., Li, E., Serrano, M., Millar, S., Hannon, G., Blasco, M. A., 2008. A mammalian microRNA cluster controls DNA methylation and telomere recombination via Rbl2-dependent regulation of DNA methyltransferases. *Nat Struct Mol Biol.* 15, 268-79.
- Bessa, M., Saville, M. K., Watson, R. J., 2001. Inhibition of cyclin A/Cdk2 phosphorylation impairs B-Myb transactivation function without affecting interactions with DNA or the CBP coactivator. *Oncogene.* 20, 3376-86.
- Blais, A., Dynlacht, B. D., 2004. Hitting their targets: an emerging picture of E2F and cell cycle control. *Curr Opin Genet Dev.* 14, 527-32.
- Bolton, V. N., Oades, P. J., Johnson, M. H., 1984. The relationship between cleavage, DNA replication, and gene expression in the mouse 2-cell embryo. *J Embryol Exp Morphol.* 79, 139-63.
- Bradford, M. M., 1976. A rapid and sensitive method for the quantitation of microgram quantities of protein utilizing the principle of protein-dye binding. *Anal Biochem.* 72, 248-54.
- Bradley, A., Evans, M., Kaufman, M. H., Robertson, E., 1984. Formation of germ-line chimaeras from embryo-derived teratocarcinoma cell lines. *Nature.* 309, 255-6.
- Burdon, T., Smith, A., Savatier, P., 2002. Signalling, cell cycle and pluripotency in embryonic stem cells. *Trends Cell Biol.* 12, 432-8.
- Ceol, C. J., Horvitz, H. R., 2001. dpl-1 DP and efl-1 E2F act with lin-35 Rb to antagonize Ras signaling in *C. elegans* vulval development. *Mol Cell.* 7, 461-73.
- Ceol, C. J., Horvitz, H. R., 2004. A new class of *C. elegans* synMuv genes implicates a Tip60/NuA4-like HAT complex as a negative regulator of Ras signaling. *Dev Cell.* 6, 563-76.
- Chazaud, C., Yamanaka, Y., Pawson, T., Rossant, J., 2006. Early lineage segregation between epiblast and primitive endoderm in mouse blastocysts through the Grb2-MAPK pathway. *Dev Cell.* 10, 615-24.
- Ciemerych, M. A., Sicinski, P., 2005. Cell cycle in mouse development. *Oncogene.* 24, 2877-98.
- Clarke, A. R., Maandag, E. R., van Roon, M., van der Lugt, N. M., van der Valk, M., Hooper, M. L., Berns, A., te Riele, H., 1992. Requirement for a functional Rb-1 gene in murine development. *Nature.* 359, 328-30.
- Cobrinik, D., Lee, M. H., Hannon, G., Mulligan, G., Bronson, R. T., Dyson, N., Harlow, E., Beach, D., Weinberg, R. A., Jacks, T., 1996. Shared role of the pRB-related p130 and p107 proteins in limb development. *Genes Dev.* 10, 1633-44.
- Coller, H. A., 2007. What's taking so long? S-phase entry from quiescence versus proliferation. *Nat Rev Mol Cell Biol.* 8, 667-70.
- Coverley, D., Pelizon, C., Trewick, S., Laskey, R. A., 2000. Chromatin-bound Cdc6 persists in S and G2 phases in human cells, while soluble Cdc6 is destroyed in a cyclin A-cdk2 dependent process. *J Cell Sci.* 113 ( Pt 11), 1929-38.
- Dagnino, L., Fry, C. J., Bartley, S. M., Farnham, P., Gallie, B. L., Phillips, R. A., 1997a. Expression patterns of the E2F family of transcription factors during mouse nervous system development. *Mech Dev.* 66, 13-25.
- Dagnino, L., Fry, C. J., Bartley, S. M., Farnham, P., Gallie, B. L., Phillips, R. A., 1997b. Expression patterns of the E2F family of transcription factors during murine epithelial development. *Cell Growth Differ.* 8, 553-63.

- Dannenberg, J. H., van Rossum, A., Schuijff, L., te Riele, H., 2000. Ablation of the retinoblastoma gene family deregulates G(1) control causing immortalization and increased cell turnover under growth-restricting conditions. *Genes Dev.* 14, 3051-64.
- den Elzen, N., Pines, J., 2001. Cyclin A is destroyed in prometaphase and can delay chromosome alignment and anaphase. *J Cell Biol.* 153, 121-36.
- Dimova, D. K., Stevaux, O., Frolov, M. V., Dyson, N. J., 2003. Cell cycle-dependent and cell cycle-independent control of transcription by the Drosophila E2F/RB pathway. *Genes Dev.* 17, 2308-20.
- Draetta, G., Luca, F., Westendorf, J., Brizuela, L., Ruderman, J., Beach, D., 1989. Cdc2 protein kinase is complexed with both cyclin A and B: evidence for proteolytic inactivation of MPF. *Cell.* 56, 829-38.
- Du, W., Vidal, M., Xie, J. E., Dyson, N., 1996. RBF, a novel RB-related gene that regulates E2F activity and interacts with cyclin E in Drosophila. *Genes Dev.* 10, 1206-18.
- Dulic, V., Lees, E., Reed, S. I., 1992. Association of human cyclin E with a periodic G1-S phase protein kinase. *Science.* 257, 1958-61.
- Elling, U., Klasen, C., Eisenberger, T., Anlag, K., Treier, M., 2006. Murine inner cell mass-derived lineages depend on Sall4 function. *Proc Natl Acad Sci U S A.* 103, 16319-24.
- Evans, M. J., Kaufman, M. H., 1981. Establishment in culture of pluripotential cells from mouse embryos. *Nature.* 292, 154-6.
- Farley, F. W., Soriano, P., Steffen, L. S., Dymecki, S. M., 2000. Widespread recombinase expression using FLPeR (flipper) mice. *Genesis.* 28, 106-10.
- Fay, D. S., Han, M., 2000. The synthetic multivulval genes of *C. elegans*: functional redundancy, Ras-antagonism, and cell fate determination. *Genesis.* 26, 279-84.
- Feil, R., Wagner, J., Metzger, D., Chambon, P., 1997. Regulation of Cre recombinase activity by mutated estrogen receptor ligand-binding domains. *Biochem Biophys Res Commun.* 237, 752-7.
- Felsani, A., Mileo, A. M., Paggi, M. G., 2006. Retinoblastoma family proteins as key targets of the small DNA virus oncoproteins. *Oncogene.* 25, 5277-85.
- Ferguson, E. L., Horvitz, H. R., 1985. Identification and characterization of 22 genes that affect the vulval cell lineages of the nematode *Caenorhabditis elegans*. *Genetics.* 110, 17-72.
- Ferguson, E. L., Horvitz, H. R., 1989. The multivulva phenotype of certain *Caenorhabditis elegans* mutants results from defects in two functionally redundant pathways. *Genetics.* 123, 109-21.
- Frolov, M. V., Dyson, N. J., 2004. Molecular mechanisms of E2F-dependent activation and pRB-mediated repression. *J Cell Sci.* 117, 2173-81.
- Furuno, N., den Elzen, N., Pines, J., 1999. Human cyclin A is required for mitosis until mid prophase. *J Cell Biol.* 147, 295-306.
- Gagrica, S., Hauser, S., Kolfshoten, I., Osterloh, L., Agami, R., Gaubatz, S., 2004. Inhibition of oncogenic transformation by mammalian Lin-9, a pRB-associated protein. *Embo J.* 23, 4627-38.
- Garcia, P., Berlanga, O., Watson, R., Frampton, J., 2005. Generation of a conditional allele of the B-myb gene. *Genesis.* 43, 189-95.
- Gardner, R. L., 1983. Origin and differentiation of extraembryonic tissues in the mouse. *Int Rev Exp Pathol.* 24, 63-133.
- Gardner, R. L., 1996. Can developmentally significant spatial patterning of the egg be discounted in mammals? *Hum Reprod Update.* 2, 3-27.
- Gaubatz, S., Lees, J. A., Lindeman, G. J., Livingston, D. M., 2001. E2F4 is exported from the nucleus in a CRM1-dependent manner. *Mol Cell Biol.* 21, 1384-92.
- Gaubatz, S., Lindeman, G. J., Ishida, S., Jakoi, L., Nevins, J. R., Livingston, D. M., Rempel, R. E., 2000. E2F4 and E2F5 play an essential role in pocket protein-mediated G1 control. *Mol Cell.* 6, 729-35.
- Georlette, D., Ahn, S., MacAlpine, D. M., Cheung, E., Lewis, P. W., Beall, E. L., Bell, S. P., Speed, T., Manak, J. R., Botchan, M. R., 2007. Genomic profiling and expression studies reveal both positive and negative activities for the Drosophila Myb MuvB/dREAM complex in proliferating cells. *Genes Dev.* 21, 2880-96.
- Giacinti, C., Giordano, A., 2006. RB and cell cycle progression. *Oncogene.* 25, 5220-7.
- Girard, F., Strausfeld, U., Fernandez, A., Lamb, N. J., 1991. Cyclin A is required for the onset of DNA replication in mammalian fibroblasts. *Cell.* 67, 1169-79.
- Goetz, C. A., Harmon, I. R., O'Neil, J. J., Burchill, M. A., Farrar, M. A., 2004. STAT5 activation underlies IL7 receptor-dependent B cell development. *J Immunol.* 172, 4770-8.
- Goldbard, S. B., Warner, C. M., 1982. Genes affect the timing of early mouse embryo development. *Biol Reprod.* 27, 419-24.
- Gonda, T. J., Metcalf, D., 1984. Expression of myb, myc and fos proto-oncogenes during the differentiation of a murine myeloid leukaemia. *Nature.* 310, 249-51.
- Gudas, J. M., Payton, M., Thukral, S., Chen, E., Bass, M., Robinson, M. O., Coats, S., 1999. Cyclin E2, a novel G1 cyclin that binds Cdk2 and is aberrantly expressed in human cancers. *Mol Cell Biol.* 19, 612-22.
- Hadwiger, J. A., Wittenberg, C., Richardson, H. E., de Barros Lopes, M., Reed, S. I., 1989. A family of cyclin homologs that control the G1 phase in yeast. *Proc Natl Acad Sci U S A.* 86, 6255-9.

- Hameyer, D., Loonstra, A., Eshkind, L., Schmitt, S., Antunes, C., Groen, A., Bindels, E., Jonkers, J., Krimpenfort, P., Meuwissen, R., Rijswijk, L., Bex, A., Berns, A., Bockamp, E., 2007. Toxicity of ligand-dependent Cre recombinases and generation of a conditional Cre deleter mouse allowing mosaic recombination in peripheral tissues. *Physiol Genomics*. 31, 32-41.
- Hanahan, D., 1983. Studies on transformation of *Escherichia coli* with plasmids. *J Mol Biol*. 166, 557-80.
- Harrison, M. M., Ceol, C. J., Lu, X., Horvitz, H. R., 2006. Some *C. elegans* class B synthetic multivulva proteins encode a conserved LIN-35 Rb-containing complex distinct from a NuRD-like complex. *Proc Natl Acad Sci U S A*. 103, 16782-7.
- Heyer, B. S., MacAuley, A., Behrendtsen, O., Werb, Z., 2000. Hypersensitivity to DNA damage leads to increased apoptosis during early mouse development. *Genes Dev*. 14, 2072-84.
- Hogan, B., Beddington, R., Costantini, F., and Lacy, E., 1994. *Manipulating the Mouse Embryo: A Laboratory Manual*. Cold Spring Harbor Laboratory Press, Cold Spring Harbor. Second edition.
- Horvitz, H. R., Sulston, J. E., 1980. Isolation and genetic characterization of cell-lineage mutants of the nematode *Caenorhabditis elegans*. *Genetics*. 96, 435-54.
- Howlett, S. K., 1986. A set of proteins showing cell cycle dependent modification in the early mouse embryo. *Cell*. 45, 387-96.
- Howlett, S. K., Bolton, V. N., 1985. Sequence and regulation of morphological and molecular events during the first cell cycle of mouse embryogenesis. *J Embryol Exp Morphol*. 87, 175-206.
- Humbert, P. O., Rogers, C., Ganiatsas, S., Landsberg, R. L., Trimarchi, J. M., Dandapani, S., Brugnara, C., Erdman, S., Schrenzel, M., Bronson, R. T., Lees, J. A., 2000. E2F4 is essential for normal erythrocyte maturation and neonatal viability. *Mol Cell*. 6, 281-91.
- Iwai, N., Kitajima, K., Sakai, K., Kimura, T., Nakano, T., 2001. Alteration of cell adhesion and cell cycle properties of ES cells by an inducible dominant interfering Myb mutant. *Oncogene*. 20, 1425-34.
- Iwamori, N., Naito, K., Sugiura, K., Tojo, H., 2002. Preimplantation-embryo-specific cell cycle regulation is attributed to the low expression level of retinoblastoma protein. *FEBS Lett*. 526, 119-23.
- Jacks, T., Fazeli, A., Schmitt, E. M., Bronson, R. T., Goodell, M. A., Weinberg, R. A., 1992. Effects of an Rb mutation in the mouse. *Nature*. 359, 295-300.
- Jeganathan, K., Malureanu, L., Baker, D. J., Abraham, S. C., van Deursen, J. M., 2007. Bub1 mediates cell death in response to chromosome missegregation and acts to suppress spontaneous tumorigenesis. *J Cell Biol*. 179, 255-67.
- Jiang, Z., Zacksenhaus, E., Gallie, B. L., Phillips, R. A., 1997. The retinoblastoma gene family is differentially expressed during embryogenesis. *Oncogene*. 14, 1789-97.
- Joaquin, M., Watson, R. J., 2003. Cell cycle regulation by the B-Myb transcription factor. *Cell Mol Life Sci*. 60, 2389-401.
- Kato, J., Matsushime, H., Hiebert, S. W., Ewen, M. E., Sherr, C. J., 1993. Direct binding of cyclin D to the retinoblastoma gene product (pRb) and pRb phosphorylation by the cyclin D-dependent kinase CDK4. *Genes Dev*. 7, 331-42.
- Kaufman, M. H., 2004. *Atlas of Mouse Development*.
- Koff, A., Giordano, A., Desai, D., Yamashita, K., Harper, J. W., Elledge, S., Nishimoto, T., Morgan, D. O., Franza, B. R., Roberts, J. M., 1992. Formation and activation of a cyclin E-cdk2 complex during the G1 phase of the human cell cycle. *Science*. 257, 1689-94.
- Korenjak, M., Taylor-Harding, B., Binne, U. K., Satterlee, J. S., Stevaux, O., Aasland, R., White-Cooper, H., Dyson, N., Brehm, A., 2004. Native E2F/RBF complexes contain Myb-interacting proteins and repress transcription of developmentally controlled E2F target genes. *Cell*. 119, 181-93.
- Kornfeld, K., 1997. Vulval development in *Caenorhabditis elegans*. *Trends Genet*. 13, 55-61.
- Kurosawa, H., 2007. Methods for inducing embryoid body formation: in vitro differentiation system of embryonic stem cells. *J Biosci Bioeng*. 103, 389-98.
- Laemmli, U. K., 1970. Cleavage of structural proteins during the assembly of the head of bacteriophage T4. *Nature*. 227, 680-5.
- Lan, Z. J., Xu, X., Cooney, A. J., 2004. Differential oocyte-specific expression of Cre recombinase activity in GDF-9-iCre, Zp3cre, and Msx2Cre transgenic mice. *Biol Reprod*. 71, 1469-74.
- Latham, K. E., Litvin, J., Orth, J. M., Patel, B., Mettus, R., Reddy, E. P., 1996. Temporal patterns of A-myb and B-myb gene expression during testis development. *Oncogene*. 13, 1161-8.
- Lauper, N., Beck, A. R., Cariou, S., Richman, L., Hofmann, K., Reith, W., Slingerland, J. M., Amati, B., 1998. Cyclin E2: a novel CDK2 partner in the late G1 and S phases of the mammalian cell cycle. *Oncogene*. 17, 2637-43.
- LeCouter, J. E., Kablar, B., Hardy, W. R., Ying, C., Megeney, L. A., May, L. L., Rudnicki, M. A., 1998a. Strain-dependent myeloid hyperplasia, growth deficiency, and accelerated cell cycle in mice lacking the Rb-related p107 gene. *Mol Cell Biol*. 18, 7455-65.
- LeCouter, J. E., Kablar, B., Whyte, P. F., Ying, C., Rudnicki, M. A., 1998b. Strain-dependent embryonic lethality in mice lacking the retinoblastoma-related p130 gene. *Development*. 125, 4669-79.

- Lee, E. Y., Chang, C. Y., Hu, N., Wang, Y. C., Lai, C. C., Herrup, K., Lee, W. H., Bradley, A., 1992. Mice deficient for Rb are nonviable and show defects in neurogenesis and haematopoiesis. *Nature*. 359, 288-94.
- Lee, M. H., Williams, B. O., Mulligan, G., Mukai, S., Bronson, R. T., Dyson, N., Harlow, E., Jacks, T., 1996. Targeted disruption of p107: functional overlap between p107 and Rb. *Genes Dev.* 10, 1621-32.
- Lee, W. H., Bookstein, R., Hong, F., Young, L. J., Shew, J. Y., Lee, E. Y., 1987. Human retinoblastoma susceptibility gene: cloning, identification, and sequence. *Science*. 235, 1394-9.
- Leone, G., DeGregori, J., Jakoi, L., Cook, J. G., Nevins, J. R., 1999. Collaborative role of E2F transcriptional activity and G1 cyclin-dependent kinase activity in the induction of S phase. *Proc Natl Acad Sci U S A*. 96, 6626-31.
- Lewis, P. W., Beall, E. L., Fleischer, T. C., Georgette, D., Link, A. J., Botchan, M. R., 2004. Identification of a *Drosophila* Myb-E2F2/RBF transcriptional repressor complex. *Genes Dev.* 18, 2929-40.
- Lindeman, G. J., Dagnino, L., Gaubatz, S., Xu, Y., Bronson, R. T., Warren, H. B., Livingston, D. M., 1998. A specific, nonproliferative role for E2F-5 in choroid plexus function revealed by gene targeting. *Genes Dev.* 12, 1092-8.
- Lipinski, M. M., Jacks, T., 1999. The retinoblastoma gene family in differentiation and development. *Oncogene*. 18, 7873-82.
- Lipsick, J. S., 2004. synMuv verite--Myb comes into focus. *Genes Dev.* 18, 2837-44.
- Litovchick, L., Sadasivam, S., Florens, L., Zhu, X., Swanson, S. K., Velmurugan, S., Chen, R., Washburn, M. P., Liu, X. S., DeCaprio, J. A., 2007. Evolutionarily conserved multisubunit RBL2/p130 and E2F4 protein complex represses human cell cycle-dependent genes in quiescence. *Mol Cell*. 26, 539-51.
- Lu, X., Horvitz, H. R., 1998. lin-35 and lin-53, two genes that antagonize a *C. elegans* Ras pathway, encode proteins similar to Rb and its binding protein RbAp48. *Cell*. 95, 981-91.
- Luthardt, F. W., Donahue, R. P., 1975. DNA synthesis in developing two-cell mouse embryos. *Dev Biol*. 44, 210-6.
- Mac Auley, A., Werb, Z., Mirkes, P. E., 1993. Characterization of the unusually rapid cell cycles during rat gastrulation. *Development*. 117, 873-83.
- Martin, G. R., 1981. Isolation of a pluripotent cell line from early mouse embryos cultured in medium conditioned by teratocarcinoma stem cells. *Proc Natl Acad Sci U S A*. 78, 7634-8.
- Martin, L., Finn, C. A., 1968. Hormonal regulation of cell division in epithelial and connective tissues of the mouse uterus. *J Endocrinol*. 41, 363-71.
- Matsushime, H., Ewen, M. E., Strom, D. K., Kato, J. Y., Hanks, S. K., Roussel, M. F., Sherr, C. J., 1992. Identification and properties of an atypical catalytic subunit (p34PSK-J3/cdk4) for mammalian D type G1 cyclins. *Cell*. 71, 323-34.
- Meyerson, M., Harlow, E., 1994. Identification of G1 kinase activity for cdk6, a novel cyclin D partner. *Mol Cell Biol*. 14, 2077-86.
- Minshull, J., Golsteyn, R., Hill, C. S., Hunt, T., 1990. The A- and B-type cyclin associated cdc2 kinases in *Xenopus* turn on and off at different times in the cell cycle. *Embo J*. 9, 2865-75.
- Morgan, D. O., 1997. Cyclin-dependent kinases: engines, clocks, and microprocessors. *Annu Rev Cell Dev Biol*. 13, 261-91.
- Morita, S., Kojima, T., Kitamura, T., 2000. Plat-E: an efficient and stable system for transient packaging of retroviruses. *Gene Ther*. 7, 1063-6.
- Morris, L., Allen, K. E., La Thangue, N. B., 2000. Regulation of E2F transcription by cyclin E-Cdk2 kinase mediated through p300/CBP co-activators. *Nat Cell Biol*. 2, 232-9.
- Morrisey, E. E., Tang, Z., Sigrist, K., Lu, M. M., Jiang, F., Ip, H. S., Parmacek, M. S., 1998. GATA6 regulates HNF4 and is required for differentiation of visceral endoderm in the mouse embryo. *Genes Dev*. 12, 3579-90.
- Mountford, P., Zevnik, B., Duwel, A., Nichols, J., Li, M., Dani, C., Robertson, M., Chambers, I., Smith, A., 1994. Dicistronic targeting constructs: reporters and modifiers of mammalian gene expression. *Proc Natl Acad Sci U S A*. 91, 4303-7.
- Mucenski, M. L., McLain, K., Kier, A. B., Swerdlow, S. H., Schreiner, C. M., Miller, T. A., Pietryga, D. W., Scott, W. J., Jr., Potter, S. S., 1991. A functional c-myb gene is required for normal murine fetal hepatic hematopoiesis. *Cell*. 65, 677-89.
- Mudrak, I., Ogris, E., Rotheneder, H., Wintersberger, E., 1994. Coordinated trans activation of DNA synthesis- and precursor-producing enzymes by polyomavirus large T antigen through interaction with the retinoblastoma protein. *Mol Cell Biol*. 14, 1886-92.
- Mummery, C. L., van Rooijen, M. A., van den Brink, S. E., de Laat, S. W., 1987. Cell cycle analysis during retinoic acid induced differentiation of a human embryonal carcinoma-derived cell line. *Cell Differ*. 20, 153-60.
- Murphy, M., Stinnakre, M. G., Senamaud-Beaufort, C., Winston, N. J., Sweeney, C., Kubelka, M., Carrington, M., Brechot, C., Sobczak-Thepot, J., 1997. Delayed early embryonic lethality following disruption of the murine cyclin A2 gene. *Nat Genet*. 15, 83-6.
- Murray, A. W., 2004. Recycling the cell cycle: cyclins revisited. *Cell*. 116, 221-34.

- Nagy, A., 2000. Cre recombinase: the universal reagent for genome tailoring. *Genesis*. 26, 99-109.
- Nash, R., Tokiwa, G., Anand, S., Erickson, K., Futcher, A. B., 1988. The WHI1+ gene of *Saccharomyces cerevisiae* tethers cell division to cell size and is a cyclin homolog. *Embo J.* 7, 4335-46.
- Ness, S. A., 2003. Myb protein specificity: evidence of a context-specific transcription factor code. *Blood Cells Mol Dis.* 31, 192-200.
- Nichols, J., Zevnik, B., Anastassiadis, K., Niwa, H., Klewe-Nebenius, D., Chambers, I., Scholer, H., Smith, A., 1998. Formation of pluripotent stem cells in the mammalian embryo depends on the POU transcription factor Oct4. *Cell.* 95, 379-91.
- Nothias, J. Y., Majumder, S., Kaneko, K. J., DePamphilis, M. L., 1995. Regulation of gene expression at the beginning of mammalian development. *J Biol Chem.* 270, 22077-80.
- Obaya, A. J., Sedivy, J. M., 2002. Regulation of cyclin-Cdk activity in mammalian cells. *Cell Mol Life Sci.* 59, 126-42.
- Ogata, K., Morikawa, S., Nakamura, H., Sekikawa, A., Inoue, T., Kanai, H., Sarai, A., Ishii, S., Nishimura, Y., 1994. Solution structure of a specific DNA complex of the Myb DNA-binding domain with cooperative recognition helices. *Cell.* 79, 639-48.
- Oh, I. H., Reddy, E. P., 1999. The myb gene family in cell growth, differentiation and apoptosis. *Oncogene.* 18, 3017-33.
- Orford, K. W., Scadden, D. T., 2008. Deconstructing stem cell self-renewal: genetic insights into cell-cycle regulation. *Nat Rev Genet.* 9, 115-28.
- Osterloh, L., von Eyss, B., Schmit, F., Rein, L., Hubner, D., Samans, B., Hauser, S., Gaubatz, S., 2007. The human synMuv-like protein LIN-9 is required for transcription of G2/M genes and for entry into mitosis. *Embo J.* 26, 144-57.
- Pagano, M., Pepperkok, R., Verde, F., Ansorge, W., Draetta, G., 1992. Cyclin A is required at two points in the human cell cycle. *Embo J.* 11, 961-71.
- Pampfer, S., Donnay, I., 1999. Apoptosis at the time of embryo implantation in mouse and rat. *Cell Death Differ.* 6, 533-45.
- Papayioannou, V. E. a. B., R. R., 2005. *Mouse Phenotypes: A Handbook of Mutation Analysis*. Papayioannou, V. E. and Behringer, R. R., 235pp.
- Pardee, A. B., 1974. A restriction point for control of normal animal cell proliferation. *Proc Natl Acad Sci U S A.* 71, 1286-90.
- Parr, M. B., Parr, E. L., 1989. *The implantation reaction*. R. M. Wynn and W. P. Jollie, Editors, The Uterus, Plenum, New York 233-277.
- Pelton, T. A., Sharma, S., Schulz, T. C., Rathjen, J., Rathjen, P. D., 2002. Transient pluripotent cell populations during primitive ectoderm formation: correlation of in vivo and in vitro pluripotent cell development. *J Cell Sci.* 115, 329-39.
- Perera, D., Tilston, V., Hopwood, J. A., Barchi, M., Boot-Handford, R. P., Taylor, S. S., 2007. Bub1 maintains centromeric cohesion by activation of the spindle checkpoint. *Dev Cell.* 13, 566-79.
- Pesce, M., Scholer, H. R., 2000. Oct-4: control of totipotency and germline determination. *Mol Reprod Dev.* 55, 452-7.
- Petersen, B. O., Lukas, J., Sorensen, C. S., Bartek, J., Helin, K., 1999. Phosphorylation of mammalian CDC6 by cyclin A/CDK2 regulates its subcellular localization. *Embo J.* 18, 396-410.
- Pfister, S., Steiner, K. A., Tam, P. P., 2007. Gene expression pattern and progression of embryogenesis in the immediate post-implantation period of mouse development. *Gene Expr Patterns.* 7, 558-73.
- Pilkinton, M., Sandoval, R., Colamonici, O. R., 2007. Mammalian Mip/LIN-9 interacts with either the p107, p130/E2F4 repressor complex or B-Myb in a cell cycle-phase-dependent context distinct from the *Drosophila* dREAM complex. *Oncogene.* 26, 7535-43.
- Planas-Silva, M. D., Weinberg, R. A., 1997. The restriction point and control of cell proliferation. *Curr Opin Cell Biol.* 9, 768-72.
- Poirier, F., Chan, C. T., Timmons, P. M., Robertson, E. J., Evans, M. J., Rigby, P. W., 1991. The murine H19 gene is activated during embryonic stem cell differentiation in vitro and at the time of implantation in the developing embryo. *Development.* 113, 1105-14.
- Psychoyos, S., Bax, M., Atkins, C., 1986. Differences in Ca<sup>2+</sup> entry blockers revealed by effects on adenosine- and adrenergic- receptors and cyclic AMP levels of [2-3H]adenine-prelabeled vesicles prepared from guinea pig brain. *Biochem Pharmacol.* 35, 1639-46.
- Putkey, F. R., Cramer, T., Morphew, M. K., Silk, A. D., Johnson, R. S., McIntosh, J. R., Cleveland, D. W., 2002. Unstable kinetochore-microtubule capture and chromosomal instability following deletion of CENP-E. *Dev Cell.* 3, 351-65.
- Ram, P. T., Schultz, R. M., 1993. Reporter gene expression in G2 of the 1-cell mouse embryo. *Dev Biol.* 156, 552-6.
- Rayman, J. B., Takahashi, Y., Indjeian, V. B., Dannenberg, J. H., Catchpole, S., Watson, R. J., te Riele, H., Dynlacht, B. D., 2002. E2F mediates cell cycle-dependent transcriptional repression in vivo by recruitment of an HDAC1/mSin3B corepressor complex. *Genes Dev.* 16, 933-47.

- Rempel, R. E., Saenz-Robles, M. T., Storms, R., Morham, S., Ishida, S., Engel, A., Jakoi, L., Melhem, M. F., Pipas, J. M., Smith, C., Nevins, J. R., 2000. Loss of E2F4 activity leads to abnormal development of multiple cellular lineages. *Mol Cell.* 6, 293-306.
- Rivera-Perez, J. A., 2007. Axial specification in mice: ten years of advances and controversies. *J Cell Physiol.* 213, 654-60.
- Robanus-Maandag, E., Dekker, M., van der Valk, M., Carrozza, M. L., Jeanny, J. C., Dannenberg, J. H., Berns, A., te Riele, H., 1998. p107 is a suppressor of retinoblastoma development in pRb-deficient mice. *Genes Dev.* 12, 1599-609.
- Rodriguez, C. I., Buchholz, F., Galloway, J., Sequerra, R., Kasper, J., Ayala, R., Stewart, A. F., Dymecki, S. M., 2000. High-efficiency deleter mice show that FLPe is an alternative to Cre-loxP. *Nat Genet.* 25, 139-40.
- Sadowski, P. D., 1995. The Flp recombinase of the 2-microns plasmid of *Saccharomyces cerevisiae*. *Prog Nucleic Acid Res Mol Biol.* 51, 53-91.
- Sage, J., Mulligan, G. J., Attardi, L. D., Miller, A., Chen, S., Williams, B., Theodorou, E., Jacks, T., 2000. Targeted disruption of the three Rb-related genes leads to loss of G(1) control and immortalization. *Genes Dev.* 14, 3037-50.
- Sala, A., 2005. B-MYB, a transcription factor implicated in regulating cell cycle, apoptosis and cancer. *Eur J Cancer.* 41, 2479-84.
- Sanchez, I., Dynlacht, B. D., 2005. New insights into cyclins, CDKs, and cell cycle control. *Semin Cell Dev Biol.* 16, 311-21.
- Sandoval, R., Xue, J., Tian, X., Barrett, K., Pilkinton, M., Ucker, D. S., Raychaudhuri, P., Kineman, R. D., Luque, R. M., Baida, G., Zou, X., Valli, V. E., Cook, J. L., Kiyokawa, H., Colamonici, O. R., 2006. A mutant allele of BARA/LIN-9 rescues the cdk4<sup>-/-</sup> phenotype by releasing the repression on E2F-regulated genes. *Exp Cell Res.* 312, 2465-75.
- Santamaria, D., Barriere, C., Cerqueira, A., Hunt, S., Tardy, C., Newton, K., Caceres, J. F., Dubus, P., Malumbres, M., Barbacid, M., 2007. Cdk1 is sufficient to drive the mammalian cell cycle. *Nature.* 448, 811-5.
- Sardet, C., Vidal, M., Cobrinik, D., Geng, Y., Onufryk, C., Chen, A., Weinberg, R. A., 1995. E2F-4 and E2F-5, two members of the E2F family, are expressed in the early phases of the cell cycle. *Proc Natl Acad Sci U S A.* 92, 2403-7.
- Sauer, B., 1993. Manipulation of transgenes by site-specific recombination: use of Cre recombinase. *Methods Enzymol.* 225, 890-900.
- Sauer, B., Henderson, N., 1988. Site-specific DNA recombination in mammalian cells by the Cre recombinase of bacteriophage P1. *Proc Natl Acad Sci U S A.* 85, 5166-70.
- Savatier, P., Huang, S., Szekely, L., Wiman, K. G., Samarut, J., 1994. Contrasting patterns of retinoblastoma protein expression in mouse embryonic stem cells and embryonic fibroblasts. *Oncogene.* 9, 809-18.
- Schmit, F., Korenjak, M., Mannefeld, M., Schmitt, K., Franke, C., von Eyss, B., Gargica, S., Hanel, F., Brehm, A., Gaubatz, S., 2007. LINC, a human complex that is related to pRB-containing complexes in invertebrates regulates the expression of G2/M genes. *Cell Cycle.* 6, 1903-13.
- Schultz, R. M., 1993. Regulation of zygotic gene activation in the mouse. *Bioessays.* 15, 531-8.
- Schwenk, F., Baron, U., Rajewsky, K., 1995. A cre-transgenic mouse strain for the ubiquitous deletion of loxP-flanked gene segments including deletion in germ cells. *Nucleic Acids Res.* 23, 5080-1.
- Sellers, W. R., Novitch, B. G., Miyake, S., Heith, A., Otterson, G. A., Kaye, F. J., Lassar, A. B., Kaelin, W. G., Jr., 1998. Stable binding to E2F is not required for the retinoblastoma protein to activate transcription, promote differentiation, and suppress tumor cell growth. *Genes Dev.* 12, 95-106.
- Sherr, C. J., 1996. Cancer cell cycles. *Science.* 274, 1672-7.
- Sherr, C. J., Roberts, J. M., 1999. CDK inhibitors: positive and negative regulators of G1-phase progression. *Genes Dev.* 13, 1501-12.
- Sherr, C. J., Roberts, J. M., 2004. Living with or without cyclins and cyclin-dependent kinases. *Genes Dev.* 18, 2699-711.
- Silver, D. L., Montell, D. J., 2003. A new trick for Cyclin-Cdk: activation of STAT. *Dev Cell.* 4, 148-9.
- Silver, D. P., Livingston, D. M., 2001. Self-excising retroviral vectors encoding the Cre recombinase overcome Cre-mediated cellular toxicity. *Mol Cell.* 8, 233-43.
- Sinkkonen, L., Hugenschmidt, T., Berninger, P., Gaidatzis, D., Mohn, F., Artus-Revel, C. G., Zavolan, M., Svoboda, P., Filipowicz, W., 2008. MicroRNAs control de novo DNA methylation through regulation of transcriptional repressors in mouse embryonic stem cells. *Nat Struct Mol Biol.* 15, 259-67.
- Sitzmann, J., Noben-Trauth, K., Kamano, H., Klempnauer, K. H., 1996. Expression of B-Myb during mouse embryogenesis. *Oncogene.* 12, 1889-94.
- Snow, M. H. L., 1977. Gastrulation in the mouse: Growth and regionalisation of the epiblast. *J. Embryol. Exp. Morphol.*, 293-303.
- Solter, D., Knowles, B. B., 1975. Immunology of mouse blastocyst. *Proc Natl Acad Sci U S A.* 72, 5099-102.
- Stead, E., White, J., Faast, R., Conn, S., Goldstone, S., Rathjen, J., Dhingra, U., Rathjen, P., Walker, D., Dalton, S., 2002. Pluripotent cell division cycles are driven by ectopic Cdk2, cyclin A/E and E2F activities. *Oncogene.* 21, 8320-33.

- Stevaux, O., Dyson, N. J., 2002. A revised picture of the E2F transcriptional network and RB function. *Curr Opin Cell Biol.* 14, 684-91.
- Sutherland, A., 2003. Mechanisms of implantation in the mouse: differentiation and functional importance of trophoblast giant cell behavior. *Dev Biol.* 258, 241-51.
- Tanaka, Y., Patestos, N. P., Maekawa, T., Ishii, S., 1999. B-myb is required for inner cell mass formation at an early stage of development. *J Biol Chem.* 274, 28067-70.
- Tarasov, K. V., Tarasova, Y. S., Tam, W. L., Riordon, D. R., Elliott, S. T., Kania, G., Li, J., Yamanaka, S., Crider, D. G., Testa, G., Li, R. A., Lim, B., Stewart, C. L., Liu, Y., Van Eyk, J. E., Wersto, R. P., Wobus, A. M., Boheler, K. R., 2008a. B-MYB is essential for normal cell cycle progression and chromosomal stability of embryonic stem cells. *PLoS ONE.* 3, e2478.
- Tarasov, K. V., Testa, G., Tarasova, Y. S., Kania, G., Riordon, D. R., Volkova, M., Anisimov, S. V., Wobus, A. M., Boheler, K. R., 2008b. Linkage of pluripotent stem cell-associated transcripts to regulatory gene networks. *Cells Tissues Organs.* 188, 31-45.
- Thomson, J. A., Itskovitz-Eldor, J., Shapiro, S. S., Waknitz, M. A., Swiergiel, J. J., Marshall, V. S., Jones, J. M., 1998. Embryonic stem cell lines derived from human blastocysts. *Science.* 282, 1145-7.
- Toscani, A., Mettus, R. V., Coupland, R., Simpkins, H., Litvin, J., Orth, J., Hatton, K. S., Reddy, E. P., 1997. Arrest of spermatogenesis and defective breast development in mice lacking A-myb. *Nature.* 386, 713-7.
- Trauth, K., Mutschler, B., Jenkins, N. A., Gilbert, D. J., Copeland, N. G., Klempnauer, K. H., 1994. Mouse A-myb encodes a trans-activator and is expressed in mitotically active cells of the developing central nervous system, adult testis and B lymphocytes. *Embo J.* 13, 5994-6005.
- Trimarchi, J. M., Lees, J. A., 2002. Sibling rivalry in the E2F family. *Nat Rev Mol Cell Biol.* 3, 11-20.
- Uren, A. G., Wong, L., Pakusch, M., Fowler, K. J., Burrows, F. J., Vaux, D. L., Choo, K. H., 2000. Survivin and the inner centromere protein INCENP show similar cell-cycle localization and gene knockout phenotype. *Curr Biol.* 10, 1319-28.
- van den Heuvel, S., 2005. The *C. elegans* cell cycle: overview of molecules and mechanisms. *Methods Mol Biol.* 296, 51-67.
- Varmuza, S., Prideaux, V., Kothary, R., Rossant, J., 1988. Polytene chromosomes in mouse trophoblast giant cells. *Development.* 102, 127-34.
- Verona, R., Moberg, K., Estes, S., Starz, M., Vernon, J. P., Lees, J. A., 1997. E2F activity is regulated by cell cycle-dependent changes in subcellular localization. *Mol Cell Biol.* 17, 7268-82.
- Wang, H., Dey, S. K., 2006. Roadmap to embryo implantation: clues from mouse models. *Nat Rev Genet.* 7, 185-99.
- Weaver, B. A., Silk, A. D., Montagna, C., Verdier-Pinard, P., Cleveland, D. W., 2007. Aneuploidy acts both oncogenically and as a tumor suppressor. *Cancer Cell.* 11, 25-36.
- Welsh, A. O., Enders, A. C., 1991. Chorioallantoic placenta formation in the rat: II. Angiogenesis and maternal blood circulation in the mesometrial region of the implantation chamber prior to placenta formation. *Am J Anat.* 192, 347-65.
- Wheatley, S. P., Hinchcliffé, E. H., Glotzer, M., Hyman, A. A., Sluder, G., Wang, Y., 1997. CDK1 inactivation regulates anaphase spindle dynamics and cytokinesis in vivo. *J Cell Biol.* 138, 385-93.
- Wu, L., de Bruin, A., Saavedra, H. I., Starovic, M., Trimboli, A., Yang, Y., Opavska, J., Wilson, P., Thompson, J. C., Ostrowski, M. C., Rosol, T. J., Woollett, L. A., Weinstein, M., Cross, J. C., Robinson, M. L., Leone, G., 2003. Extra-embryonic function of Rb is essential for embryonic development and viability. *Nature.* 421, 942-7.
- Wu, L., Timmers, C., Maiti, B., Saavedra, H. I., Sang, L., Chong, G. T., Nuckolls, F., Giangrande, P., Wright, F. A., Field, S. J., Greenberg, M. E., Orkin, S., Nevins, J. R., Robinson, M. L., Leone, G., 2001. The E2F1-3 transcription factors are essential for cellular proliferation. *Nature.* 414, 457-62.
- Yamauchi, T., Ishidao, T., Nomura, T., Shinagawa, T., Tanaka, Y., Yonemura, S., Ishii, S., 2008. A B-Myb complex containing clathrin and filamin is required for mitotic spindle function. *Embo J.* 27, 1852-62.
- Yan, Y., Frisen, J., Lee, M. H., Massague, J., Barbacid, M., 1997. Ablation of the CDK inhibitor p57Kip2 results in increased apoptosis and delayed differentiation during mouse development. *Genes Dev.* 11, 973-83.
- Yoshikawa, T., Piao, Y., Zhong, J., Matoba, R., Carter, M. G., Wang, Y., Goldberg, I., Ko, M. S., 2006. High-throughput screen for genes predominantly expressed in the ICM of mouse blastocysts by whole mount in situ hybridization. *Gene Expr Patterns.* 6, 213-24.
- Yu, H., Tang, Z., 2005. Bub1 multitasking in mitosis. *Cell Cycle.* 4, 262-5.
- Zariwala, M., Liu, J., Xiong, Y., 1998. Cyclin E2, a novel human G1 cyclin and activating partner of CDK2 and CDK3, is induced by viral oncoproteins. *Oncogene.* 17, 2787-98.
- Zhang, S. L., DuBois, W., Ramsay, E. S., Bliskovski, V., Morse, H. C., 3rd, Taddesse-Heath, L., Vass, W. C., DePinho, R. A., Mock, B. A., 2001. Efficiency alleles of the *Pctrl* modifier locus for plasmacytoma susceptibility. *Mol Cell Biol.* 21, 310-8.
- Zhu, W., Giangrande, P. H., Nevins, J. R., 2004. E2Fs link the control of G1/S and G2/M transcription. *Embo J.* 23, 4615-26.



## 7.8 Acknowledgement

I am deeply thankful to Prof. Stefan Gaubatz for the opportunity to work in his lab and for the supervision of my thesis. Thank you for your continuous encouragement, your helpful suggestions and optimism.

Thank you to Prof. Brand for the supervision of my thesis as a representative for the faculty of biology.

Special thanks goes to Prof. Renate Renkawitz-Pohl (Developmental Biology, Marburg) for her continuous support, Prof. Martin Eilers (IMT, Marburg) and Prof. Manfred Scharl (PCI, Würzburg) for providing a stimulating working environment in their institutes.

I want to thank all my present and former lab members for all their help, support, interest and valuable hints, as well as for numerous “Feierabendbierchen”, especially to Fabienne Schmit (trying to teach me German), Kathrin Schmitt (reading the polnische Zusammenfassung), Mirijam Mannefeld (playing my music, sometimes), Susi Spahr (mouse support), Lisa Osterloh, Markus Kleinschmidt, Steffi Hauser, Adelgunde Wolpert, Marianne Frings (best bachelorette), Katharina Brauburger & Sarah Cremer.

Thanks to all my colleagues in the PCI (Würzburg) and IMT (Marburg) for support, discussions, distractions & tea breaks.

Very special thanks to Fabienne Schmit and Conny Schmidt for always being there, sharing the weal and woe, as well as food supply and entertainment.

Thanks to all my friends for having a good time and for always being there, especially Tanja & Isabel for the good start in Wü.

Thank you to my family for their understanding and continuous support, especially to my sister Silke & Oliver Föst, and my parents Karin & Reinhard Reichert.

Very special thanks go to Oliver Kawach, for his love, continuous encouragement, and who I could always rely on.

Sincere thanks are given to them all!!

## 7.9 Own publications

- 2008 Reichert, N., Spahr, S., Gaubatz, S. Generation of Mice with a Conditional Allele of Lin9 (in submission).
- Kehoe, S.M., Oka, M., Hankowski, K.E., Reichert, N., Garcia, S., McCarrey, J.R., Gaubatz, S., and Terada, N. (2008). A Conserved E2F6-Binding Element in Murine Meiosis-Specific Gene Promoters. Biol Reprod. 2008 Jul 30. [Epub ahead of print]
- 2006 Kreiskother, N., Reichert, N., Buttgerit, D., Hertenstein, A., Fischbach, K.F., and Renkawitz-Pohl, R. (2006). Drosophila Rolling pebbles colocalises and putatively interacts with alpha-Actinin and the Sls isoform Zormin in the Z-discs of the sarcomere and with Dumbfounded/Kirre, alpha-Actinin and Zormin in the terminal Z-discs. J Muscle Res Cell Motil. 2006;27 (1):93-106.
- 2005 Storre, J., Schafer, A., Reichert, N., Barbero, J.L., Hauser, S., Eilers, M., and Gaubatz, S. (2005). Silencing of the meiotic genes SMC1beta and STAG3 in somatic cells by E2F6. J Biol Chem. 2005 Dec 16;280 (50):41380-6.

### Conference contributions (Talks & Posters)

- 06.-07.02.2008 Sonderforschungsbereich Transregio 17 Meeting, University of Würzburg.
- Poster: Reichert N., Schmitt K, Spahr S, Götz R, Rapp UR, Gaubatz S. The role of LIN9 in Ras-dependent tumorigenesis.
- 26.-30.08.2006 The 7th Transcription Meeting, EMBL, Heidelberg.
- Poster: Reichert N., Osterloh L, von Eyss B, Schmit F, Gaubatz S. The pRB-associated LIN9 protein is required for embryonic viability.
- 18.-23.02.2006 4th Winter School of the International Graduiertenkolleg "Transcriptional control in developmental processes" meeting, Kleinwalsertal (AT).
- Talk: Generating a knockout-mouse model for the RB associated lin-9 protein.
- 19.-24.02.2005 3rd Winter School of the International Graduiertenkolleg "Transcriptional control in developmental processes" meeting, Kleinwalsertal (AT).
- Talk: The role of LIN-9 for tumor suppression by the retinoblastoma protein.

## 7.10 Curriculum Vitae

### Personal Details

|                 |   |
|-----------------|---|
| Name            | Nina Reichert                                 |
| Private Address | Gegenbaurstr. 17<br>97074 Würzburg<br>Germany |
| D.O.B           | 20 June 1979                                  |
| Birthplace      | Marburg                                       |

### Education

|                 |  |
|-----------------|--|
| 10.2004-12.2008 | PhD. student in the laboratory of Prof. Dr. S. Gaubatz, PCI, Biocenter Julius-Maximilians-University Würzburg (04.2006-12.2008) and Institute of Molecular Biology and Tumor Research (IMT), University of Marburg (10.2004-03.2006).<br><br>Thesis title: The Role of LIN9 in Mouse Development.  |
| 09.1999-09.2004 | Undergraduate student at the Philipps-University Marburg.<br><br>Degree: Diploma in Biology (Major Subjects: Developmental Biology, Cell Biology and Virology), Grade: 1.2.<br><br>Diploma thesis in the laboratory of Prof. Dr. R. Renkawitz-Pohl, Developmental Biology.<br><br>Thesis title: Entwicklung von Myotuben bei <i>Drosophila melanogaster</i> : Analyse zweier EMS induzierter Mutanten und Protein-Protein Wechselwirkungen zwischen Rolling pepples und weiteren Fusions-relevanten Proteinen. |
| 09.1990-06.1999 | Student at the Werkgymnasium Heidenheim.<br><br>Degree: Abitur, Grade: 2.0.  |
| 08.1996-07.1997 | Exchange student at the Otter Valley Union High School, Vermont (USA). Organized by the Deutsch-Amerikanische Studiengesellschaft e.V. (DASG).   |

### Internship Abroad

|             |  |
|-------------|--|
| 04.-06.2003 | Practical course in the laboratory of Prof. Dr. MV Taylor, Cardiff School of Biosciences, Cardiff University (UK).<br><br>Topic: Gene Function and Expression in <i>Drosophila</i> Muscle and Heart Differentiation. |
|-------------|--|

---

## 7.11 Eidesstattliche Erklärung

Hiermit erkläre ich an Eides statt, dass ich die vorliegende Dissertation selbständig verfasst habe und dabei keine anderen, als die von mir angegebenen Hilfsmittel und Quellen benutzt habe. Zitate sind als solche gekennzeichnet.

Ich erkläre außerdem, dass die vorliegende Dissertation weder in gleicher noch in ähnlicher Form bereits in einem anderen Prüfungsverfahren vorgelegen hat. Ich habe früher, außer den mit dem Zulassungsantrag urkundlich vorgelegten Graden, keine weiteren akademischen Grade erworben oder zu erwerben versucht.

Würzburg, den 29. September 2008

---

Nina Reichert